ISSN 0915-9916

Readout

HORIBA Technical Reports

December 2025
English Edition No. 59

Analytical and Measurement Technologies for a Clean Water Environment and Sustainable Society

2024 Masao Horiba Awards

HORIBA

Readout
HORIBA Technical Reports
March 2025 No.59

Analytical and Measurement Technologies for a Clean Water Environment and Sustainable Society
2024 Masao Horiba Awards

In recent years, with changes in the global environment, there has been growing interest in sustainable development in various industries, and the efficient use and reuse of water is being emphasized. The measurement requirements vary widely, from drinking water to lakes and marshes, where organic matter floats, and ultra-pure water for semiconductors to factory wastewater. In this issue, we will introduce content relevant to the theme of the 2024 Masao Horiba Award, which was "Analytical and Measurement Technologies for a Clean Water Environment and Sustainable Society", highlighting HORIBA's initiatives in this field.

I visited a mountain stream when the cherry blossoms were falling. The light sparkling in the water and the petals floating on the surface looked like they were dancing, and I felt a sense of peace for a while.
-Photographer MATSUI Hideo-
(Member of Nikakai Association of Photographers)

Name of this Journal

This Journal is named "Readout" in the hope that "the products and technology we have created and developed will be read out and so become widely known".

Foreword

Water Tells Us, We Talk With Them for Our Global Future.

NISHIKATA Kentaro

Corporate Officer
HORIBA, Ltd.
President,
HORIBA Advanced Techno Co., Ltd.
Ph. D.

According to the 2024 United Nations World Water Development Report[1], roughly half of the global population is affected by water scarcity, a situation projected to worsen due to climate change, population growth, and urbanization. The depletion of water resources and water pollution have severe impacts on drinking water supply, agriculture, industrial activities, and entire ecosystems. Addressing these challenges requires a scientific understanding of water environments and concrete actions to build a sustainable, circular society.

The semiconductor industry exemplifies this issue. Semiconductor manufacturing processes require large quantities of ultrapure water, with a single plant's water usage sometimes equating to that of an entire city. These facilities are implementing thorough purification and recycling measures to utilize water resources effectively. Similarly, the rapidly expanding data center sector is increasing its water usage. To cool high-performance servers, efficient water-cooling systems are being introduced alongside traditional air-cooling methods. While this improves energy efficiency, it also necessitates consideration of regional water usage impacts.

In light of these circumstances, efforts toward realizing a circular society emphasize efficient water use, recycling, and pollution prevention. For instance, the European Union's Circular Economy Action Plan[2] and groundwater conservation and water quality management technologies advancing in North America and Asia highlight the importance of accurate, data-driven water management. Analytical and measurement technologies supporting these initiatives provide the scientific foundation for understanding water conditions, enabling appropriate management and decision-making.
Electrochemical sensing technologies play a crucial role in water quality monitoring.

Foreword

Advancements in new electrode materials have enhanced the precision of detecting trace components and pollutants. This progress contributes to monitoring river and lake water quality, optimizing water purification processes, and improving wastewater reuse. Additionally, spectroscopic analysis technologies precisely analyze the concentrations of chemical substances and pollutants in water, serving as powerful tools for real-time monitoring of water quality changes. Combining these technologies with artificial intelligence, machine learning, and big data analysis enables the prediction of water environment changes and the proposal of sustainable management methods.

HORIBA Group's mission, "Shape our future with solutions based on HONMAMON[3] and Diversity," reflects our commitment to contributing to society through innovative technologies that exceed expectations and a team that leverages diversity. To realize this mission, HORIBA Advanced Techno Co., Ltd., the headquarters for water and liquid measurement within the HORIBA Group, upholds the value of "Water tells us, we talk with them for our global future." This expresses our determination to build a sustainable future by listening to the voice of water through analysis and measurement. Our mission is to develop solutions based on scientific principles, contributing to a circular society and the global environment, thereby shaping our future.

We hope this issue prompts readers to contemplate the future of water environments and leads to concrete actions. Utilizing the power of analysis and measurement, let's achieve Joy and Fun for All!

* Editorial note: This content is based on HORIBA's investigation at the year of issue unless otherwise stated.

References

[1] UN World Water Development Report 2024
https://www.unwater.org/publications/un-world-water-development-report-2024
[2] EU Circular economy action plan
https://eur-lex.europa.eu/resource.html?uri=cellar:9903b325-6388-11ea-b735-01aa75ed71a1.0017.02/DOC_1&format=PDF
[3] HORIBA website . What is "HONMAMON?" | HORIBA Our Future [Online]. 2024
https://www.horiba.com/our-future/en/honmamon/

2024 Masao Horiba Awards Award Details

About Masao Horiba Awards

The Masao Horiba Award is an encouragement and recognition given to researchers and engineers who are making remarkable achievements in the field of science and technology related to analysis, measurement, and their applications at universities or public research institutions both domestically and internationally.

Eligible fields

Analytical and Measurement Technologies for a Clean Water Environment and Sustainable Society

Comments

2024 Masao Horiba Awards Screening Committee Chairperson
KUWABATA Susumu
Professor Emeritus at Osaka University

Congratulations to all the recipients of the Masao Horiba Award. You have been selected from among many outstanding applicants through a rigorous screening. I hope you will take pride in this award with confidence. I would like to report on the screening process for this year's Masao Horiba Award. A total of 25 applications were received, including 14 from Japan and 11 from overseas. With nearly half of the applications coming from overseas, this award has become an international award indeed.

The rigorous screening was conducted in two stages by seven committee members from Japan and overseas, including myself. In the first stage, we assessed whether the research aligned with this year's application theme, "Analysis and measurement technologies that contribute to the formation of a circular society by maintaining healthy water environments." We also evaluated the academic novelty, originality, and future potential of the analysis and measurement technologies as part of the screening criteria. In addition, the future potential of the applicants was also taken into consideration based on the extent of their contribution to the submitted research. In the second stage, the Screening Committee convened in person and engaged in thorough discussions while listening to the opinions of each committee member. As a result, three recipients of the Masao Horiba Award and two Honorable Mentions were selected as research with strong future potential for contributing to the creation of the sustainable water environment in the future. All of the research skillfully employs cutting-edge trace substance detection methods that were not yet developed during my time as a student, such as Excitation Emission Matrix (EEM) Spectroscopy, Three-Dimensional Ultrafast Infrared Spectroscopy, and Holographic Imaging, and involves the use of cutting-edge techniques such as Vacuum Ultraviolet Radiation (VUV) and Diamond Electrode. This is highly commendable research that will ensure the safety of water, which is essential for us and all living things. That concludes my brief comments on the screening. Once again, congratulations to all the award recipients.

Screening Committee

Chairperson :	KUWABATA Susumu	Professor Emeritus at Osaka University
Judges :	Paul K. WESTERHOFF	Professor, School of Sustainable Engineering and the Built Environment, Arizona State University
	Qinghui HUANG	Associate Professor, College of Environmental Science and Engineering, Tongji University
	IMAI Akio	Research Director, Center for Environmental Science in Saitama
	TAKAI Madoka	Professor, Department of Bioengineering, School of Engineering, The University of Tokyo
	ICHINARI Yuichi	Deputy General Manager, Advanced Technology Development Department, Development Division, HORIBA Advanced Techno Co., Ltd.
	NISHIO Yuji	Senior Meister, Advanced Technology Development Department, Development Division, HORIBA Advanced Techno Co., Ltd.

Masao Horiba Awards Winners

Dr. IDEGUCHI Takuro

Associate Professor
Institute for Photon Science and Technology, Graduate School of Science, The University of Tokyo
[Research Theme]
Development of Super-Resolution Infrared Microscopy and Ultrafast Infrared Spectroscopy

Dr. Chen QIAN

Associate Professor
Department of Environmental Science and Engineering, University of Science and Technology of China
[Research Theme]
Lab to Lake: Excitation-Emission Matrix's Voyage from Theory to Practice

Dr. SHIRASAKI Nobutaka

Associate Professor
Division of Environmental Engineering, Faculty of Engineering, Hokkaido University
[Research Theme]
Investigating of the Occurrence of Pathogenic Viruses in Drinking Water Sources and Their Reduction Efficiencies in Drinking Water Treatment Processes

Honorable Mention Winners

Dr. TAKAHASHI Tomoko

Researcher
Marine Biodiversity and Environmental Assessment Research Center, Research Institute for Global Change, Japan Agency for Marine-Earth Science and Technology
[Research Theme]
Development of in Situ Continuous In-Flow Microplastic Monitoring Techniques Using Spectroscopic Techniques

Dr. Tania Louise READ

Assistant Professor
Department of Chemistry, University of Warwick
[Research Theme]
Development of Boron-Doped Diamond Electrodes for Key Analytes in the Aqueous Environment and Beyond

Award Ceremony Thursday, October 17, 2024 Hotel Granvia Kyoto Taketori Room

* Editorial note: This content in based on HORIBA's investigation at the time of the award unless otherwise stated.

Development of Super-Resolution Infrared Microscopy and Ultrafast Infrared Spectroscopy

IDEGUCHI Takuro

Infrared spectroscopy is a standard analytical method for identifying microplastics. However, conventional techniques, such as Fourier-transform infrared spectroscopy (FTIR) and FTIR microscopy, have inherent limitations. Traditional FTIR measurements are constrained to a throughput of up to approximately 100 spectra per second, rendering them unsuitable for high-throughput analysis. Furthermore, FTIR microscopy has a spatial resolution limited to several micrometers, making it challenging to analyze fine plastic particles. To address these limitations, we developed ultrafast infrared spectroscopy techniques and super-resolution infrared microscopes, paving the way for large-scale microplastic analysis and the detection of nanoplastics.

Introduction

Microplastics have infiltrated ecosystems through the food chain, raising serious concerns about their impact on human health. In response, governments and research institutions worldwide are advancing studies to develop reliable methods for assessing microplastics. Broadband vibrational spectroscopy in the mid-infrared region (2.5–25 μm) is considered one of the most promising identification techniques, offering unique molecular fingerprints for various polymers and enabling non-contact, non-destructive measurement and analysis of microplastics. Currently, commercial Fourier-transform infrared spectrometers (FTIR) and FTIR microscopes are commonly used to analyze particles. Although these conventional methods are widely recognized as effective for measuring microplastics, they are insufficient to address the challenges posed on a global scale. This research seeks to propose advancements from two critical perspectives.

Firstly, we examine the impact on human health. Nanoplastics smaller than 1 μm pose a significant concern as they are difficult for the body to eliminate, leading to accumulation in organs such as the heart and brain via the bloodstream. This buildup can trigger inflammation, increasing the risk of conditions such as heart attacks and strokes. Traditional FTIR microscopes, with a spatial resolution limited to several micrometers, are incapable of detecting nanoplastics. As this limitation is dictated by the diffraction limit of mid-infrared light, there is an urgent need for new technologies that operate on alternative principles.

Secondly, we address the challenge of acquiring large-scale data for statistical analysis. Microplastics are not only found in rivers and seas but also in drinking water and food, infiltrating agriculture, industry, and residential areas. Addressing this global issue requires extensive sampling from diverse locations and the accumulation of robust datasets. Flow particle measurement, capable of analyzing thousands of particles per second, is a promising method for generating such data. In cell biology and medical research, flow cytometry leverages high-speed fluorescence measurements to analyze cells. However, this technique is unsuitable for microplastics, which require molecular vibrational spectroscopy without the need for fluorescent staining. Conventional FTIR measurements, with a maximum throughput of approximately 100 spectra per second, remain inadequate for flow-based analyses. To date, high-throughput flow measurement using infrared spectroscopy has not been demonstrated, underscoring the urgent need for substantial advancements in measurement rates.

Super-resolution infrared microscopy

FTIR microscopes have been utilized as standard infrared microscopes for many years. Recently, infrared microscopes employing quantum cascade lasers—a type of semiconductor laser operating in the infrared range—have been developed, significantly improving the signal-to-noise ratio (SNR). However, the spatial resolution of these methods is constrained by the diffraction limit determined by the wavelength of infrared light, achieving only several micrometers of spatial resolution.

To enhance the spatial resolution of infrared microscopy, various techniques have been proposed. These include methods leveraging near-field effects using nanoscale probes and far-field imaging techniques that combine fluorescence imaging or utilize vibrational sum-frequency generation. While these methods successfully achieve super-resolution capabilities surpassing the diffraction limit of infrared light, they face certain limitations. The former requires physical contact between the probe and the sample, while the latter depends on fluorescence or second-order nonlinear optical effects, inherently restricting the range of measurable samples. Recently, advancements in mid-infrared photothermal microscopy have addressed these challenges.

The principle of mid-infrared photothermal microscopy is as follows: when monochromatic infrared light irradiates a sample, molecules with resonant vibrations absorb the infrared photons and start vibrating. The vibrational energy is rapidly dissipated, transferring to surrounding molecules and generating heat—a phenomenon known as the photothermal effect. This localized temperature increase causes a change in the refractive index of the material. By detecting and quantifying this refractive index change using visible light microscopy, the system achieves image contrast corresponding to infrared absorption, with spatial resolution defined by the wavelength of visible light. Figure 1 illustrates the principle of mid-infrared photothermal (MIP) microscopy.

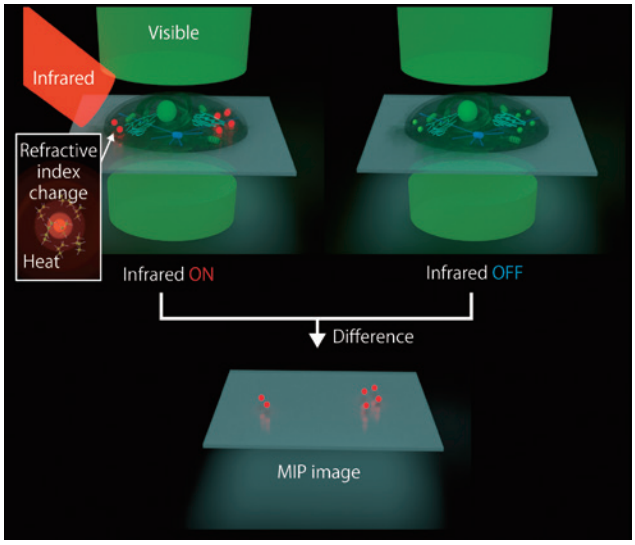

Figure 1 Principle of mid-infrared photothermal microscopy.

We have demonstrated wide-field mid-infrared photothermal (MIP) microscopy techniques. Initially, we utilized a commercially available phase-contrast microscope and successfully validated the proof-of-concept[1]. However, phase-contrast microscopy introduces image artifacts, such as halo and shade-off effects, which also affect MIP images. To address this, we replaced the phase-contrast microscope with a quantitative phase microscope, enabling the accurate measurement of phase shifts caused by refractive index changes without image artifacts[2]. Furthermore, we demonstrated three-dimensional imaging by applying the principle of optical diffraction tomography[3]. By incorporating a single-objective imaging configuration and aperture synthesis technology, we further enhanced spatial resolution, achieving 120 nm (Nyquist resolution) or 175 nm (full width at half maximum of the point spread function)[4].

We have also prioritized improving the SNR in MIP microscopy. Initially, quantum cascade lasers were employed, and their low pulse energies limited the SNR. To overcome this, we developed a nanosecond optical parametric oscillator capable of delivering pulse energies two orders of magnitude higher. By pairing this with a high-full-well-capacity image sensor, we achieved more than two-orders-of-magnitude improvement in SNR, enabling the world's first video-rate measurements[5]. Furthermore, we expanded the dynamic range of MIP quantitative phase imaging through the application of wavefront control technologies[6].

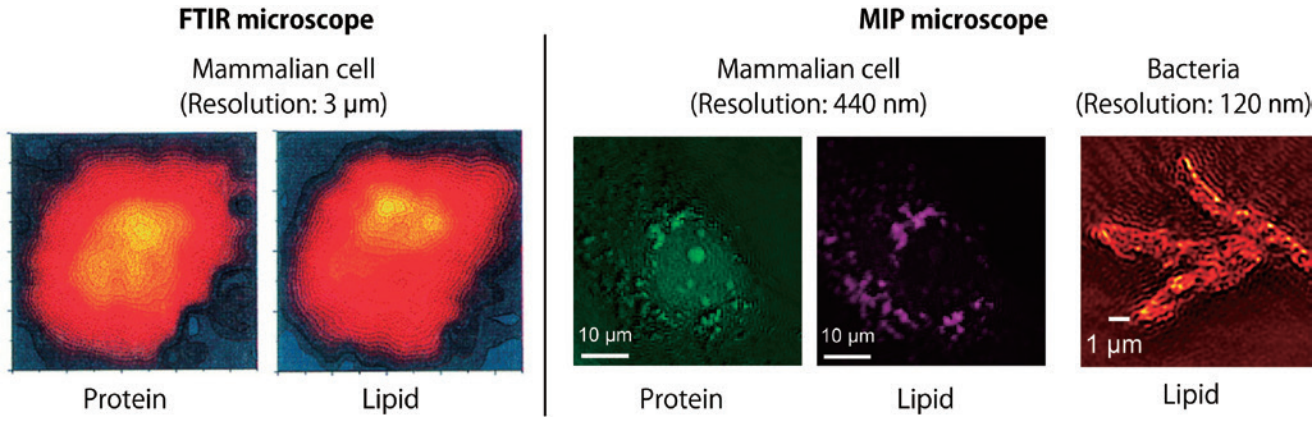

Figure 2 Comparison of cellular MIP images captured with a conventional FTIR microscope and MIP microscopes. (Left) Cellular images acquired using a conventional FTIR microscope with a spatial resolution of 3 μm[7]. (Right) MIP images of a mammalian cell with a resolution of 440 nm and bacteria with a resolution of 120 nm.

Figure 2 compares infrared microscopic images of cells obtained using a conventional FTIR microscope and our MIP microscope. The intracellular structures of cells are not visualized with FTIR microscopy but are clearly visible with MIP microscopy. The high spatial resolution allows the observation of finer structures inside bacteria. This novel technology enables the non-destructive imaging of detailed chemical information with unprecedentedly high spatial resolution, paving the way for new studies, such as investigating the interactions between nanoplastics and cells.

Ultrafast infrared spectroscopy

Fourier-transform infrared spectroscopy (FTIR) has been the standard method for infrared spectroscopy for over half a century. This technique enables the acquisition of broadband vibrational spectra but requires a relatively long measurement time—typically one second per spectrum—making it best suited for static measurements. For capturing dynamic changes in vibrational spectra, rapid-scan FTIR is often used. This approach enables high-speed measurements at approximately 100 spectra per second with commercially available instruments.

In recent years, we developed a faster FTIR technique, known as phase-controlled FTIR, capable of achieving measurement speeds of 10^4 to 10^5 spectra per second[8]. This breakthrough was enabled by the integration of a high-speed delay scanner utilizing an angle-scanning mirror and a spectral phase manipulation technique. Additionally, dual-comb spectroscopy—employing two optical frequency combs with slightly detuned repetition rates—provides a mechanical-scanner-free, high-speed FTIR technology[9]. This approach achieves the maximum measurement rate of approximately 10^6 spectra per second, allowing for time resolutions of 1 microsecond. Applications of these advanced techniques include studies of protein structural changes and combustion dynamics.

The measurement speed of dual-comb spectroscopy is fundamentally limited by the signal-to-noise ratio (SNR), posing challenges for further acceleration. Frequency-swept spectroscopy (FSS), however, offers higher SNR than Fourier-transform spectroscopy (FTS), including dual-comb spectroscopy, under equivalent conditions of measurement time, sampling rate, and detected light power. The SNR of FSS increases proportionally to the square root of the number of spectral components. Figures 3(a) and 3(b) show the SNR versus the number of spectral elements and measurement time under typical conditions. For example, with 1,000 spectral elements, the SNR for FTS is approximately 1 for a measurement time of 1 μs. In contrast, for FSS, the same SNR is achieved with a measurement time of about 1 ns, corresponding to a measurement rate of approximately 1 GHz. This highlights the potential of FSS for even faster measurements.

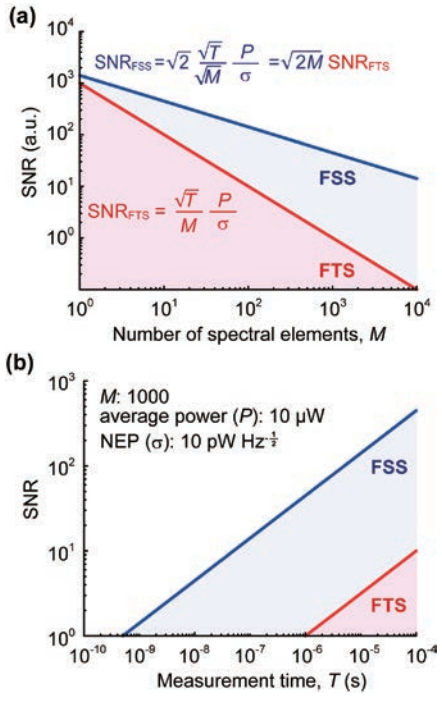

Figure 3 SNR comparison between FSS and FTS as a function of (a) the number of spectral elements and (b) the measurement time under typical conditions.

Time-stretch spectroscopy is a high-speed FSS technique that continuously measures the spectrum of each pulse from a high-repetition-rate ultrashort pulsed laser. The pulses are temporally stretched to generate chirped pulses with significant wavelength dispersion. When second-order dispersion dominates, the temporal intensity waveform directly corresponds to the spectral shape of the pulse. By recording this waveform with a high-speed photodetector and an oscilloscope, the spectrum of each pulse can be measured. However, this method had been limited to the near-infrared region, particularly within telecommunications wavelengths. Implementing time-stretch spectroscopy requires substantial dispersion, typically achieved using optical fibers typically 10 km in length. While ultra-low-loss optical fibers are readily available for telecommunications wavelengths, those suitable for the mid-infrared region suffer from high losses and are impractical. Furthermore, high-speed photodetectors with ~10 GHz bandwidth are commercially available for telecommunications wavelengths, but mid-infrared photodetectors are restricted to ~1 GHz bandwidth. These limitations had thus precluded the application of time-stretch spectroscopy in the mid-infrared region.

We pioneered time-stretch spectroscopy in the mid-infrared region by utilizing a free-space time stretcher and a high-speed quantum cascade detector[10]. Figure 4(a) illustrates the experimental setup. Femtosecond pulses from a mid-infrared pulsed laser (a femtosecond optical parametric oscillator) with an 80 MHz repetition rate were temporally stretched using a free-space angular-chirp-enhanced delay (FACED) system. This free-space time-stretcher enabled time-stretch spectroscopy in the mid-infrared region. The stretched pulses passed through the sample were captured by a quantum cascade detector with ~5 GHz bandwidth and then digitized using a 16 GHz oscilloscope. Figure 4(b) presents the time-stretched spectra of phenylacetylene, showing approximately 30 spectral components with a resolution of 15 nm (7.7 cm^{-1}). Continuous spectral measurements at 80 MHz, governed by the laser repetition rate, were successfully demonstrated.

Although this method enabled time-stretch infrared spectroscopy, challenges such as losses from multiple mirror reflections in the free-space time-stretcher limited the number of spectral elements and resolution. Since time-stretch spectroscopy achieves superior SNR compared to FTIR, particularly with a larger number of spectral elements, an improved approach was demanded. To overcome these limitations, we employed a nonlinear wavelength conversion (upconversion) technique to map mid-infrared spectra into the near-infrared region[11]. This allowed for low-loss time stretching using telecommunications optical fibers. Furthermore, the use of high-speed,

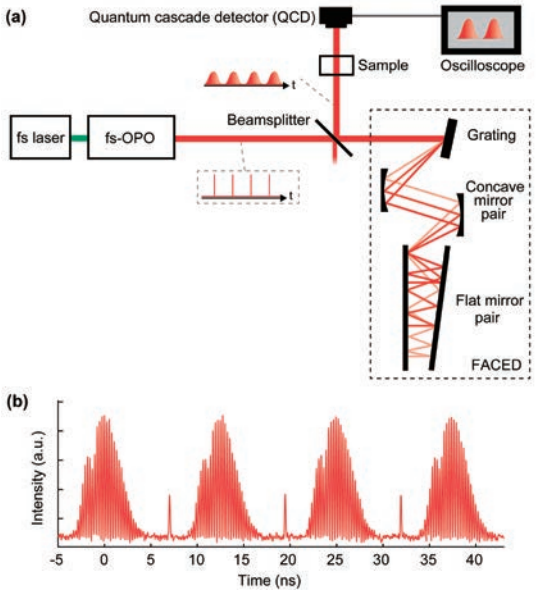

Figure 4 (a) Schematic diagram of time-stretch infrared spectroscopy utilizing a free-space time stretcher. (b) Time-stretched spectra of phenylacetylene.

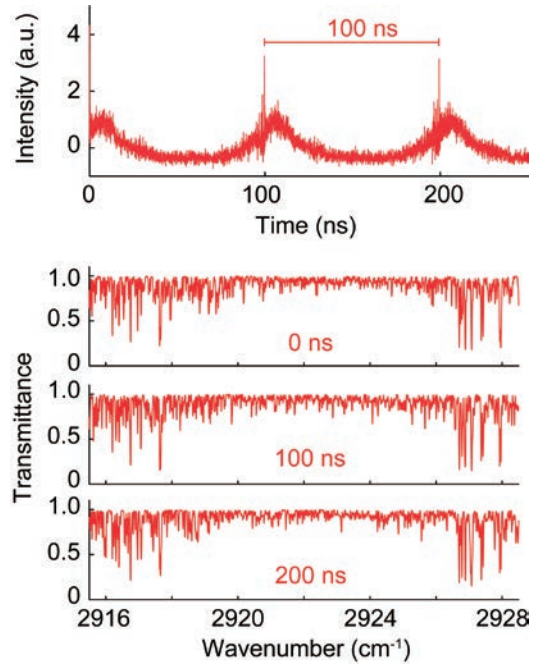

Figure 5 Methane gas spectra measured using upconversion time-stretch infrared spectroscopy.

high-sensitivity photodetectors in the telecommunications range significantly enhanced both spectral resolution and SNR. Figure 5 illustrates methane gas spectra measured using upconversion time-stretch infrared spectroscopy, employing a 60-km dispersion-compensating fiber. This setup achieved a measurement rate of 10 MHz, a spectral resolution of 0.017 cm^{-1}, and captured 1,000 spectral elements. Fiber-based time stretching improved resolution by more than two orders of magnitude, enabling high-speed infrared spectroscopy for gas molecules.

Conclusion

The super-resolution infrared microscope and ultrafast infrared spectroscopy developed in this research have thus far been primarily demonstrated through proof-of-concept measurements of cells and liquid or gaseous molecular samples. Looking ahead, these technologies are envisioned to be applied to the measurement of nano- and microplastics. In super-resolution microscopy, it will become possible to analyze nanoplastics absorbed by cells, advancing research into the effects of nanoplastics on biological functions—a field that has been challenging to study until now. For ultrafast infrared spectroscopy, its application can be extended to large-scale flow measurements in combination with microfluidic channels. High-speed infrared spectroscopy for flow particle analysis will enable high-throughput measurements of water samples from various sources, facilitating the identification of regions potentially at risk from microplastic contamination.

References

[1] K. Toda et al., *Sci. Rep.* 9, 9957 (2019).
[2] M. Tamamitsu et al., *Opt. Lett.* 44, 3729–3732 (2019).
[3] M. Tamamitsu et al., *Optica* 7, 359–366 (2020).
[4] M. Tamamitsu et al., *Nat. Photonics* 18, 738–743 (2024).
[5] G. Ishigane et al., *Light Sci. Appl.* 12, 174 (2023).
[6] K. Toda et al., *Light Sci. Appl.* 10, 1 (2021).
[7] N. Jamin et al., *PNAS 95*, 4837-4840 (1998).
[8] K. Hashimoto et al., *Nat. Commun.* 9, 4448 (2018).
[9] T. Ideguchi, *Opt. Photonics News* 28, 32-39 (2017).
[10] A. Kawai et al., *Commun. Phys.* 3, 152 (2020).
[11] K. Hashimoto et al., *Light Sci. Appl.* 12, 48 (2023).

Dr. IDEGUCHI Takuro

Associate Professor,
Institute for Photon Science and Technology,
Graduate School of Science,
The University of Tokyo

Lab to Lake: Excitation-Emission Matrix's Voyage from Theory to Practice

Chen QIAN

Dissolved organic matters (DOMs) significantly impact water quality and contaminant behavior, making their monitoring essential for water treatment. Excitation-emission matrix (EEM) fluorescence spectroscopy is a powerful tool for this purpose but faces challenges such as complex fluorescence property of DOM, turbidity interference, and limitations in field applications. To address these challenges, we developed an advanced algorithm based on the charge transfer model for accurate DOM decomposition and a new method to reduce scattering interference, improving EEM accuracy. Additionally, we introduced a sparse EEM reconstruction algorithm, leading to a miniaturized, portable device for real-time, in-situ monitoring. This innovation enhances the feasibility of EEM spectroscopy in field monitoring, contributing to efficient, precise water quality assessments and supporting sustainable water management practices.

Introduction

Dissolved organic matter (DOM), a heterogeneous mixture of polysaccharides, proteins, peptides, humic substances, and lipids, is pervasively present in waters and serves as a key environmental indicator[1],[2]. Containing various aromatic chromophoric groups such as phenols, quinones, and indoles, DOM significantly alters the water's hue, engaging as both reactants and mediators in hydrochemical processes[3],[4]. The diverse functional groups enable the DOM-pollutants interactions, thus influencing their properties, transportation, transformation, and ultimate fate[5],[6]. Due to the pivotal roles of DOMs in the migration and transformation of pollutants and the formation of disinfection by-products, an efficient monitoring of their contents and composition is of vital importance for better comprehension of aquatic environments and improving the water treatment process[7],[8].

Ultraviolet-visible (UV-Vis) and fluorescence spectroscopies are particularly adept at characterizing DOM's aromatic groups, which are linked to molecular weight distribution, hydrophilicity and hydrophobicity, reactivity, and concentration quantification[9],[10]. These techniques, sensitive to the absorption or emission of electromagnetic radiation, are thereby unveiling DOM's intrinsic properties in diverse chemical environments[11],[12]. Compared to UV-Vis spectra, fluorescence spectra can identify more nuanced changes in DOM's structure or composition by detecting peaks located at different excitation or emission wavelengths[13],[14].

With advancements in fluorescence spectrometry, it's now possible to generate excitation-emission matrix (EEM) fluorescence spectra that offer richer information by collecting emission spectra at a series of excitation wavelengths. EEM

heralded for its rapidity, precision, selectivity, and depth of insight, has been instrumental in delineating the migration dynamics and transformation mechanisms of DOM[15],[16]. However, it is very challenging to adapt such technologies from controlled laboratory settings to the monitoring of complicated natural waters, because the intricate fluorescence behaviors of DOM impede the accurate interpretation of EEM spectra. Moreover, the presence of turbidity in water samples substantially hampers precise spectral analysis. Additionally, the prohibitive costs and rigorous operational prerequisites of conventional EEM spectrometers further confine their usage predominantly to laboratory investigations. These drawbacks have severely restricted a broader application of the EEM spectroscopy in environmental surveillance.

To address these challenges, we have investigated into the intricate fluorescence mechanisms of DOM, and based on which optimized the EEM analytical algorithms for enhanced speed and accuracy and enabling miniaturization of EEM spectrometers. Initially, we developed an algorithm for the precise decomposition of the EEM of DOM, based on the charge transfer model. Subsequently, we established a model to deduce the absorption spectrum from Rayleigh scattering, grounded in the principles of light scattering. Leveraging these spectral analysis enhancements, we engineered a compact EEM pollution traceability device. This innovation provides essential technological and instrumental support for implementing EEM spectroscopy in the real-time surveillance and identification of pollutants within aquatic environments.

Non-trilinear independence nature of DOM's EEM

The Parallel Factor Analysis (PARAFAC) is one of the most popular methods for DOM characterization. it decomposes the original dataset composed of a series of EEMs into several linear independent components (Figure 1A)[17],[18]. Due to the rapidity and plentiful information obtained from PARAFAC, it has become the most popular approaches and widely be applied in analyzing EEMs with complex unidentified components, such as DOM from various sources. However, PARAFAC decomposes the EEMs mathematically and cannot provide a physical interpretation for each component. Thus, the number of factors and their explanations are usually further clarified through methods like peak-picking and fluorescence regional integration. This problem occurred because PARAFAC assumed that the complex EEM of DOM are a linear superposition of fluorescence signals from independent fluorescent groups. However, environmental monitoring data have revealed that DOM, especially its major components like humic and fulvic acids, do not conform to this assumption, resulting in spectral distortion and errors in quantitative results. This limitation arises from the fact that PARAFAC is only applicable when the excitation and emission spectra are independent, making it unsuitable for scenarios involving charge transfer processes.

The charge transfer model is a fluorescence mechanism model that describes the transfer of electrons from donor molecules to acceptor molecules. This model emphasizes the importance of the electron transfer process in the fluorescence behavior of dissolved organic matter, especially in complex molecules containing both electron donors and acceptors. Compared to the basic principles of the traditional fluorescence model, the charge transfer model exhibits significant differences. Traditional fluorescence models focus on electron transitions within the molecule, assuming that fluorescence emission is solely related to changes in the molecule's excited state energy levels, typically applicable to simple organic molecules. In contrast, the charge transfer model posits that electrons not only transition within the molecule but can also undergo intermolecular charge transfer, a process that significantly impacts fluorescence intensity and wavelength.

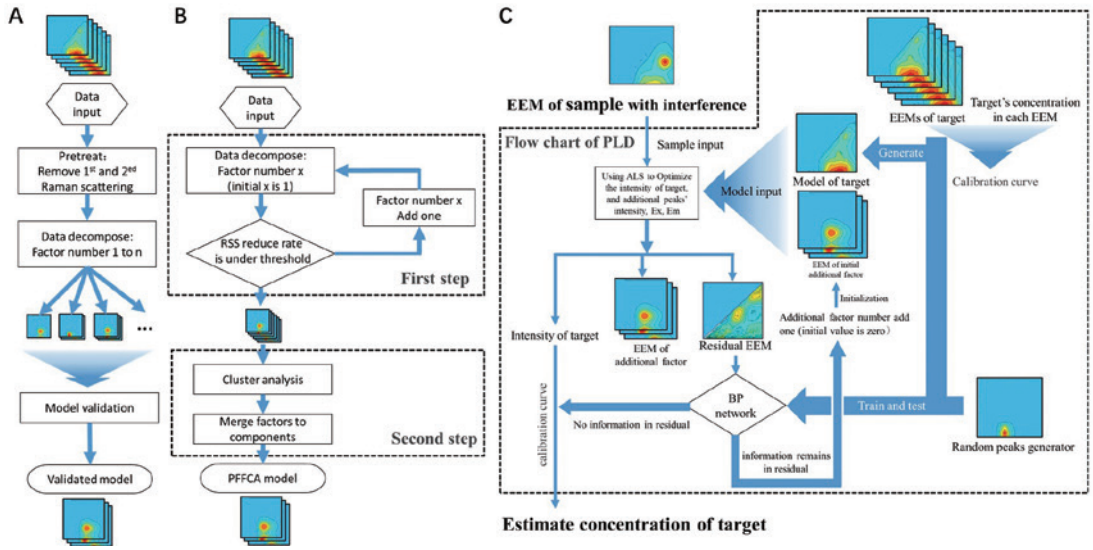

Figure 1 Workflow of (A) Parallel Factor Analysis (PARAFAC), (B) Parallel Factor Framework with Cluster Analysis (PFFCA) and (C) Prior Linear Decomposition (PLD).

Due to these mechanistic differences, the charge transfer model is particularly applicable to molecules with complex structures and electron donor-acceptor functionalities, such as dissolved organic matter like humic acid and fulvic acid[19]. Traditional fluorescence models fail to adequately describe the fluorescence emission of such substances, particularly in complex environments, where the fluorescence behavior of dissolved organic matter is significantly influenced by environmental factors and the charge transfer process. Therefore, the peak attribution results from the analysis method based on traditional fluorescence model can sometimes vary, potentially causing confusion or misleading the accurate identification of DOM components.

Analyze the EEM of DOM with a charge transfer model

The charge transfer model provides a more complex framework for a deeper understanding of the fluorescence characteristics of these dissolved organic compounds in real-world environments. Therefore, it should have important applications in environmental science fields such as water quality monitoring and pollutant tracking. However, traditional fluorescence analysis methods are based on the traditional fluorescence model, lacking consideration of the charge transfer process. This limitation can lead to inaccurate or constrained analysis when dealing with DOM.

Therefore, we simulated the EEM of DOM under conditions of charge transfer, and developed a novel method integrating the parallel factor framework with cluster analysis (PFFCA)[20]. The PFFCA method principally assumes that all of the components are independent and that the dataset is decomposed into many factors without considering charge transfer model. Afterwards, the factors whose scores are highly correlated was combined into one component because they may individually represent only a proportion of the component due to the charge transfer (Figure 1B). Therefore, in the first step, EEM dataset was decomposed into a set of trilinear terms and a residual array using the PARAFAC model. The factor number was determined when the residual was not decreased with the increasing of the factor number. This process is based on the idea that if the increase in factor number cannot reduce the residual, the increase is no longer necessary.

For the second step, PFFCA clusters these factors into several practical DOM components by calculating the coefficient of the scores from different components. If the scores of several factors correlate consistently with each other, they are likely derived from the same DOM component due to the charge transfer. Consequently, both trilinear and non-trilinear DOM fractions can be accurately identified. This approach, by decoupling the data decomposition and analysis processes, eliminates the impact of non-linear superposition of fluorescent groups on the analysis. PFFCA achieves stable and interpretable information on DOM components by clustering the variation patterns of different factors with disturbances.

This work represents a breakthrough from the traditional understanding of linear superposition assumed by PARAFAC, reversing the common practice of introducing errors from non-trilinear components in quantitative analysis. Compared to traditional methods, PFFCA can more accurately reflect the composition of DOM in water (with a reduction in the sum of squared residuals of the spectra by at least an order of magnitude), providing a reliable method for analysis of the DOM components. For the quantification applications, the scores from standard solution samples can also be linearly fitted with concentration vectors to determine their contributions. Then, the unknown concentration samples' scores are calculated with the EEMs of each component, followed by concentration calculations via linear regression[21].

Despite that the new method partially overcome the obstacles of PARAFAC, the analysis procedures are relatively time-consuming, due to the reserve of PARAFAC framework and the subsequent cluster analysis or multiple regression fitting. Therefore, we optimized the PFFCA by reevaluating the independence of data, thereby refining the linear iterative approach[22]. This prior linear decomposition (PLD) method firstly involves linear regression of sample EEMs with the standard solution, followed by residual analysis via a backpropagation artificial neural network. If there are still additional peaks in the residual, the factor number will be increased by one until a residual EEM with random noise is obtained (Figure 1C). The final concentrations of the target and the EEMs of the additional factors will be simultaneously estimated, allowing PLD to quantify the DOM and diagnose potential fluorescent interfering substances. By incorporating known EEMs as prior knowledge, the optimization process transcended the limitations of the linear superposition model. Furthermore, integrating machine learning enabled rapid alerts for abnormal fluorescence peaks without human intervention, significantly reducing analysis time from PFFCA's 30 minutes to less than 40 seconds. Our method revolutionizes the traditional regression-based "needle in a haystack" workflow for estimating unknown pollutants, providing a new approach for faster, more interference-resistant EEM analysis. Leveraging these innovative algorithms, we developed an EEM-based method for detection of non-fluorescent saccharides[21], enabling simultaneous quantification of aldoses and ketoses, and optimized the selection of protein standards, thereby expanding the scope of EEM's application in environmental monitoring.

Eliminates scattering interference in turbid water samples

Spectral analysis methods typically require samples to be clear, true solutions. However, the presence of particles in actual water environments is inevitable and can cause turbidity, posing challenges to practical environmental monitoring application. Conventional spectral testing often necessitates preprocessing steps like centrifugation or membrane filtration to remove particulate interference. However, these processes not only significantly restrict the development of in-situ water environment spectral monitoring techniques but also risk omitting crucial environmental information since these particles themselves could be pollutants. Therefore, a thorough understanding of the light scattering behavior of particles in the environment is crucial for accurately interpreting the environmental spectral data.

EEM spectroscopy naturally includes Rayleigh scattering signals, where the excitation wavelength equals the emission wavelength. However, traditional analysis methods often cannot resolve complex scattering signals and thus typically set these scattering signals to zero to avoid interference with EEM analysis. Based on the deep understanding of light scattering and EEM, we develop our estimation method based on the following two hypotheses:
obedience to Beer's law ($I=I_0e^{-\alpha_{ext}h}$), and the far smaller illuminated area than the cuvette cross-section. By applying Beer's law, the strength of the Rayleigh scattering signal was given as (Figure 2A):

$$S(\lambda) = I_0 \int_{x_1}^{x_2} \alpha_{sca}(\lambda) e^{-(\alpha_{sca}(\lambda)+\alpha_{abs}(\lambda))x}\, dx \cdot k_{\frac{\pi}{2}}(\lambda) \int_{y_1}^{y_2} e^{-(\alpha_{sca}(\lambda)+\alpha_{abs}(\lambda))y}\, dy \quad (1)$$

where I_0 refers to the incident light intensity while $\alpha_{sca}(\lambda)$ and $\alpha_{abs}(\lambda)$ represent the coefficients of Rayleigh scattering and absorption[23] with the unit of cm^{-1}, their sum is the attenuation coefficient α_{ext} in Beer's Law. Meanwhile, $k_{\frac{\pi}{2}}(\lambda)$ is the proportion of Rayleigh scattered photons detected by the right-angle observation[24] sensor to all Rayleigh scattered photons in the region of integration.

For the second hypothesis when the illuminated area is far smaller than the cuvette cross-section, the approximation of eq. 1 can be given as:[25],[26]

$$S(\lambda) = \alpha_{sca}(\lambda) k_{\frac{\pi}{2}}(\lambda) I_0 (x_2 - x_1)(y_2 - y_1) e^{-(\alpha_{sca}(\lambda)+\alpha_{abs}(\lambda))(C_{ex}+C_{em})} \quad (2)$$

where x_1, x_2, y_1 and y_2, expressed in two-dimensional Cartesian coordinates, define the boarder of illuminated area in the top view of a cuvette. Moreover, C_{ex} and C_{em}, representing midpoint coordinates of the optical path in cuvette along the x and y axis in an ordinary circumstance[26]. As a result, eq. 2 could be rewritten as:

$$S(\lambda) = \gamma(\lambda)\alpha_{sca}(\lambda) e^{-(\alpha_{sca}(\lambda)+\alpha_{abs}(\lambda))} \quad (3)$$

where $\gamma(\lambda)$ is the multiplication of $k_{\frac{\pi}{2}}(\lambda)$, I_0, $x_2 - x_1$, and $y_2 - y_1$ in eq. 2 that can be seen as a constant. With the blank control of the sample written as $S_{blank}(\lambda) = \gamma(\lambda)\alpha_{sca}(\lambda) e^{-\alpha_{sca}(\lambda)}$, a deduction can be made to estimate the absorbance of the sample by introducing a relationship of $\alpha_{abs}(\lambda) = ln(10) \cdot A(\lambda)$ for any cuvette with 1 cm light path:

$$A(\lambda) = log_{10}\left(S_{blank}(\lambda)\right) - log_{10}\left(S_{sample}(\lambda)\right) \quad (4)$$

where A(λ) is the absorbance of sample in wavelength λ, S_{sample} and S_{blank} are Rayleigh scattering signal strength for sample and blank control detected under the same configuration of measurement (Figure 2B). Therefore, the estimated absorbance can be used to calibrate the inner filter effects in EEM measurement, overcoming the bottleneck that EEM requires additional light sources or detectors for accurate quantification. Our method provides a theoretical basis for the optimization of fluorescence spectroscopy instrument optical paths and offers methodological support for the structural optimization of EEM monitoring instruments in actual water environments[27].

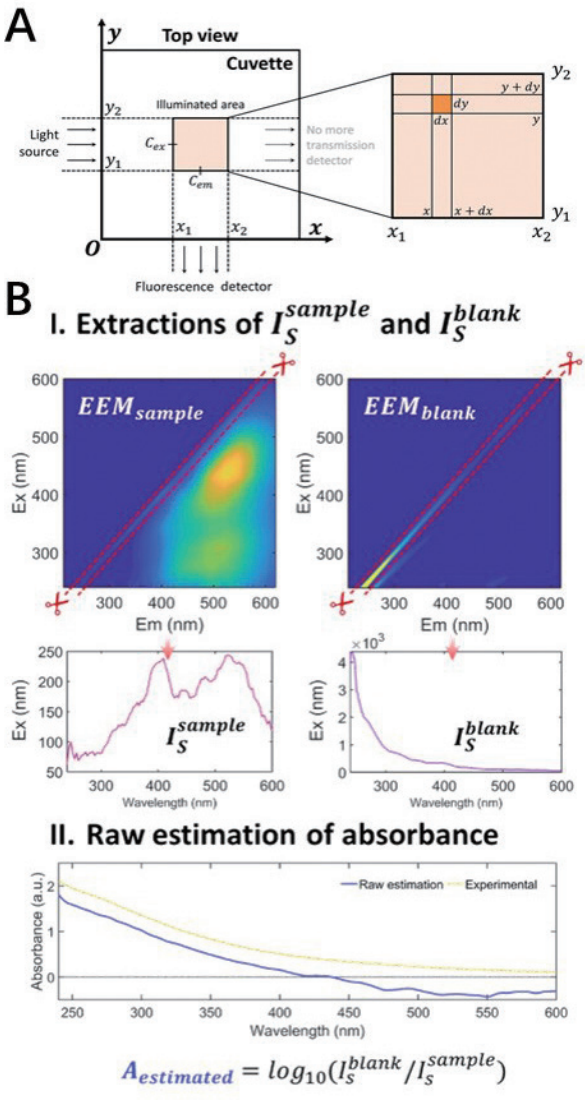

Figure 2 (A) The geometry of infinitesimal analysis in the model. (B) Workflow of the absorbance estimation with the Rayleigh scattering.

In aquatic environments, the adsorption and distribution of DOM on particles largely affect the migration and transformation of both DOM and pollutants. However, such processes can result in organic matter concentrations exceeding the linear range of the Beer-Lambert law. Thus, traditional analysis methods based on radiative transfer theory, which decouple scattering and absorption spectra, often lead to spectral distortions and fail to quantitatively resolve the distribution process. Leveraging a new understanding of the scattering model, we established a distribution model for the adsorption process of environmental particles. This model corrected for the nonlinear changes in adsorption spectra with concentration, and analyzed the distribution process, proportion, and rate of pollutants in water and on particle surfaces. Using this method in conjunction with infrared spectroscopy, we elucidated how the DOM interacts through π-π conjugation with polystyrene microplastics containing benzene rings and large condensed domains, providing essential support for analyzing the migration behaviors of pollutants carried by microplastics in actual environments[28].

Development of miniaturized EEM monitoring device

Although we have deciphered the EEM of DOM in actual environmental water samples, transitioning the EEM spectrometer from laboratory analysis to in-situ monitoring in the field introduces new challenges such as harsh and variable environments, the need for low power consumption, and the requirement for long-term stability with minimal maintenance. Therefore, due to the short lifespan of mercury/xenon lamps and the high sensitivity of monochromator to temperature and vibrations, the traditional EEM spectrometers struggles to cope with the complex and harsh conditions of actual monitoring scenarios. Although light-emitting diodes (LEDs) offer longer lifespans and stable performance, their poor monochromaticity and discontinuous spectra make obtaining comprehensive spectral information challenging due to spectral sparsity.

To address this issue, we introduced the manifold embedding hypothesis, theoretically proving that, under appropriate wavelength selection, sparse spectra collected with LEDs contain equivalent information to continuous spectra. Based on this, we developed a deep learning network with an encoder-decoder architecture, creating a method for the continuous reconstruction of sparse spectra. This approach allows the use of LED light sources in EEM spectrometers, breaking free from the constraints of traditional mercury/xenon lamp-monochromator structures and providing methodological support for the miniaturization of EEM spectrometers.

Building on the innovations in analytical algorithms, we developed a portable water quality monitoring and traceability device based on EEM spectroscopy. Compared to existing EEM spectrometers that are mainly confined to lab use, this device not only maintains the quality and quantitative accuracy of EEM but also offers advantages such as interference resistance, compact size, extended lifespan, and rapid testing. Therefore, we integrated this device onto autonomous surface vehicle (ASV) for high-density navigational monitoring of the Chao Lake, China's third-largest freshwater lake (Figure 3). It enabled monitoring changes in water quality as tributaries merge, and identifying potential sources of wastewater discharge or leaks through the abnormal fluctuations in EEM components. With the new method powered EEM spectrometer, we have provided technical support for the management and regulation of the Chao Lake.

In addition, EEMs with high spatial and temporal density can also provide sufficient data support for big data analysis of the water environment. For example, only with dense spatiotemporal data can we unveil whether environmental variables show gradual or abrupt changes over time and space. Therefore, we conduct a field tests covered 8.3 km of the Nanfei River in Hefei, China provided 132 samples with the spatial resolution less than 63 m. With these data, we could use the noise color[29]-[31] to explore the structure of spatial autocorrelation of fluorescent noise along the Nanfei

Figure 3 Homemade compact EEM spectrometers

River, which is impossible for the manual EEM data collection. Noise color, informed by power spectrum density[29], reflects the frequency variation of a variable. This allowed us to distinguish between fluorescence components that exhibit low-frequency, spatially continuous changes, and those with high-frequency variations linked to specific geographical locations.

Predominantly, white noise represented about 83% of the EEM spectral area, indicating random variation in fluorescence, particularly in the coordinates of humic-like substance (Figure 4). However, pink noise was primarily associated with the T peak of protein-like substance, indicating a smoother variation of protein-like substances along the river. These findings imply that humic-like substance exhibits relative local heterogeneity, while protein-like substance demonstrates a more uniform distribution within the river, indicating that the differing origins of humic-like and protein-like substances play a crucial role. Thus, the miniaturized EEM monitoring device has the potential to enrich our comprehension of water variations.

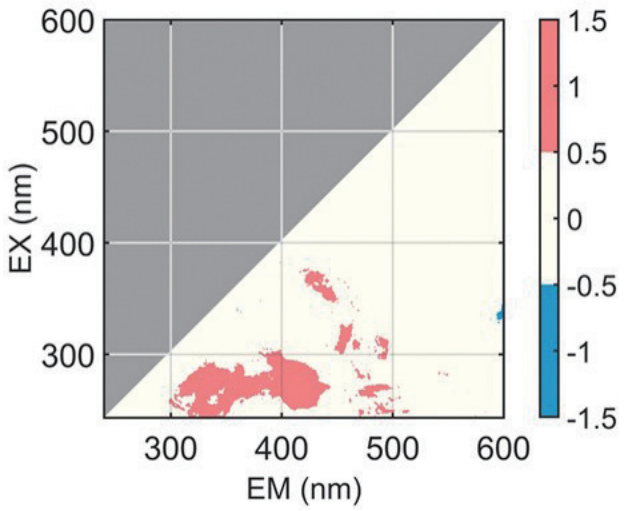

Figure 4 Noise colors of elements in EEM across 132 ASV sampling points.

Conclusion

By addressing the intricate challenges of accurate DOM analysis in natural waters, we made advancements in EEM analytical algorithms and instrumental innovation, enabling EEM spectroscopy applied to actual environmental monitoring. The development of the algorithm based on the charge transfer model for precise DOM decomposition, and spectral analysis method to eliminate scattering interference, fundamentally enhances the accuracy and practical applicability of EEM spectroscopy. Furthermore, we successfully miniaturized the EEM spectrometer, culminating in a compact, portable device for real-time environmental surveillance, representing a significant leap towards practical, field-deployable solution. This work not only bridges the gap between sophisticated laboratory analyses and the exigencies of in-situ environmental monitoring, but also opens new avenues to assist the enforcement of sustainable water management practices. By enabling more precise, efficient, and accessible monitoring of water quality, these works offer profound implications for environmental science, water treatment technologies, and policy-making, aligning with the global imperatives of environmental conservation and public health.

References

[1] Croué, J. A. L. J.-P., Peer Reviewed: Characterizing Aquatic Dissolved Organic Matter. *Environmental Science & Technology* **2003,** *37,* (1), 18A-26A.

[2] Nebbioso, A.; Piccolo, A., Molecular characterization of dissolved organic matter (DOM): a critical review. *Anal. Bioanal. Chem.* **2013,** *405,* (1), 109-124.

[3] Shah Walter, S. R.; Jaekel, U.; Osterholz, H.; Fisher, A. T.; Huber, J. A.; Pearson, A.; Dittmar, T.; Girguis, P. R., Microbial decomposition of marine dissolved organic matter in cool oceanic crust. *Nature Geoscience* **2018,** *11,* (5), 334-339.

[4] Connolly, C. T.; Cardenas, M. B.; Burkart, G. A.; Spencer, R. G. M.; McClelland, J. W., Groundwater as a major source of dissolved organic matter to Arctic coastal waters. *Nat Commun* **2020,** *11,* (1), 1479.

[5] Aiken, G. R.; Hsu-Kim, H.; Ryan, J. N., Influence of dissolved organic matter on the environmental fate of metals, nanoparticles, and colloids. *Environmental Science & Technology* **2011,** *45,* (8), 3196-3201.

[6] Philippe, A.; Schaumann, G. E., Interactions of Dissolved Organic Matter with Natural and Engineered Inorganic Colloids: A Review. *Environ. Sci. Technol.* **2014,** *48,* (16), 8946-8962.

[7] Tang, W. W.; Zeng, G. M.; Gong, J. L.; Liang, J.; Xu, P.; Zhang, C.; Huang, B. B., Impact of humic/fulvic acid on the removal of heavy metals from aqueous solutions using nanomaterials: a review. *Sci. Total Environ.* **2014,** *468-469,* 1014-1027.

[8] Yang, X.; Rosario-Ortiz, F. L.; Lei, Y.; Pan, Y.; Lei, X.; Westerhoff, P., Multiple Roles of Dissolved Organic Matter in Advanced Oxidation Processes. *Environmental Science & Technology* **2022,** *56,* (16), 11111-11131.

[9] Hansen, A. M.; Kraus, T. E. C.; Pellerin, B. A.; Fleck, J. A.; Downing, B. D.; Bergamaschi, B. A., Optical properties of dissolved organic matter (DOM): Effects of biological and photolytic degradation. *Limnol. Oceanogr.* **2016,** *61,* (3), 1015-1032.

[10] Li, P.; Hur, J., Utilization of UV-Vis spectroscopy and related data analyses for dissolved organic matter (DOM) studies: A review. *Crit. Rev. Environ. Sci. Technol.* **2017,** *47,* (3), 131-154.

[11] Fellman, J. B.; Hood, E.; Spencer, R. G. M., Fluorescence spectroscopy opens new windows into dissolved organic matter dynamics in freshwater ecosystems: A review. *Limnology and Oceanography* **2010,** *55,* (6), 2452-2462.

[12] Chen, W.; Yu, H. Q., Advances in the characterization and monitoring of natural organic matter using spectroscopic approaches. *Water Research* **2021,** *190,* 116759.

[13] Lakowicz, J. R., Instrumentation for Fluorescence Spectroscopy. In *Principles of Fluorescence Spectroscopy,* Lakowicz, J. R., Ed. Springer US: Boston, MA, 2006; pp 27-61.

[14] Lakowicz, J. R.; Masters, B. R., Principles of Fluorescence Spectroscopy, Third Edition. *Journal of Biomedical Optics* **2008,** *13,* 029901.

[15] Yu, J. L.; Xiao, K.; Xue, W. C.; Shen, Y. X.; Tan, J. H.; Liang, S.; Wang, Y. F.; Huang, X., Excitation-emission matrix (EEM) fluorescence spectroscopy for characterization of organic matter in membrane bioreactors: Principles, methods and applications. *Frontiers of Environmental Science & Engineering* **2020,** *14,* (2), 31.

[16] Li, L.; Wang, Y.; Zhang, W. J.; Yu, S. L.; Wang, X. Y.; Gao, N. Y., New advances in fluorescence excitation-emission matrix spectroscopy for the characterization of dissolved organic matter in drinking water treatment: A review. *Chemical Engineering Journal* **2020,** *381,* 122676.

[17] Stedmon, C. A.; Markager, S.; Bro, R., Tracing dissolved organic matter in aquatic environments using a new approach to fluorescence spectroscopy. *Marine Chemistry* **2003,** *82,* (3), 239-254.

[18] Stedmon, C. A.; Bro, R., Characterizing dissolved organic matter fluorescence with parallel factor analysis: a tutorial. *Limnology and Oceanography: Methods* **2008,** *6,* (11), 572-579.

[19] Baker, A., Fluorescence excitation− emission matrix characterization of some sewage-impacted rivers. *Environ. Sci. Technol.* **2001,** *35,* (5), 948-953.

[20] Qian, C.; Wang, L. F.; Chen, W.; Wang, Y. S.; Liu, X. Y.; Jiang, H.; Yu, H. Q., Fluorescence Approach for the Determination of Fluorescent Dissolved Organic Matter. *Anal. Chem.* **2017,** *89,* (7), 4264-4271.

[21] Qian, C.; Chen, W.; Gong, B.; Yu, H. Q., Determination of Saccharides in Environments Using a Sulfuric Acid-Fluorescence Approach. *Environ Sci Technol* **2020,** *54,* (11), 6632-6638.

[22] Qian, C.; Chen, W.; Gong, B.; Wang, L. F.; Yu, H. Q., Diagnosis of the unexpected fluorescent contaminants in quantifying dissolved organic matter using excitation-emission matrix fluorescence spectroscopy. *Water Research* **2019,** *163,* 114873.

[23] Bohren, C. F.; Huffman, D. R., *Absorption and scattering of light by small particles.* John Wiley & Sons: 2008.

[24] Lakowicz, J. R., *Principles of fluorescence spectroscopy.* Springer: 2006.

[25] Kubista, M.; Sjoback, R.; Eriksson, S.; Albinsson, B., Experimental Correction for the Inner-Filter Effect in Fluorescence-Spectra. *Analyst* **1994,** *119,* (3), 417-419.

[26] MacDonald, B. C.; Lvin, S. J.; Patterson, H., Correction of fluorescence inner filter effects and the partitioning of pyrene to dissolved organic carbon. *Anal. Chim. Acta* **1997,** *338,* (1-2), 155-162.

[27] Du, M.; Chen, W.; Qian, C.; Chen, Z.; Chen, G. L.; Yu, H. Q., Using Rayleigh Scattering to Correct the Inner Filter Effect of the Fluorescence Excitation-Emission Matrix. *Anal. Chem.* **2023,** *95,* (33), 12273-12283.

[28] Yang, X. D.; Gong, B.; Chen, W.; Qian, C.; Du, M.; Yu, H. Q., In-situ quantitative monitoring the organic contaminants uptake onto suspended microplastics in aquatic environments. *Water Res.* **2022**, *215.*

[29] Tu, T. B.; Comte, L.; Ruhi, A., The color of environmental noise in river networks. *Nat Commun* **2023,** *14,* (1).

[30] Vasseur, D. A.; Yodzis, P., The color of environmental noise. *Ecology* **2004,** *85,* (4), 1146-1152.

[31] Yang, Q.; Fowler, M. S.; Jackson, A. L.; Donohue, I., The predictability of ecological stability in a noisy world. Nat Ecol Evol **2019,** *3,* (2), 251-259.

Dr. Chen QIAN

Associate Professor,
Department of Environmental Science and Engineering,
University of Science and Technology of China

Investigating of the Occurrence of Pathogenic Viruses in Drinking Water Sources and Their Reduction Efficiencies in Drinking Water Treatment Processes

SHIRASAKI Nobutaka

To control waterborne diseases and to ensure a stable supply of safe drinking water, it is essential to understand the occurrence of pathogenic viruses in drinking water sources and their reduction efficiencies in drinking water treatment processes. Here, we improved and optimized a method that combines a photoreactive intercalating dye with a PCR assay for virus quantification, and developed a novel virus concentration method using two membranes, making it possible to investigate the occurrence of pathogenic viruses and to discuss the presence or absence of infectious viruses in drinking water sources. By applying the developed virus concentration method to water samples collected at actual drinking water treatment plants, we successfully evaluated the virus treatment properties in full-scale drinking water treatment processes. Furthermore, we prepared virus-like particles (VLPs) of human norovirus, which is difficult to culture, and developed a method to quantify them in high sensitivity, and then successfully evaluated the removal efficiencies of human norovirus particles in drinking water treatment processes. In addition, we established a method for producing purified solutions of human sapovirus at high concentrations, and a method for evaluating its infectivity, and then successfully evaluated the removal and inactivation efficiencies of human sapovirus in drinking water treatment processes.

Introduction

Water supply is a key infrastructure indispensable for people to lead healthy and cultured lives, and at the same time, it plays an important role in the control of infectious diseases. On the other hand, climate change is expected to bring about problems that threaten the safety and security of people's lives in the future in terms of both the quality and quantity of water, such as the increased risk of drought and floods and deterioration of water quality in rivers and lakes, which are the raw water for drinking water, due to frequent extreme low and high rainfall events. In particular, waterborne infectious diseases caused by viral contamination of water are an international water problem that still occurs not only in developing countries but also in developed countries including Japan, where sanitary conditions have improved due to advances in medical and pharmaceutical sciences and the

spread of water supply and sewage systems. Control of this problem is an essential issue for the use/reuse of low-quality water with high levels of pathogenic viral contamination, which is expected to increase in the future. In Japan, unintentional reuse of wastewater for drinking is widely practiced, in which surface water including treated wastewater with high virus concentrations discharged upstream is used as raw water for drinking water downstream (commonly referred to as *de facto* reuse), a situation that cannot be avoided in the future. Under these circumstances, to ensure a stable supply of safe and reliable drinking water in the future, it is essential to understand the occurrence of pathogenic viruses, especially infectious viruses, in drinking water sources, and their removal and inactivation efficiencies in the drinking water treatment processes. Based on these findings, it is extremely important to apply effective and efficient drinking water treatment to reduce the risk of waterborne infection by pathogenic viruses to an acceptable level.

Pathogenic viruses that cause waterborne diseases are more infectious than pathogenic bacteria, and infection can be established at doses as low as 1 to 100 virus particles, therefore the World Health Organization (WHO) estimates an acceptable concentration of 1 virus particle/90,000 L (approximately 10^{-5} virus particles/L) in drinking water[1]. Although it is ideal to evaluate the reduction efficiencies of pathogenic viruses in actual drinking water treatment plants, it is virtually impossible to evaluate the efficacy of drinking water treatment processes to reduce pathogenic viruses based on direct quantification of those because the concentrations of pathogenic viruses in treated water after drinking water treatment are extremely low and are usually below the quantification limit of PCR assay even when >1,000 L of water are concentrated to several milliliters. Therefore, it is realistic to estimate the concentration of pathogenic viruses in treated water including drinking water using the concentration of pathogenic viruses in drinking water sources obtained from investigation of the occurrence of pathogenic viruses in drinking water sources and the removal and inactivation efficiencies of pathogenic viruses in drinking water treatment processes evaluated through lab-scale drinking water treatment experiments using artificially propagated virus-spiked water. However, although the PCR assay is widely used to investigate the presence of viruses in the water environment including drinking water sources, since it is fast, highly sensitive, and highly specific, the PCR assay detects and quantifies the viral DNA/RNA of both infectious and inactivated viruses, and does not discriminate the presence or absence of infectious viruses, which is important for accurately assessing the risk of infection in the water environment. In addition, for some of the pathogenic viruses such as human noroviruses, it is difficult to propagate a large number of virus particles enough to conduct lab-scale virus-spiking experiments because of the lack of an effective *in vitro* cell-culture system. Therefore, little is known about the behaviors of difficult-to-culture pathogenic viruses including human norovirus during the drinking water treatment processes.

Against this background, we focused on the viability PCR, which combines the photoreactive intercalating dye such as propidium monoazide (PMA) and DNA/RNA quantification by PCR assay, used to determine whether bacteria are alive or dead, and tried to improve and optimize it as a method to determine viral infectivity. Also, we attempted to develop a novel virus concentration method that can effectively concentrate a wide variety of viruses from large volumes of water samples, and combine with the improved and optimized assay to investigate the occurrence of infectious pathogenic viruses in drinking water sources. In addition, we focused on pepper mild mottle virus, a plant virus that is present at high concentrations in drinking water sources, and investigated its effectiveness as a potential surrogate for pathogenic viruses in physical and physicochemical drinking water treatment processes, and then attempted to investigate the reduction efficiencies of the indigenous pepper mild mottle virus in actual drinking water treatment plants by applying the developed virus concentration method. Furthermore, we focused on virus-like particles (VLPs), which can be produced in a large number of particles without relying on a cell-culture system (i.e., without waiting for the establishment of an effective *in vitro* cell-culture system) and are morphologically and antigenically the same as native virus particles, and tried to prepare VLPs of human norovirus that is difficult to culture. Also, we attempted to develop a novel virus quantification method that can quantify VLPs with high sensitivity, and combine with VLPs to investigate the reduction efficiencies of human norovirus particles in drinking water treatment processes through lab-scale virus-spiking experiments. In addition, we tried to prepare the purified solution of human sapovirus, which belongs to the same family as human norovirus, by applying an *in vitro* cell-culture system for human sapovirus. Also, we attempted to develop a virus quantification method that can quantify the infectivity of human sapovirus, and combine it with the purified solution of human sapovirus to investigate the reduction efficiencies of human sapovirus in drinking water treatment processes through lab-scale virus-spiking experiments.

Occurrence of pathogenic viruses in drinking water sources

We focused on the integrity of the viral capsid, which is one of the main factors that determine whether the virus is infectious or not, and customized the viability PCR to determine whether the viral capsid is damaged. The

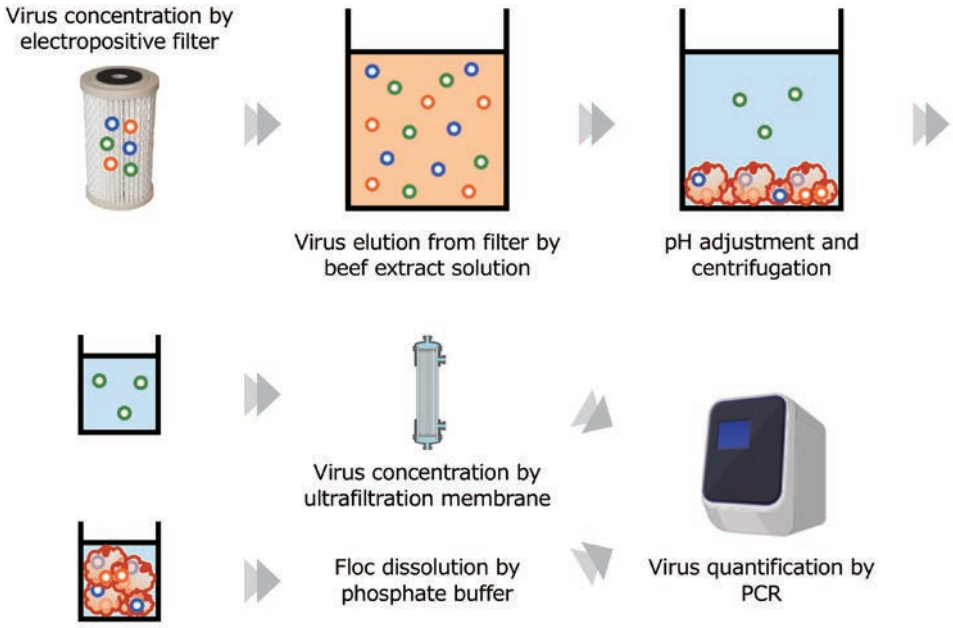

Figure 1 Schematic diagram of a novel virus concentration method using a combination of an electropositive filter and an ultrafiltration membrane.

PMAxx-Enhancer-PCR, which combines PMAxx, a newly improved version of PMA, and PMA Enhancer for Gram Negative Bacteria, was used and optimized the type and concentration of photoreactive intercalating dyes, reaction time, and duration of visible light irradiation, to improve the ability of the viability PCR to discriminate between infectious and inactivated viruses. In addition, to effectively concentrate a wide variety of viruses from large volumes of water samples, we developed a novel virus concentration method (a method combining an electropositive filter and a tangential-flow ultrafiltration membrane; Figure 1). By combining PMAxx-Enhancer-PCR and the developed virus concentration method, we were able to investigate the occurrence of pathogenic viruses (i.e., adenoviruses, astroviruses, noroviruses, sapoviruses, enteroviruses, parechoviruses, hepatitis A virus, hepatitis E virus, and rotaviruses: all nine viruses listed in the WHO *Guidelines for Drinking-water Quality* as pathogenic viruses transmitted through drinking water[1]) in drinking water sources all over Japan, and discuss the presence or absence of infectious viruses based on the integrity of the viral capsid. Indeed, adenovirus, human noroviruses GI, and rotavirus present in drinking water sources tended to have damaged capsids and to be inactivated by damaging the viral capsid. In contrast, astrovirus, human norovirus GII, and enteroviruses present in drinking water sources tended to have intact capsids and to be potentially infectious. We also found that pepper mild mottle virus was ≥100 times more abundant than pathogenic viruses (Figure 2a), and that pepper mild mottle virus is highly likely to present in an infectious without damage to its viral capsid, making it the usefulness of pepper mild mottle as a target virus to determine the virus reduction efficiencies in actual drinking water treatment plants.

Investigation of virus reduction efficiencies in actual drinking water treatment plants

We focused on pepper mild mottle virus and demonstrated that pepper mild mottle virus appears to be a potential surrogate for pathogenic viruses such as adenovirus, norovirus, sapovirus, and enteroviruses in the conventional drinking water treatment processes, coagulation-sedimentation–rapid sand filtration processes, and in next-generation water purification technologies, coagulation–microfiltration processes, through lab-scale virus-spiking experiments[2]-[4]. In addition, we found that the developed virus concentration method using a combination of an electropositive filter and a tangential-flow ultrafiltration membrane can effectively concentrate pepper mild mottle virus from water samples of ≥1,000 L. By focusing on pepper mild mottle virus and applying the developed virus concentration method, we were able to investigate the reduction efficiencies of indigenous pepper mild mottle virus in multiple actual drinking water treatment plants with different treatment processes. Indeed, the concentrations of indigenous pepper mild mottle virus in raw and treated water samples were always above the quantification limit of the PCR assay. We therefore were able to determine the reduction ratios of pepper mild mottle virus: 0.9–2.7-$\log_{10}$ in full-scale coagulation-sedimentation–rapid sand filtration processes and 0.7–2.9-$\log_{10}$ in full-scale coagulation–microfiltration processes (the reduction ratios at Plant A and B were 1.0 ± 0.3-$\log_{10}$ and 2.2 ± 0.6-$\log_{10}$, respectively; Figure 2b, c)[5].

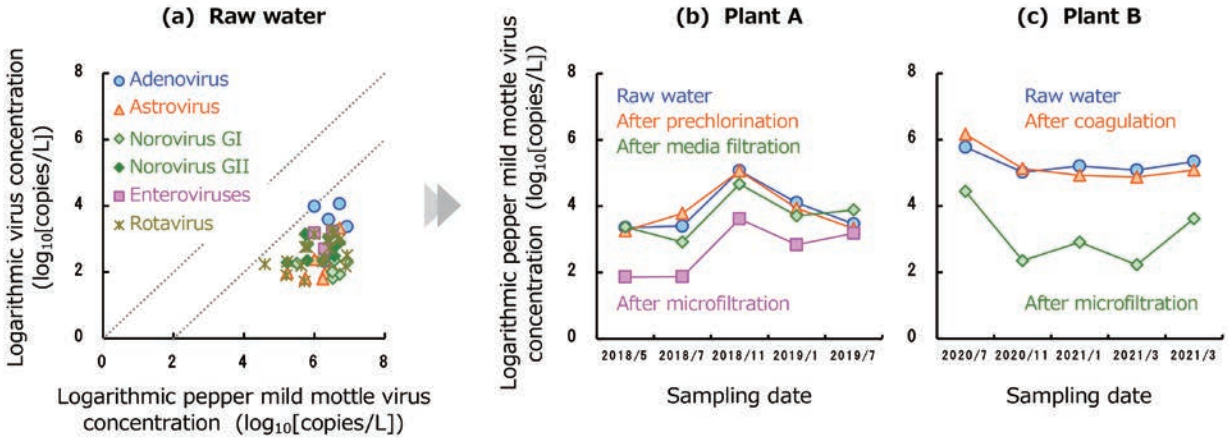

Figure 2 Relationship between the concentrations of indigenous pepper mild mottle virus and pathogenic viruses in drinking water sources (a), and concentrations of indigenous pepper mild mottle virus in raw and treated water at Plants A (b) and B (c). Virus concentrations were determined by PCR.

Investigation of reduction efficiencies of human norovirus in drinking water treatment processes

For human noroviruses, which are difficult to culture, we successfully evaluated the removal efficiencies of human norovirus particles in the coagulation-sedimentation–rapid sand filtration processes, by applying recombinant human norovirus VLPs, which were prepared using the genome sequence of human norovirus and a baculovirus-silkworm protein expression system (Figure 3). Approximately 3-$\log_{10}$ removals were observed for human norovirus VLPs in the coagulation-sedimentation–rapid sand filtration processes[6]. In addition, to increase the sensitivity of VLP quantification, we developed an immuno-PCR (a method combining antigen-antibody reaction and DNA tag quantification by PCR assay; Figure 3) that is 1,000 times more sensitive than the conventional enzyme-linked immunosorbent assay. By combining VLPs and the developed immuno-PCR, we were able to evaluate the removal efficiencies of human norovirus particles in membrane filtration processes. Whereas microfiltration processes with a nominal pore size of 0.1 μm could not remove human norovirus VLPs, approximately 4-$\log_{10}$ removals were obtained by ultrafiltration processes with a molecular weight cutoff of 1 kDa. In addition, >4-$\log_{10}$ removals of human norovirus VLPs were achieved by a combination of coagulation and microfiltration, i.e., coagulation–microfiltration processes[7]. To the best of our knowledge, this is the first study assessing the efficacy of drinking water treatment processes for the removal of human norovirus particles through lab-scale experiments by applying VLPs without waiting for the establishment of an effective *in vitro* cell-culture system for human norovirus.

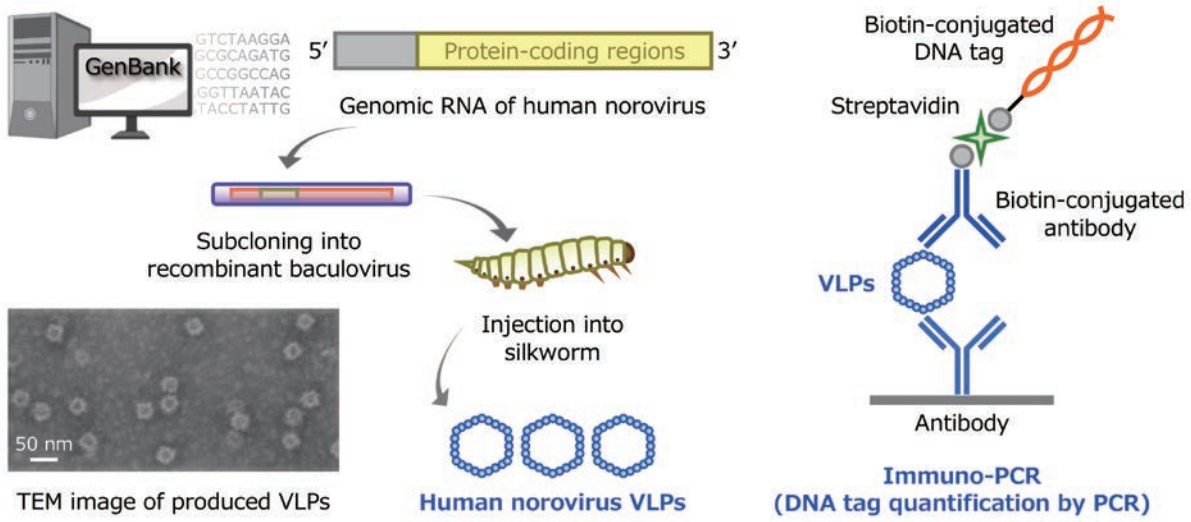

Figure 3 Schematic diagrams of preparation of human norovirus VLPs and VLP quantification by an immuno-PCR.

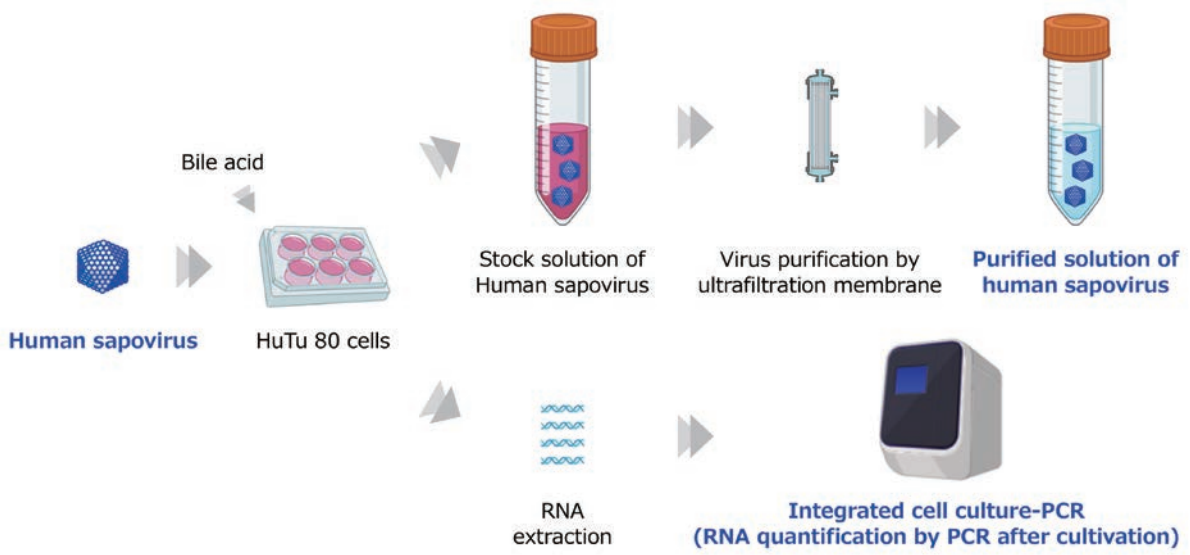

Figure 4 Schematic diagrams of preparation of purified human sapovirus solution and human sapovirus quantification by an integrated cell culture-PCR.

Investigation of reduction efficiencies of human sapovirus in drinking water treatment processes

For human sapoviruses, which were difficult to culture and belong to the same Caliciviridae family as human noroviruses, an *in vitro* cell-culture system using commercially available cell lines and bile acid was discovered in 2020. We prepared the purified solution of human sapovirus (Figure 4) containing virus concentration high enough to conduct lab-scale virus-spiking experiments, and developed an integrated cell culture-PCR (a method combining cell culture and DNA/RNA quantification by PCR assay ; Figure 4) that can quantify the infectivity of human sapoviruses, by applying an *in vitro* cell-culture system. By combining the purified solution of human sapovirus and the developed integrated cell culture-PCR, we were able to evaluate the removal efficiencies of human sapovirus in coagulation-sedimentation–rapid sand filtration processes and membrane filtration processes as well as the inactivation efficiencies of human sapovirus in free-chlorine disinfection processes. In the coagulation-sedimentation–rapid sand filtration processes and the coagulation–microfiltration processes, human sapovirus removals of approximately 2–3-$\log_{10}$ and >4-$\log_{10}$, respectively, were observed[4]. When the efficacy of chlorine treatment was examined by using the developed integrated cell culture-PCR, approximately 4-$\log_{10}$ inactivation of human sapovirus was observed at a CT value (free-chlorine concentration [C] multiplied by contact time [T]) of 0.02 mg-Cl_2·min/L[4]. To the best of our knowledge, this is the first study assessing the efficacy of drinking water treatment processes for the removal and inactivation of human sapovirus through lab-scale experiments by applying an *in vitro* cell-culture system for human sapovirus.

Conclusions

We investigated the occurrence of pathogenic viruses in drinking water sources and their reduction efficiencies in drinking water treatment processes by applying novel virus quantification and concentration methods developed in the present study.

The improved and optimized viability PCR, i.e., the PMAxx-Enhancer-PCR, can determine the presence or absence of viral infectivity quickly and easily (in a few hours), without the use of cell culture. The novel virus concentration method, which can effectively concentrate a wide variety of viruses from a large volume of water samples, can be applied to various types and volumes of water samples, including environmental water and treated drinking water. Therefore, the evaluation method for the presence of infectious pathogenic viruses in environmental water using the PMAxx-Enhancer-PCR and the novel virus concentration method has the potential to be widely used as a method that does not depend on cell-culture methods.

By focusing on pepper mild mottle virus and applying the novel virus concentration method, it is possible to evaluate virus treatability in various actual drinking water treatment plants with different raw water quality, treatment processes, treatment capacity, etc., thereby providing evidence for the safety of drinking water against pathogenic viruses. This approach has the potential to contribute to the establishment of a framework for risk management and control of pathogenic viruses in sustainable drinking water use and the water cycle.

VLPs do not require virus culture using host cells and can be produced in large amounts based on the viral genome

sequence, making them applicable to viruses for which an effective *in vitro* cell-culture system has not yet been established as long as the genome sequence data is available. With the rapid development of genome analysis technology, the metagenomic analysis of viruses in water environments will accelerate in the future, and the prevalence of a wide variety of pathogenic viruses in various water environments around the world will become clear, and their genome sequence data will be accumulated in databases. VLPs are morphologically and antigenically the same as native virus particles, but do not have any genes. Therefore, by applying the new method that combines VLPs and the immuno-PCR, it is possible not only to clarify the treatability of difficult-to-culture pathogenic viruses in drinking water treatment processes, but also to produce VLPs of various virus species, genotypes, and strains, which will provide many findings, such as the differences in behaviors of viruses during drinking water treatment processes among genotypes and strains, and the elucidation of genetic factors (e.g., differences in the amino acids that make up proteins) that affect the differences in behaviors of viruses. The combined use of VLPs and the immuno-PCR has the potential to be used not only for drinking water treatment, but also for understanding the treatability of difficult-to-culture pathogenic viruses in wastewater treatment and water reclamation treatment, clarifying the treatment mechanism, and clarifying the behaviors of difficult-to-culture pathogenic viruses in environmental water.

By applying the purified solution of human sapovirus and the integrated cell culture-PCR, it is possible not only to clarify the treatability of human sapoviruses in various water treatment processes, but also to isolate new strains of human sapoviruses from water samples, develop new, rapid, and easy methods for the quantification of human sapoviruses, the identification of infection receptors, and the development of new disinfectants, vaccines, and infection inhibitors. Therefore, it has cross-disciplinary development potential not only in the field of water environment, but also in the fields of medicine and pharmacology.

References

[1] WHO (World Health Organization), *Guidelines for Drinking-water Quality, fourth ed., incorporating the first addendum.* World Health Organization, Geneva, Switzerland, 2017.

[2] Shirasaki, N., Matsushita, T., Matsui, Y. and Murai, K. Assessment of the efficacy of membrane filtration processes to remove human enteric viruses and the suitability of bacteriophages and a plant virus as surrogates for those viruses. *Water Research* 115: 29-39, 2017.

[3] Shirasaki, N., Matsushita, T., Matsui, Y. and Yamashita, R. Evaluation of the suitability of a plant virus, pepper mild mottle virus, as a surrogate of human enteric viruses for assessment of the efficacy of coagulation-rapid sand filtration to remove those viruses. *Water Research* 129: 460-469, 2018.

[4] Shirakawa, D., Shirasaki, N., Hu, Q., Matsushita, T., Matsui, Y., Takagi, H. and Oka, T. Investigation of removal and inactivation efficiencies of human sapovirus in drinking water treatment processes by applying an *in vitro* cell-culture system. *Water Research* 236: 119951, 2023.

[5] Shirakawa, D., Shirasaki, N., Matsushita, T., Matsui, Y., Yamashita, R., Matsumura, T. and Koriki, S. Evaluation of reduction efficiencies of pepper mild mottle virus and human enteric viruses in full-scale drinking water treatment plants employing coagulation-sedimentation-rapid sand filtration or coagulation-microfiltration. *Water Research* 213: 118160, 2022.

[6] Shirasaki, N., Matsushita, T., Matsui, Y., Oshiba, A. and Ohno, K. Estimation of norovirus removal performance in a coagulation-rapid sand filtration process by using recombinant norovirus VLPs. *Water Research* 44(5): 1307-1316, 2010.

[7] Matsushita, T., Shirasaki, N., Tatsuki, Y. and Matsui, Y. Investigating norovirus removal by microfiltration, ultrafiltration, and precoagulation-microfiltration processes using recombinant norovirus virus-like particles and real-time immuno-PCR. *Water Research* 47(15): 5819-5827, 2013.

Dr. SHIRASAKI Nobutaka

Associate Professor,
Division of Environmental Engineering,
Faculty of Engineering,
Hokkaido University

Development of in Situ Continuous In-Flow Microplastic Monitoring Techniques Using Spectroscopic Techniques

TAKAHASHI Tomoko

Microplastics are serious pollutants in marine environments, and it is essential to know the distribution and composition of microplastics on local and global scales, as well as the temporal dynamic change, for a better understanding of pollution. However, very little data in deep waters is currently available due to the difficulty in accessibility. In addition, distributions/amounts of small plastics with a size of <100μm are not well known due to the limitation of measurement techniques. Aiming to monitor microplastics in water continuously, we have developed a novel in situ deep-sea analyser of marine particles by integrating holography and Raman spectroscopy. In addition, using coherent anti-Stokes Raman scattering(CARS), the classification of in-flow microplastics and other natural particles with a size of <100μm has been successfully demonstrated. The methods being developed in this research will enable continuous measurements of microplastics at much higher spatial and temporal scales than what is possible with the current methods and so allow for tracking dynamic variations of microplastics in terms of types, number densities and distributions.

Introduction

In recent years, pollution of marine environments by microplastics has become a global environmental issue and has come to the attention not only of researchers but also the wider public. Microplastic particles are transported all over the oceans like natural particles and are becoming a serious threat to various marine organisms[1]. As the density of plastic debris in the ocean has been selected as an indicator of the Sustainable Development Goals set by the United Nations for the year 2030[2], it is a global urgent task to understand dynamic temporal and spatial distributions of microplastics for a long-term scale.

Typically, the surveys of microplastics in the ocean are conducted by manually collecting and analysing samples in the laboratory. Microplastics on the sea surface are often collected using nets deployed from ships. The net mesh size of ~100 μm is typically used to collect samples as otherwise the nets are easily clogged. However, smaller microplastics can cause more serious impacts on marine animals[3], and measurement techniques for these smaller particles are required. Plastic surveys in deeper water layers are also a challenging task. Particles in the water column are typically collected by filtering sampled water in situ or on board or using sediment traps, as it is difficult to tow a net at a constant depth in the water column. Still, little is known about the distribution of microplastics in deep waters compared to the sea surface, as the sampling chances in deep waters are limited due to difficulty in accessibility.

In situ underwater measurement techniques have a large potential to increase survey efficiency. Conventional in situ techniques for marine particles use imaging for zooplankton and fluorescence analysis for phytoplankton detection. While the morphological or specific chemical (e.g. chlorophyll) information can be obtained in a non-contact manner using these devices, there are currently few methods that can directly measure the general chemical compositions to identify microplastics in water among other particles. Therefore, while it is crucial to survey the dynamic spatial and temporal changes of microplastics to understand the current situation of the pollution, methods for the surveys, particularly of the particles in the deep water column and with a size of <100 µm have not been established.

In our work, continuous non-contact, label-free and real-time monitoring methods of microplastics in water are developed by applying Raman spectroscopic-based and imaging techniques. The research consists of two topics:

1. Development of the in situ deep-sea marine particle analyser

2. Classification of microplastics by applying coherent anti-Stokes Raman scattering (CARS)

Development of the in situ deep-sea marine particle analyser

Digital in-line holography is a volumetric imaging technique that can take monochrome images of suspended particles by analysing interference patterns created by the collimated laser beam and scattered light at a suspended particle. While this has been widely applied to the imaging of underwater planktonic animals, it has been reported that 30 – 70 % of marine particles are not able to be identified only by morphological characteristic[4]. In our work, Raman spectroscopy, a molecular analytical technique that also observes scattered light directed at an object with shifted wavelengths due to molecular vibration/rotation/stretching modes, has been efficiently combined with holography to enable fast particle identification with both morphological and chemical information in a single, large-volume channel using a compact setup[5].

The laboratory setup is shown in Figure 1 (a). The measurement process is the following: a 20 cm measurement cell where the water flows using a pump is constantly illuminated using a collimated laser beam. Using the beam, holographic images are captured at a high frame rate (several tens of Hz) to detect a particle. When a particle is detected, the pump stops to trap the particle and a Raman measurement is initiated using a laser beam at the same beam path as holography. After the Raman measurement, which typically takes several to several tens of seconds, the pump and holographic imaging start again to wait for the next particle. The advantages of this measurement method are that both image and chemical information of particles can be taken in a large volume of water; the whole process can be fully automated; and the system is compact and simple without a filter or mesh to collect particles, which does not require frequent maintenance and is ideal for a long-term in situ deployment. Using a laboratory setup, different plastic pellets and representative marine particles (i.e. polypropylene (PP) pellet, polyethylene (PE) pellet, PE fragment collected from the sea, zooplankton, foraminifera), were measured, as shown in Figure 1 (b). Both holographic images and Raman spectra were successfully obtained for each particle.

The 3000 m depth-rated in situ device, called “RamaCam”, as shown in Figure 2 was developed and deployed at a water depth of 1000-2000 m during the research cruise of KM24-03 conducted by the research vessel (R/V) Kaimei, and KS-24-11 conducted by the R/V Shinseimaru, in 2024. While the detailed data analysis obtained during the cruises is ongoing, automatic holography and Raman measurements of marine particles in the deep water were successfully performed for the first time using the device.

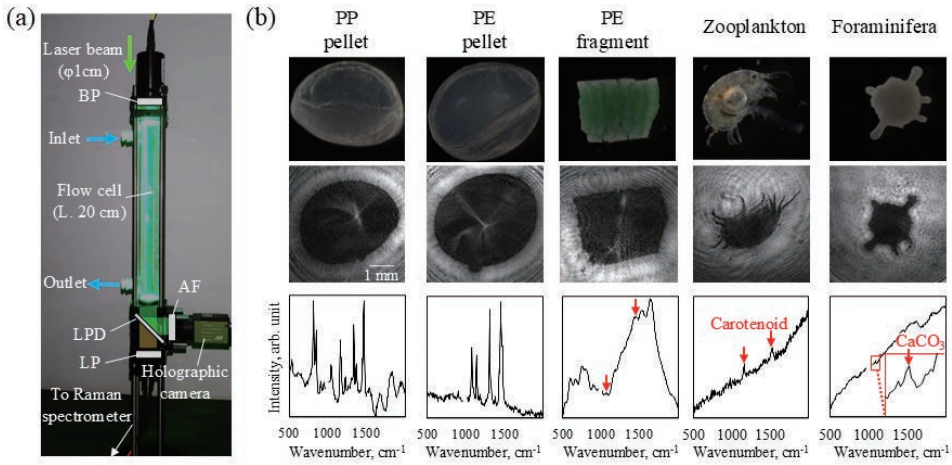

Figure 1 (a) Experimental setup of the integrated system of holography and Raman spectroscopy and (b) the data obtained for typical marine particles using the setup. BP: bandpass filter; LPD: long-pass dichroic filter; LP: longpass filter; AF: attenuation filter.

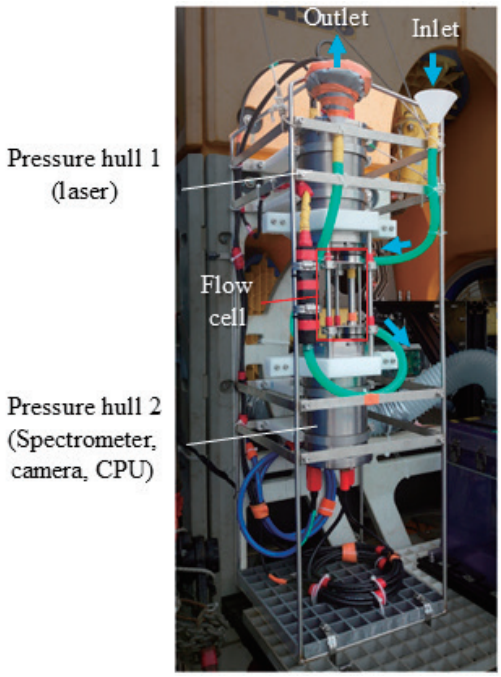

Figure 2 Deep-sea in situ marine particle analyser.

Particle classification method using images and spectra

For the interpretation of multimodal data obtained from the setup of the integrated holography-Raman spectroscopic analyser, a data fusion analysis of images and spectra was developed[6]. While data fusion applications have been expanded to a wide range of multi-sensory data analysis[7], the previous methods have not been applied to the identification of marine particle types/materials due to the limitation of multiple sensory applications to analyse particles. We investigated autoencoder-based unsupervised feature learning approaches to group the different particle types. Autoencoders are a generic type of unsupervised feature learner that has been well-established for analysing imagery, including holographic images[8]. They consist of an encoder network, which reduces the input data down to smaller latent representations, and a decoder network that attempts to reconstruct the original data from the compressed latent representation. The latent representations, through optimising both networks to minimise the difference between the original inputs and their reconstructions, can be used as features for clustering and classification tasks[9]. A key advantage is that they are unsupervised and can flexibly manage different sizes and dimensionality of data inputs as well as the size of the latent feature space representations they output, without significant modification of their underlying form, which is suitable for multimodal data[7]. Figure 3 illustrates the proposed multimodal holographic image and Raman spectrum feature learning. For holographic images with a large data size (227 × 227 pixels, downsized from the original image size prior to the feature learning to reduce the computational time), a convolutional autoencoder, which can handle a complex dataset was used to extract features.

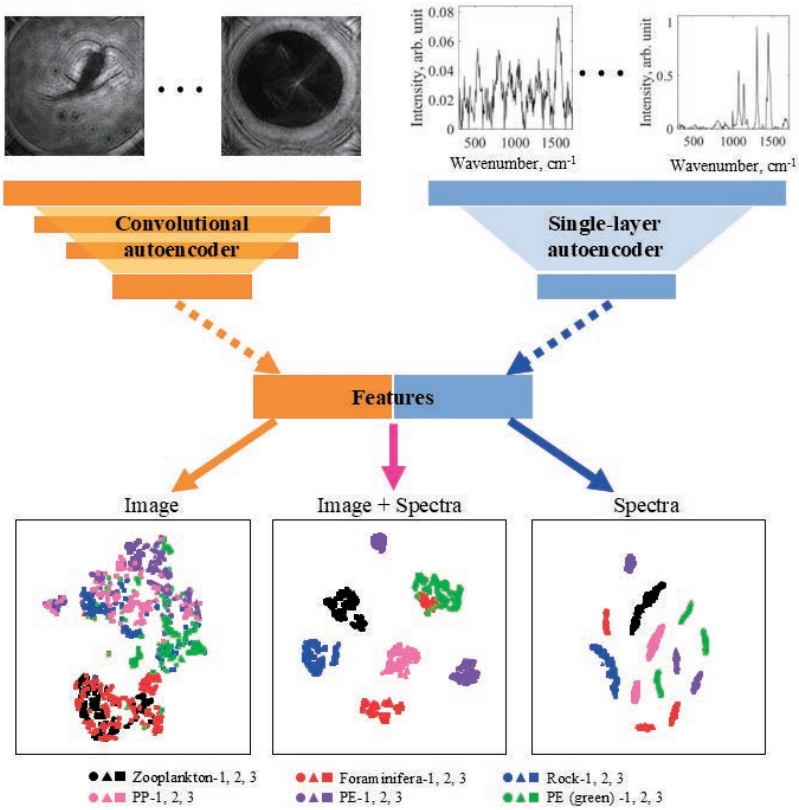

Figure 3 Classification algorithms using features extracted from holographic images and Raman spectra and the t-SNE visualisation of features extracted from holography (left), blended features (middle), and extracted from Raman spectra (right).

For Raman spectra with a small data size (309 × 1 pixels) compared to images, a simple single-layer autoencoder was used. The extracted latent representations from each image and spectra were blended using the t-distributed stochastic neighbour embedding (t-SNE), a method to non-linearly reduce the dimensions of the data to two.

The classification was performed for the data of six typical marine particles (three different individuals per type) taken using the laboratory setup introduced in the previous section. As seen in Figure 3, only two main clusters were formed when only holographic images were used, while too many clusters were formed when only Raman spectra were used for classification. This might be because some types of particles are morphologically too similar to distinguish each other, while the features of Raman spectra pick the difference between individuals. When the combined features were used, the classification accuracy was enhanced by 44 % compared to the accuracy obtained through the analysis only of holographic images or Raman spectra.

Classification of microplastics by applying CARS

Although the device introduced in the previous section is a novel and powerful tool to identify marine particles in situ in the ocean, the measurable size is limited to >1 mm due to the weak Raman scattering light. The diameter of the collimated beam is ~1 cm to scan a large volume of water without filtering, while this can be a disadvantage for Raman spectroscopy as the laser power density at a target is weak, which linearly affects the intensity of the Raman scattering light.

To monitor smaller particles, particularly with a size of <100 µm, we applied CARS to the measurement of flowing particles as a proof of concept[10]. CARS is an advanced Raman spectroscopic-based method where a specific Raman scattering is enhanced by two laser beams with a wavelength difference equal to the wavelength of the scattering light. In the field of biomedical science, CARS is known as a technique for non-destructive and high-speed analysis of living cells, including in-flow measurements in microfluidic devices[11]. While CARS is promising for measuring suspended particles in water, few studies using CARS to aim at continuous monitoring of microplastics in natural environments have been reported, possibly because of strict flow control to align a wide size range of particles in a microfluidic device. We demonstrated the detection of in-flow microplastics with wide size ranges in a relatively large channel (500 µm depth) to avoid clogging by proposing reconstruction analysis of two-dimensional CARS line scanning with a wide view (0.5 mm width, 1.6 times wider than typically used views for CARS images). Selective detection of polystyrene (PS), Poly(methyl methacrylate) (PMMA), and low-density polyethene (LDPE) beads with the size of several tens to hundreds of µm flowing and with the speed of 4 mm/s was successfully performed when the CARS signals of the corresponding frequencies (3050 cm^{-1} for PS, 2940 cm^{-1} for PMMA, and 2840 cm^{-1} for LDPE) was detected as shown in Figure 4 (a) and (b). With this method, the number density and diameters of flowing particles can be calculated. We also demonstrated the classification of flowing microplastics (PMMA) and bio-organic particles (algae) by taking CARS and two-photon excited autofluorescence (TPEAF) signals simultaneously.

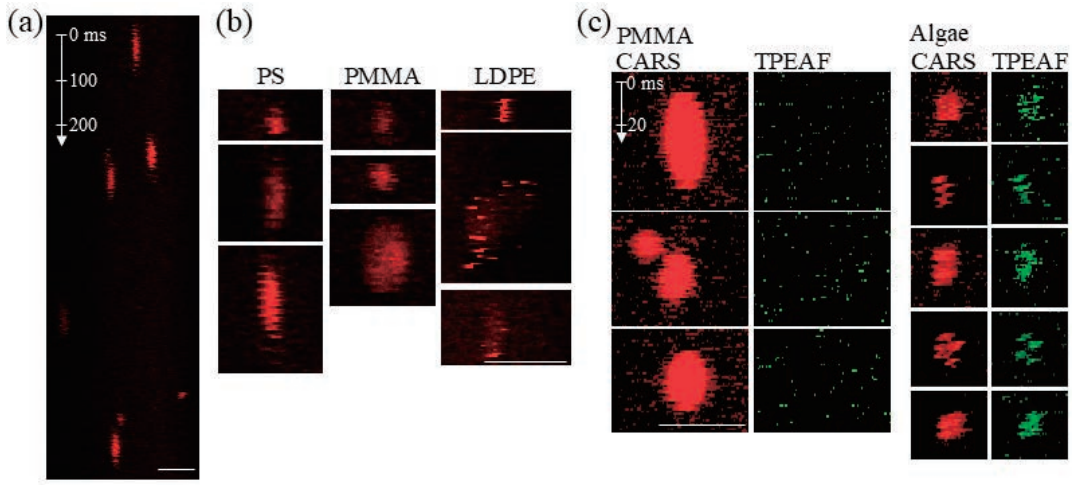

Figure 4 (a) Example of CARS images of PS beads in flow. (b) Zoomed CARS images of different microplastics detected with the corresponding frequencies. The scale bars indicate 100 µm. (c) CARS (red) and TPEAF (green) signals for PMMA and alga particles in flow. The scale bar indicates 50 µm. The scan speed and direction are indicated in (a) and (c). Adapted with permission from Ref [10]. *© 2021 American Chemical Society.*

The average intensity of both PMMA and alga particles in the CARS signals at the frequency for C-H bonds (2940 cm^{-1}) was higher than the background level, while only algae emit TPEAF signals because of the existence of chlorophyll. Classification of PMMA and alga particles in flow has been successfully performed by simultaneous detection of CARS and TPEAF signals, as shown in Figure 4 (c).

Conclusions

In this paper, we first reported the development of the integrated device of Raman spectroscopy and holography for in situ deep-sea particle measurements. Different marine particles, including plastic pellets with a size of ~1 mm, were successfully identified using the laboratory setup. The classification algorithm of marine particle types using both holographic images and Raman spectra was also proposed. In 2024, the in situ device was developed and deployed in the sea, and fully automated in situ measurements of marine particles were successfully performed at the water depth of 1000-2000 m. Secondly, for measurements of smaller microplastics with a size of <100 μm, a method based on CARS was reported. In-flow microplastics and bio-organic particles (algae) were successfully detected and classified by simultaneous detection of CARS and TPEAF signals.

This research opens new possibilities for monitoring of microplastics. Measurements that are currently made manually by sampling will be performed in situ and continuously. With the method being developed in this research, the efficiency of surveys of microplastics in the ocean can significantly be increased, which will be game-changing for future surveys. Acquisition of global-scale chemical data on microplastics with high spatial and temporal resolution will be possible, which will lead to the accurate estimation of microplastic pollution. It is hoped that this will also feed back into the public awareness for the protection of our oceans and the establishment of government policies.

References

[1] Andrady, A. L. "Microplastics in the marine environment." *Marine pollution bulletin* 62, pp. 1596-1605, 2017.

[2] United Nations General Assembly, "Work of the Statistical Commission Pertaining to the 2030 Agenda for Sustainable Development, "A/RES/71/313 (United Nations, 2017).

[3] Ašmonaitė, G and Almroth, B. C. "Effects of Microplastics on Organisms and Impacts on the Environment." *Goteborgs Universitet* pp. 1-70, 2018.

[4] Silva, N. L., Marcolin, C. R. and Schwamborn, R. "Using image analysis to assess the contributions of plankton and particles to tropical coastal ecosystems." *Estuarine, Coastal and Shelf Science* 219, pp. 252-261, 2019.

[5] Takahashi, T., Liu, Z., Thangavel, T., et al. "Identification of microplastics in a large water volume by integrated holography and Raman spectroscopy", *Applied Optics* 59, pp. 5073-5078, 2020.

[6] Takahashi, T., Liu, Z., Thangavel, T., et al. "Multimodal image and spectral feature learning for efficient analysis of water-suspended particles", *Optics Express* 31, pp. 7492-7504, 2023.

[7] Bayoudh, K., Knani, R., Hamdaoui, F. and Mtibaa, A. "A survey on deep multimodal learning for computer vision: advances, trends, applications, and datasets", *The Visual Computer*, pp. 1–32, 2021.

[8] Zeng, T., Zhu, Y. and Lam, E. Y. "Deep learning for digital holography: a review," *Optics Express* 29, pp. 40572–40593, 2021.

[9] Bank, D., Koenigstein, N. and Giryes, R. "Autoencoders," arXiv, arXiv:2003.05991, 2020.

[10] Takahashi, T., Herdzik, K. P., Bourdakos, K. N., et al. "Selective imaging of microplastic and organic particles in flow by multimodal coherent anti-stokes Raman scattering and two-photon excited autofluorescence analysis", *Analytical Chemistry* 93, pp. 5234-5240, 2021.

[11] Hiramatsu, K., Ideguchi, T., Yonamine, Y., et al. "High-throughput label-free molecular fingerprinting flow cytometry." *Science Advances* 5, eaau0241, 2019.

Dr. TAKAHASHI Tomoko

Researcher,
Marine Biodiversity and Environmental Assessment Research Center,
Research Institute for Global Change,
Japan Agency for Marine-Earth Science and Technology

Development of Boron-Doped Diamond Electrodes for Key Analytes in the Aqueous Environment and Beyond

Tania Louise READ

Dissolved oxygen and pH are two of the most important factors in analytical science, affecting processes in the environment and beyond. Given their impact their importance is twofold, firstly their measurement is key to understanding the condition of a given environment, and secondly their control aids in managing the health and quality of those environments for example, the toxicity of potential pollutants such as heavy metals with pH dependent availability. Electrochemistry offers a relatively simple, cheap, and clean analytical method however, conventional electrode materials often struggle with long-term in situ measurements due to fouling, chemical, or physical degradation. Herein, we exploit the robust properties of Boron Doped Diamond electrode materials to explore methods of analysis and in situ control of key environmental analytes such as oxygen, pH, and heavy metals. Negating the need to remove and chemically alter samples before analysis.

Introduction

Although in the modern analytical science world we are able to measure countless aqueous species via an array of techniques, each important in its own way to a given field of interest, dissolved oxygen and pH are perhaps two of the most widely important analytes of interest. Dissolved oxygen is unequivocally key to the existence of life on our planet, and thus it can be of no surprise that its quantitation is vital in fields from the aqueous environment, to healthcare, and from agriculture all the way through the chain to the food and drinks industry[1],[2]. Furthermore, life and the environment exist in a finely balanced homeostasis of which pH forms a key pillar that when disturbed can have devastating results[3]. Not only is the pH value itself important, but its influence on the speciation and complexation of other key analytes (e.g. heavy metals) can change their bioavailability and thus impact the toxicity of a system[4]. Whilst technologies exist to measure each of these analytes, the sheer breadth of conditions and matrices under which measurement is necessary and range of relevant concentrations necessitates continued development and innovation. For many applications existing technologies suffer drawbacks such as long-term measurement stability, fragility, corrosion, size, and (bio)fouling. Under potentially changeable environmental conditions subtle changes in e.g. pH may cause release of, and therefore increased toxicity of heavy metals[5], it is therefore important to measure both their available and total concentrations; normally achieved by removal and acidification of samples thus prohibiting in situ and continuous monitoring[6]. One of the most commonly used analytical

tools in this field is electrochemistry, appealing due to its potential for sensitive, selective, low cost, and easy to use sensing. The body of research highlighted herein aims to combat some of these drawbacks through exploring the use of high-quality Boron Doped Diamond (BDD) for electrochemical control of pH and for the measurement of key environmental analytes[7]-[9]. The superior electrode qualities of BDD have generated much interest in the electrochemistry field over the past few decades, such as chemical and thermal stability, low biofouling, ability to in situ electrochemically clean, low background currents etc[10]-[13]. These same qualities are what give the BDD sensors much potential for solving some of the issues experienced by those interested in measuring dissolved oxygen, pH and pH dependent systems, such as heavy metals. Firstly, this work takes advantage of the robustness of BDD at extreme potentials to explore the ability to control the local pH environment of the measurement electrode[7],[8]; For traditional electrode materials such as gold, or sp^2 carbon (e.g. glassy carbon, screen printed carbon) it is not possible to work at these extremes of potential without causing damage (corrosion) to the electrode surface over time. The resistance to corrosion afforded by the sp^3 bonded structure of BDD offers considerable advantage; in the research highlighted here we demonstrate the use of electrochemical water splitting to produce and control proton concentration at a generator electrode, in turn influencing the pH environment local to a sensing electrode, where the speciation, and concentration of heavy metals of environmental importance can be assessed. This sensor technology is applied to the detection of heavy metals (here Hg[7] and Cu[8]) in aqueous solutions where the pH is non-ideal for the measurement of interest. The sp^3 bonded nature of BDD which produces these excellent qualities also results in a lack of surface sites required for inner sphere reactions, such as the oxygen reduction reaction (ORR), and is not sensitive to pH. Previous research has demonstrated that through surface engineering via laser machining, controlled incorporation of very robust (corrosion stable) forms of sp^2 carbon into the BDD surface is possible. The quinone surface terminations (BDD-Q) introduced with the sp^2 carbon have been demonstrated in previous work to undergo proton-coupled electron transfer, resulting in a Nernstian (~59 mV/pH unit) shift in the voltammetric peak with changing pH[14],[15]. The work discussed herein expands on this, exploring the use of selective incorporation of these sp^2 carbon regions into BDD to enable the simultaneous detection of both pH and dissolved oxygen in aqueous systems on a single electrode (taking ~4 s)[9]. The possibility of negating reference electrode (RE) drift by implementing an internal-referencing mechanism based on the relationship between the two analytical signals is also explored.

BDD Sensor Design For Electrochemical pH Control

An individually addressable ring-disk electrode system is designed; Ring and disk shaped electrodes are each laser machined out of a wafer of freestanding BDD and placed concentrically, separated and encapsulated by electrically-insulating material such that the electrode faces are co-planar but not touching. The electrochemistry at each electrode is separately controlled via copper wires connected to the BDD through Ohmic sputtered Ti-Au contacts. This arrangement enables the control of local pH through water electrolysis on the ring electrode upon the application of a sufficiently large current, whilst analytical voltammetric measurements of a species of interest can be conducted independently on the disk. The relationship between applied ring-current and resultant local pH at the disk surface were characterised through use of an electrodeposited pH sensitive IrOx film for both applications. Figure 1 illustrates (a) the ring-disk format and (b)

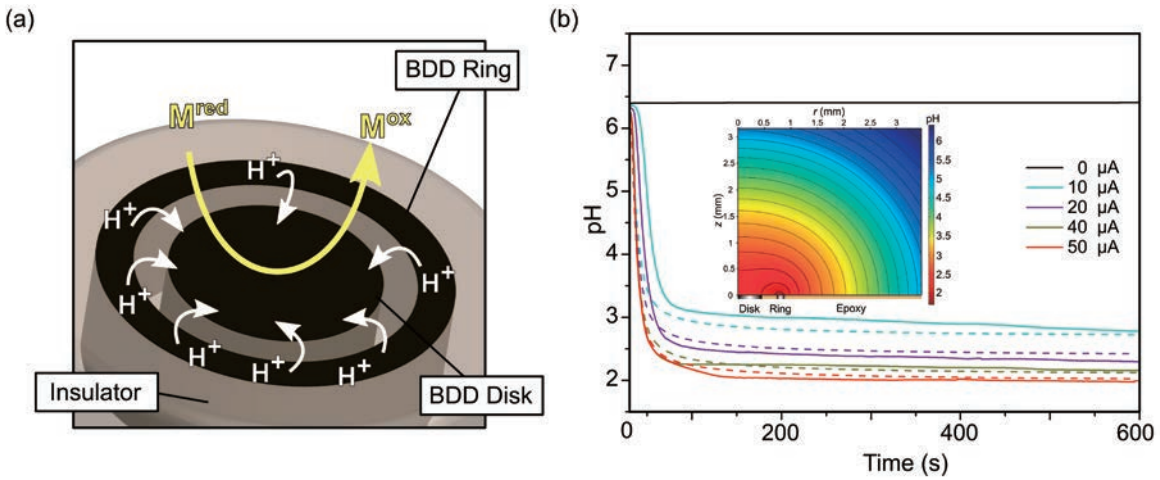

Figure 1 (a) Illustration of the BDD ring-disk design for pH control and simultaneous electrochemical heavy metal analysis.
(b) Comparing simulated (dashed line) and experimental (solid line) data for the pH change generated at different applied ring currents. Inset shows 2D axisymmetric simulation of the pH profile extending into bulk solution.
Figure adapted from [7] *copyright 2014 American Chemical Society.*

experimental data for the pH change associated with different applied ring-currents compared with data produced using finite element methods[7].

Electrochemical Measurement of Hg with simultaneous pH Control

Stripping voltammetry measurements conducted in Hg containing solutions at different bulk pH values, Figure 2(a), demonstrate the effect of pH on the analytical signal. At low pH values, where Hg is completely in the Hg2+ form, a single sharp stripping peak is observed. However, as the pH increases the peak is seen to shift on the potential axis, broadening and decreasing in current magnitude as the Hg speciation changes to less electroactive forms. In Figure 2(b) measurements conducted in bulk pH 6.40 and pH 2.0 solutions are compared to the resulting data when a current is applied to the ring electrode during measurement in bulk pH 6.40 solution. Application of a 50 µA current is expected to result in a pH change to ~pH 2.0 as found in Figure 1(b), here we see the stripping peak transformed from a broad peak at ~0.2 V in bulk pH 6.4 solution to a much sharper peak at ~0.5 V, which is similar to that recorded in bulk pH 2.0 solution. Some shoulder peaks are observable, indicating that the local pH may not have completely reached pH 2.0 at the point of measurement however, this data demonstrates the power of such electrodes for in situ analysis of heavy metals such as Hg in solutions of non-ideal pH without the need for manual acidification.

Controlling Cu speciation and detection with simultaneous pH Control

Copper is another common contaminant in natural water, which can cause issues such as Wilsons Disease when it accumulates in the body[16]. The binding of copper by ligands in water systems or therapeutics can be used to remove it – but this process is also pH dependent. In this work the same ring disk pH control sensor format is applied to measurement and manipulation of the speciation of copper by common therapeutic ligand triethylenetetramine (TETA). The effect of Cu-ligand binding is demonstrated using UV-Vis Spectroscopy in combination with speciation simulations in Figure 3(a), here demonstrating good agreement and a move from free copper to bound systems as pH increases. Electrochemical measurements using the disk electrode to measure in solutions at

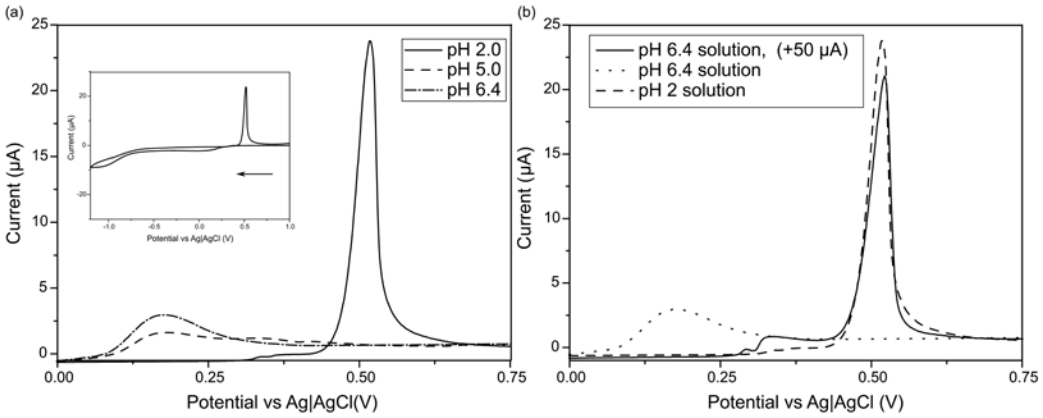

Figure 2 (a) Comparing Hg stripping peaks from cyclic voltammetry at different bulk solution pH values. inset shows full CV and direction of scan. (b) Comparing stripping peaks for Hg in bulk pH 2 and pH 6.4 solutions with that in bulk pH 6.4 solution with 50 µA simultaneously applied to the ring electrode. Figure adapted from [7] *copyright 2014 American Chemical Society.*

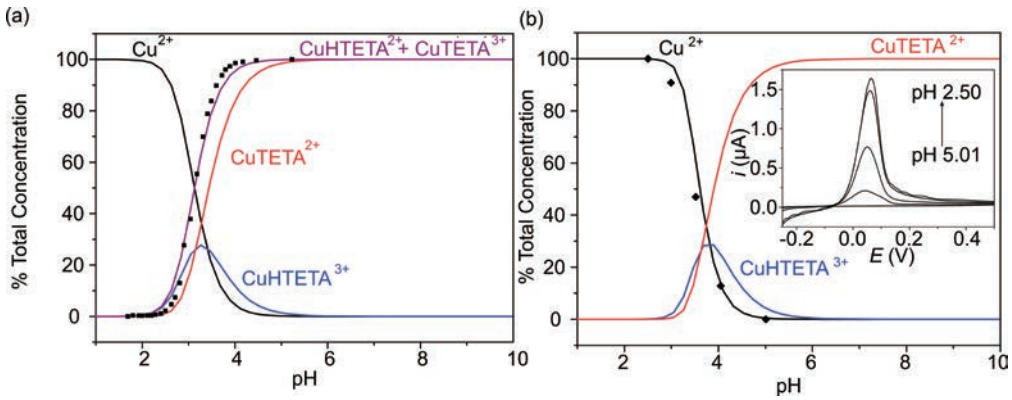

Figure 3 (a) Simulated speciation curves for copper in TETA containing solutions at different pH compared to experimental UV-Vis data (black squares), (b) Copper speciation simulation compared with peak currents (black dots) for electrochemical stripping peaks of Cu in solutions at different pH.
Figure adapted from [8].

chemically adjusted pH values showed good agreement to simulated speciation curves, confirming that the change in binding was observable via electrochemical measurement, Figure 3(b).

Finally, the ring electrode was used to influence the local pH enabling in situ local control over the binding of the copper with simultaneous electroanalysis. The current density applied to the ring is compared to the resultant Cu detection peak current measured on the ring as a percentage of the maximum recorded current (representing complete availability of all copper species) in Table 1; Used in combination with the electrochemical speciation curve in Figure 3(b) it is therefore possible to calculate the local pH generated at each current density. This study further highlights potential of BDD electrodes for control of metal ligand binding and therefore measurement of free and total metal concentrations in complex aqueous systems.

BDD Sensor Design for Electrochemical pH and Oxygen Measurement

The ability to measure pH using BDD based electrode materials with robust laser-induced sp^2 carbon regions (BDD-sp^2) has been demonstrated by researchers in the Macpherson group[14],[15]. Sp^2 carbon also catalyses reactions which require surface interaction and are therefore not measurable by high quality sp^3 diamond carbon surfaces, such as the key environmental analyte dissolved oxygen. This study aimed to assess the use of such sensors for simultaneous pH and oxygen measurement. In order to achieve this it was first necessary to optimize the pattern of sp^2 regions to achieve clear and sensitive electrochemical signals for both analytes (not just pH). Figure 4 presents the three patterns assessed: (a) a microspot array of pits with overlapping diffusional fields akin to a microelectrode array, (b) a single pit of equivalent total machined area to (a), and (c) a microspot array of smaller, diffusionally isolated spots. Cyclic voltammetry was used to assess the electrochemical performance of each, and the resultant

Table 1 Comparing data for the applied current at the ring electrode with electroanalytical response on the disk electrode for Cu detection and the effective local pH change. Table from [8].

Applied Current Density (mA cm^{-2})	% Maximum LSV Peak Current	Generated pH from Speciation Curve
0.10	0	5.01 ≤
0.20	34.98	3.76
0.395	78.92	3.35
1.98	100	≤ 2.50

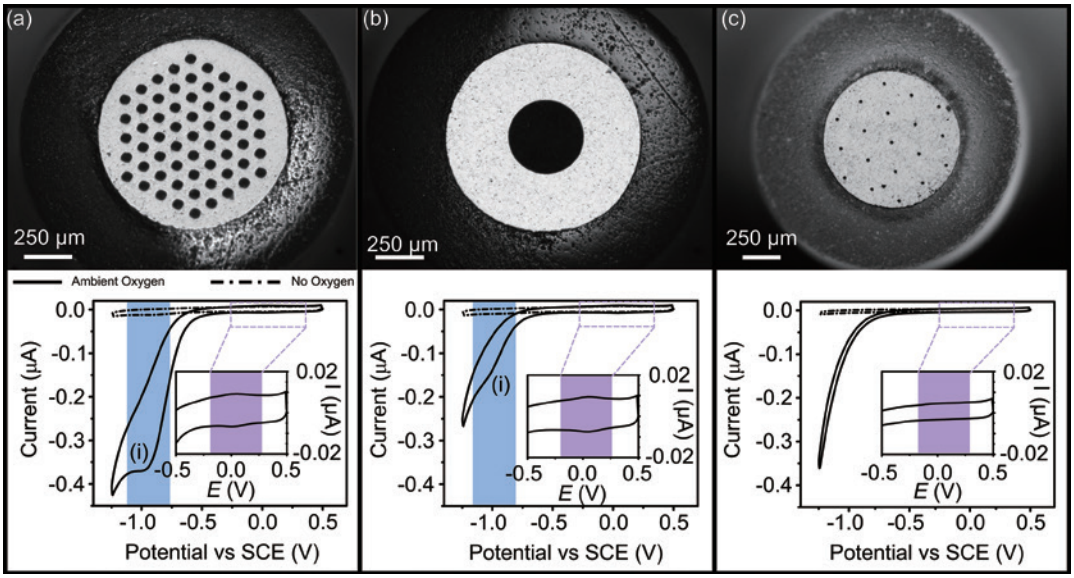

Figure 4 Optical images and cyclic voltammograms comparing BDD electrodes with (a) a microarray of machined spots with diffusional overlap, (b) a single spot of equivalent machined area to (a), and (c) a microspot array with no diffusional overlap and decreased machining area. Cyclic voltammograms show pH signatures (purple highlighted region) and oxygen signatures (blue highlighted region labelled (i)) under ambient and degassed conditions. Figure adapted from [9] *copyright 2019 American Chemical Society.*

data is also presented. For each electrode a clear signal at ~0.1 V associated with the proton coupled electron transfer reaction at quinone surface terminations is observed (purple highlighted regions) as expected based on previous work. It is notable that the signature for (c) whilst present is significantly smaller, which is expected as the lower machined area results in a lower surface coverage of quinone species. For (a) and (b) a signal associated with the reduction of oxygen can also be observed at ~-1.0 V (blue highlighted region, labelled (i)), however this is not present in (c) and is likely masked by the onset of solvent reduction. As the signal for oxygen reduction was found to be larger and more clearly distinguishable from solvent reduction in (a) and no significant difference in pH response was observed this pattern was used for further studies.

Rapid Simultaneous Measurement of Oxygen and pH

For full characterization of simultaneous oxygen and pH response on BDD-sp^2 electrodes, square wave voltammetry was applied as it enables reduction of background currents increasing signal-to-noise and is significantly faster than other voltammetric techniques. Calibration curves were collected for both analytes simultaneously, where the concentration of oxygen in a series of solutions at different pH values was varied using mass flow controllers to change the ratio of oxygen to balance gas (argon). Figure 5 presents an example measurement (centre) with the resultant aggregate mean data from measurements conducted at 5 different pH values in the range 4.00-10.20, with 5 different oxygen values over 0.1-8 mgL^{-1} in each. For both oxygen (blue, left) and pH (purple, right) a clear signature is observed, and calibration plots for each (left and right respectively) are produced demonstrating linear behaviour (R^2 = 0.999 for oxygen and 0.998 for pH). The slope of the pH calibration plot, 60 mV pH^{-1}, is also found to be close to that predicted by the Nernst equation, 59 mV pH^{-1}. Each measurement conducted to produce the calibration plots was obtained in ~4 s, clearly demonstrating the potential of these BDD-sp^2 electrodes for the rapid simultaneous measurement of oxygen and pH in aqueous media.

Potential to Correct for Reference Electrode Drift

As a linear relationship is observed between the aggregate mean oxygen peak current and the mean dissolved oxygen concentration (measured independently via commercial optical dissolved oxygen probe) across the whole pH range assessed, the assumption can be made that the magnitude of the oxygen current response is unaffected by pH over the pH range 4–10. One of the most significant issues for real-world analysis is the necessity for a long-term stable reference electrode, to which the potential at the sensing electrode is compared. However, in real-world systems these reference electrodes often suffer drift due to fouling or other influences thus impacting the accuracy of the measurement and impeding continuous or long-term in situ measurements, particularly when they rely on peak potential as with the proton coupled electron transfer reaction signals used to measure pH here. As the two analytical signals (oxygen and pH) are seemingly independent, the relationship between them has potential to act as an internal referencing mechanism where any reference electrode drift would impact both equally and thus be

Equation 1 $O_2 + 2H^+ + 2e^- \rightarrow H_2O_2$ $pH = 7$ $E^0 = 0.456\ V\ vs\ SCE$

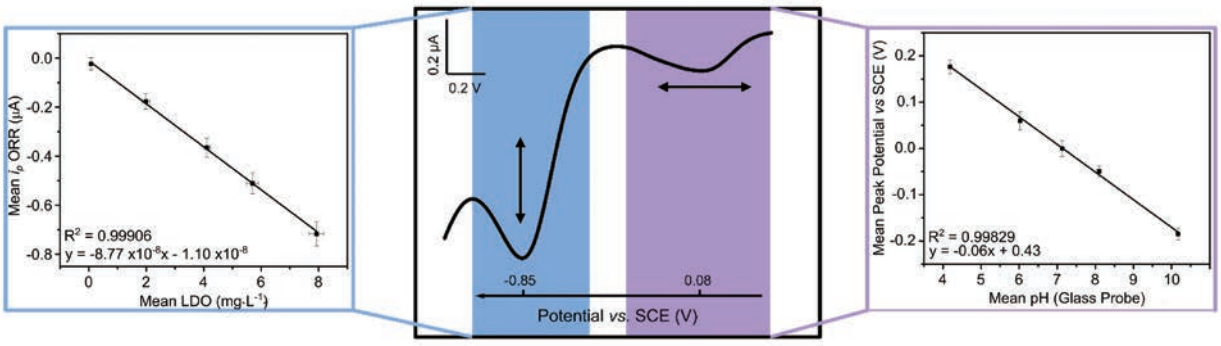

Figure 5 Example measurement of both oxygen (blue) and pH (purple), centre, compared with (left) aggregate mean oxygen calibration data and (right) aggregate mean pH calibration data conducted in solutions at a range of pH and dissolved oxygen concentrations. Figure adapted from [9] *copyright 2019 American Chemical Society.*

negated, a concept first proposed by Wrighton et al.[17]. Although the equation for two electron reduction of oxygen on sp^2 C, Equation 1, indicates the involvement of protons in the reaction, as there are no proton transfer reactions occurring before or in the rate-determining step, the peak position for electron transfer should not be affected[18]-[21].

This is assessed in Figure 6, where the relationship between the pH and oxygen signatures is explored in more detail. The peak potential for oxygen reduction from Figure 5 was analyzed for a statistically significant dependence using a Kruskal–Wallis analysis of variance (ANOVA) and a One-Way ANOVA at a 5 % significance level, with the Bonferroni correction for multiple comparisons. No statistical dependence of the oxygen reduction peak potential was observed for either dissolved oxygen concentration or pH, Figure 6(a) and (b), respectively. Figure 6(c) shows the separation between the pH and oxygen peaks in one measurement, ΔE_p, as a function of dissolved oxygen concentration, at set pH values. ΔE_p can thus be used to inform on solution pH, as shown in Figure 6(d), where a gradient of 57 mV is observed, close to that predicted by Nernst, for a plot of mean ΔE_p for all oxygen concentrations as a function of pH. This highlights the potential for using the ORR signal as an internal reference for voltammetric pH measurements, negating any reference electrode fouling when applied in real world systems.

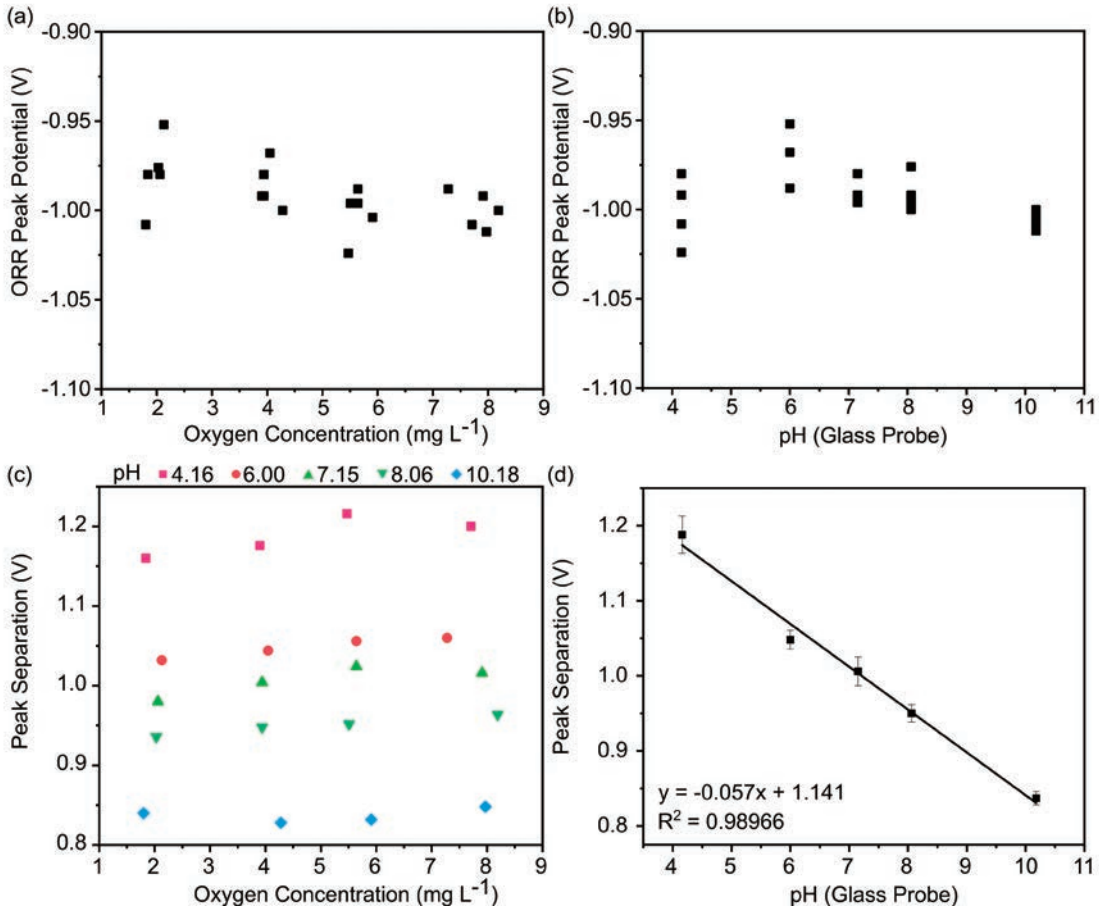

Figure 6 Comparison of oxygen and pH peak parameters to assess the potential for internal referencing. Figure from [9] *copyright 2019 American Chemical Society.*

Conclusion

This manuscript highlights the use of BDD electrodes to improve measurement and local-control of key environmental analytes. We present the first published examples of the use of electrochemical pH control in aqueous systems, and its application to heavy metal detection and speciation control. Firstly, the method is used to electrochemically measure Hg concentrations in solutions of non-ideal measurement pH without manual adjustment of the bulk pH. This technique is subsequently used to control the local speciation of Cu ions in the presence of binding ligands, thus providing a route to assess total and bound concentrations of heavy metals using a single in situ sensor. This work has since inspired further work by unrelated international research groups (see work by e.g. O'Riordan et al on interdigitated electrodes for agricultural, chlorination applications). The ability to control the local pH environment, and therefore speciation of analytes, in a system of interest could offer new approaches to in situ analyses in fields ranging from waste-water treatment and environmental analysis to medicine (e.g. chelation based cancer therapeutics) and human function (e.g. oxygen and hemoglobin interactions). Proof of concept work on the use of high quality laser-modified BDD electrodes for dissolved oxygen and pH measurements is also described; The ability to simultaneously measure both species on a single electrode (as opposed to separate sensing electrodes within a device) offers a route to the reduction of material usage and manufacturing steps, and therefore a potential decrease in the environmental impact of production. Whilst the work described herein proves the initial concept, going forwards assessments of sensor function in a wider range of environmentally relevant conditions and matrices will be conducted.

Whilst BDD may initially be considered both monetarily and resource expensive, the ability to grow it in the laboratory in a free-standing form at the wafer scale (~6" diameter) and the fact that the sensors demonstrated here are ≤1 mm in diameter (with potential to go smaller limited only by the current laboratory manual electrode fabrication and handling methods) means a huge quantity of sensors could be produced from a single wafer. Furthermore, the robustness of BDD as a material implies a significant longevity over other electrode materials and other existing methods (e.g. optical) of measuring dissolved oxygen and pH and counters these initial costs. The material qualities of BDD, such as hardness and resistance to fouling, could offer solutions for dissolved oxygen and pH measurement over long periods in challenging or hazardous to access aqueous environments, improving not only sensor longevity and measurement frequency but also personnel safety.

References

[1] Abele, D.; Vasques-Medina, J.P. ; Zenteno Savin, T. *Oxidative Stress in Aquatic Ecosystems;* John Wiley & Sons, 2011
[2] Maltepe, E. ; Saugstad, O.D., *Pediatr. Res.* 2009, 65 (3), 261-268
[3] Hoogenboom, R. et al., *Angew. Chem., Int. Ed.*, 2015, 54, 10879 – 10883
[4] Tessier, A.; Turner, D.R., *Metal speciation and bioavailability in aquatic systems,* J. Wiley, 1995
[5] Simpson, S.L. et al., *Appl. Geochem.*, 2015, 59, 1-10
[6] Aragay, G.; Pons, J.; Merkoçi, A., *Chem. Rev.*, 2011, 111, 3433-3458
[7] Read, T.L., et al., *Anal. Chem.*, 2014, 86, 367-371
[8] Read, T.L. et al., *Chem. Commun.*, 2016, 52, 1863-1866
[9] Read, T.L. et al., *ACS Sens.*, 2019, 4, 756-763
[10] Luong, J. H. T.; Male, K. B.; Glennon, J. D., *Analyst,* 2009,134, 1965−1979.
[11] Swain, G. M.; Ramesham, R., *Anal. Chem.*, 1993,65, 345−351
[12] Compton, R. G.; Foord, J. S.; Marken, F., *Electroanalysis,* 2003,15, 1349−1363
[13] McGaw, E. A.; Swain, G. M., *Anal. Chim., Acta* 2006, 575, 180−189
[14] Macpherson, J.V., et al, *Anal. Chem.*, 2016, 88, 974-980
[15] Macpherson, J.V. et al, *Electrochem. Commun.*, 2016, 72, 59-63
[16] Walshe, J.M., *Lancet*, 1982, 319, 643-647
[17] Wrighton, M.S., et al., *Science*, 1991, 252, 688-691
[18] Morcos, I.; Yeager, E. *Electrochim. Acta.*, 1970, 15, 953−975
[19] Yeager, E., *Electrochim. Acta*, 1984, 29 (11), 1527−1537
[20] Taylor, R. J.; Humffray, A. A., *J. Electroanal. Chem. Interfacial Electrochem.*, 1975, 64(1), 63−84
[21] Taylor, R. J.; Humffray, A. A., *J. Electroanal. Chem. Interfacial Electrochem.*, 1975,64, 85−94

Dr. Tania Louise READ
Assistant Professor
Department of Chemistry
University of Warwick

Analysis and Measurement Technologies that Contribute to the Formation of a Water Recycling Society

KAWANO Tadashi

MIYAMURA Kazuhiro

In recent years, the pattern of water resources has changed significantly. Securing water for daily life as the population increases and for industrial use as industry develops have become major social issues. However, the water that exists in rivers, lakes and ponds that are easily accessible to people accounts for only about 0.01% of the water on Earth, and this limited water resource is reused by purifying and circulating it. This paper describes the changes and issues in water resources, and the measurement technologies that contribute to a water-recycling society.

Introduction

Approximately two-thirds of the earth is covered with water, but only about 0.01% of Earth's water is available for human use. This limited resource is used for drinking water, industrial water, and irrigation water in the water cycle. However, population growth and climate change are causing imbalances in the supply of water resources.

According to "the United Nations World Population Prospects 1960-2060, revised in 2015", the world population was approximately 7.35 billion in 2015 and is projected to reach approximately 9.73 billion by 2050. According to the Organization for Economic Co-operation and Development (OECD) "Environmental Outlook to 2050 (2012)", water demand is expected to increase by 55% between 2000 and 2050, mainly due to increases in industrial water use in manufacturing (+400%), in power generation (+140%), and in water for daily life (+30%). By 2050, the population living in river basins and facing severe water shortages could reach 3.9 billion (more than 40% of the world's population). (Figure 1)

The amount of water available as a water resource is constantly changing due to variability in precipitation. For this reason, climate change caused by global warming, which is believed to be causing extreme weather such as heavy rains and droughts, has a significant impact on the amount of water available for use. According to the Centre for Research on the Epidemiology of Disasters (CRED), floods and droughts are occurring frequently around the world. In 2015, there were 152 national-level floods and 32 national-level droughts, affecting approximately 30 million people and 50 million people, respectively.

Measurement technologies used in a water cycle society

People use limited water resources for drinking, industrial water, and irrigation, and after purification, discharge it into rivers and oceans, forming a water cycle. In order to produce water for specific purposes, it is necessary to accurately measure the quality of raw water and appropriately treat it. For example, in order to produce ultrapure water used in semiconductor manufacturing processes, the pH, hardness, electrical conductivity, turbidity, and other properties of the raw water are continuously monitored. At the point of use, the electrical resistivity of the

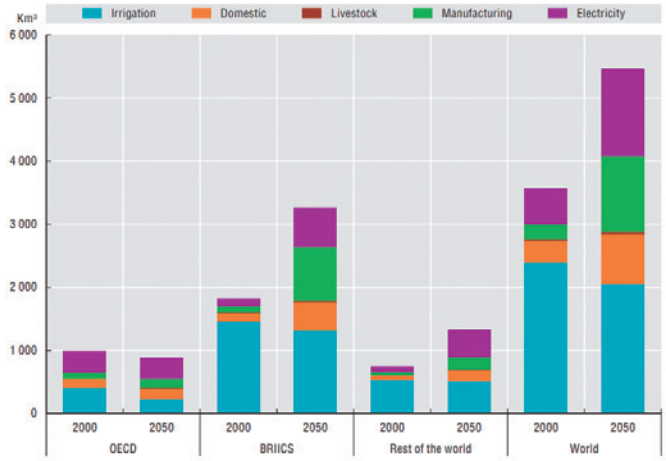

Figure 1 OECD's 2012 graph of projected global water demand to 2050

water must always be 18.20 MΩ·cm or higher, compared to the theoretical resistivity of the pure water, which is 18.24 MΩ·cm. Therefore, continuous monitoring of the electrical resistivity is used to ensure the water quality. In addition, with advances in semiconductor technologies, higher accuracy is required year by year as the water quality standards required for the ultrapure water. For example, with the miniaturization of semiconductors, it is necessary to measure even finer particle sizes. Wastewater generated in the semiconductor manufacturing process may contain hydrofluoric acid in the inorganic wastewater line. If discharged directly into rivers, it cannot be naturally purified, leading to environmental pollution and stagnation of the water cycle. Calcium chemicals are added to reduce the concentration of the hydrofluoric acid. To properly carry out this treatment, the concentration of the fluoride ions in the wastewater must be measured to determine the amount of the calcium chemicals to be added. Measuring the calcium concentration also helps to prevent excessive addition of the chemicals. After that, biological treatment improves the water quality to a level that can be naturally purified, and then the water is discharged into rivers and the ocean.

On-site industrial water quality meters, such as the H-1 series manufactured by HORIBA Advanced Techno Co., Ltd., are used for the water quality management described above (Figure 2). This measuring device is a field-installable water quality meter that can measure all the parameters necessary for comprehensive water quality measurement and management, and is used not only in the semiconductor industry but also for water quality management in water supply and sewage systems. It is used not only in the semiconductor industry, but also for water quality management in water supply and sewage systems. In addition, portable pH and water quality analyzers such as the WQ-300 series are used for water quality management in locations where installation is difficult and in rivers (Figure 3). This analyzer enables immediate measurement on site, supporting water quality management at any location.

As described above, water quality measurement is necessary throughout the water cycle and supports it globally. On the other hand, measurement technologies that contribute to food safety and security are also in demand. The following section introduces measurement technologies necessary for hygiene management in food processes.

Figure 2 On-site industrial water quality meters, H-1 series
https://www.horiba.com/jpn/water-liquid/products/se ries/h-1-series-field-installation-type/

Figure 3 Portable pH and water quality analyzers WQ-300 series
https://www.horiba.com/jpn/water-quality/handheld-meters/

Residual chlorine concentration monitor using diamond electrodes UP-400CL

Aim of developing a residual chlorine concentration monitor and on-site needs

Food hygiene management in food processing plants and related facilities is required to be more stringent under the international HACCP (Hazard Analysis and Critical Control Point) system[*1]. For example, in the process control of cut vegetable washing, the type and amount of vegetables, the temperature and pH of the washing solution, and the residual chlorine concentration must be recorded. Among these parameters, the concentration of residual chlorine decreases during washing, so it is necessary to frequently sample the washing solution to perform measurement and recording using the colorimetric method or the test paper, and to adjust the concentration as necessary. This requires considerable labor, and there is also concern about measurement errors, measurement omissions, and recording mistakes by workers. Furthermore, the current manual operations are not suitable for the rapid adoption of IoT in process control. As a means of overcoming these issues, we have developed the Residual Chlorine Concentration Monitor (UP-400CL), which can automate measurement tasks and enable data communication. We believe that this monitor contributes to food safety and security by not only improving the on-site environment, but also helping to prevent food poisoning and enhance food taste. Figure 4 shows the photo and the configuration of the residual chlorine concentration monitor.

This monitor is the world's first[*2] residual chlorine concentration monitor designed to perform measurement during vegetable washing by using a diamond electrode. Since the main unit is compact and waterproof with a built-in pump, measuring 125 mm wide × 125 mm deep × 100 mm high, just installing the monitor near the washing tank enables the measurement. The residual chlorine concentration can be also checked in real time on the screen of the monitor. In addition, data can be stored on an SD card and transmitted to an external device.

*1 Refer to the Ministry of Health, Labour and Welfare (Japan) website. https://www.mhlw.go.jp/stf/seisakunitsuite/bunya/kenkou_iryou/shokuhin/haccp/index.html

*2 According to our research in August 2022.

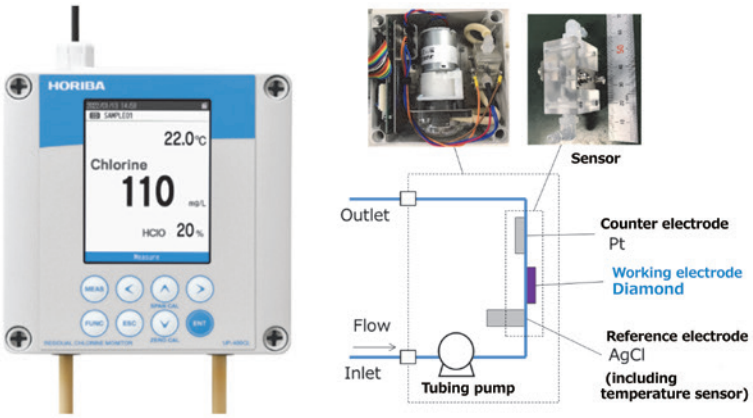

Figure 4 Photo and device configuration of residual chlorine concentration monitor.

Figure 5 Example of residual chlorine concentration monitor operation at a vegetable processing factory.

Core technology that enables measurement even during food washing

The polarography method using platinum or gold electrodes has been used for continuous measurement of residual chlorine. However, it is difficult to accurately measure the residual chlorine concentration during the vegetable washing.
This is because the reaction on the electrode surface is inhibited by organic matter eluting from the vegetables, causing the indicated value to drop rapidly. Therefore, we adopted a boron-doped diamond electrode (BDD: Boron-Doped Diamond)[1] developed by professor Yasuaki Einaga of Keio University and developed a unique measurement sequence[2] that is less susceptible to the effects of organic matter.

Compared to conventional electrode materials, BDD has a wide potential window, low noise, and high durability. Taking advantage of these characteristics, we have developed new technologies, such as a powerful electrolytic cleaning method to remove organic contaminants from the electrode, and a new measurement method capable of measuring both hypochlorous acid and hypochlorite ions with reduced influence from pH. In addition, we have developed a unique measurement sequence that reduces the influence of organic matter by applying a negative voltage immediately before measurement to remove negatively charged anionic organic matter from the electrode surface and then measuring the hypochlorous acid ion concentration immediately after (this technology is patent pending).

The function of this product is realized through these measurement methods and flow control of the pump built into the monitor.

Example of use in cut vegetable washing

Figure 5 shows an example of use in a cut vegetable washing line[*3]. The monitor is installed next to the washing line and automatically samples the washing liquid through a stainless steel filter to prevent vegetable residues from entering. This allows the concentration of the residual chlorine to be checked in real time during washing. In addition, pH and liquid temperature are measured simultaneously when necessary. The data is stored in the cloud via a separately installed gateway, enabling monitoring on-site or remotely via tablets, PCs, and other devices.

Figure 6 shows the concentration measurement and its control during vegetable washing. By pre-setting operational limits and acceptable limits, alerts are triggered before these values fall below the limits, enabling appropriate process control. Furthermore, in the event that the measured values fall below the acceptable limits, alerts can be notified with warning lights or emails.

*3 https://www.horiba.com/jpn/water-liquid/products/detail/action/show/Product/up-400cl-5075/

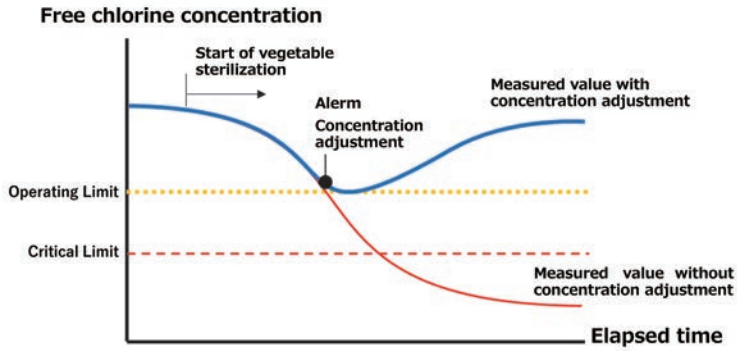

Figure 6 Image of concentration measurement and control during vegetable washing

Future challenges and prospects

Caution is required when the measurement method is switched from the conventional colorimetric method to the monitor, as the control values may not match. This is because the monitor measures free residual chlorine, whereas the colorimetric method measures total residual chlorine, which includes both free and combined residual chlorine. However, from the perspective of sterilization effectiveness, which should be the appropriate control indicator, the sterilizing power of combined residual chlorine is said to be less than one-tenth that of free residual chlorine. Accordingly, relying on colorimetric values when the concentration of the combined residual chlorine is increased may result in a significant and unintended reduction in disinfection performance. This concern stems from the previous lack of analytical method for continuously measuring the free chlorine during the vegetable washing, but the introduction of this monitor may change management practices in the future.

This monitor can be easily installed in washing tanks used for vegetable cleaning or in washing liquid supply tanks. It also supports SD card data storage and communication functions. Therefore, it is expected to play a key role in the IoT-based hygiene management and in improving on-site working environments in the future. Although this paper focuses on the washing of cut vegetables, the technology is also applicable to washing eggs and fish. In the future, since real-time measurement and automatic recording are possible, the measured concentration of residual chlorine could be considered as a monitoring item for CCP (Critical Control Point). We hope to contribute further to the food safety and security by developing technologies that meet user needs.

Conclusion

Appropriate water treatment is necessary for the efficient and effective use of limited water resources. This requires accurate and stable measurement of water quality. However, maintaining accurate measurements requires sensor maintenance, which is a significant burden for users. In order to reduce the burden of the sensor maintenance, it will be important to develop the sensors that are not affected by contamination and are highly durable. In addition, contactless measurement will be also the important technology that is conducted without any contact with liquids in the first place. Moreover, the measurement method with the multivariate analysis using multi-point measurements and multiple component measurements will be also important technologies to solve problems in measurement samples and in measurement environments that were difficult to be measured with conventional methods. We hope to contribute to the water cycle society, to support the prosperity of humankind, and to contribute to the industrial develop-

ment through the development of the liquid measurement technologies.

* Editorial note: This content is based on HORIBA's investigation at the year of issue unless otherwise stated.

References

[1] M. Murata, T. A. Ivandini, M. Shibata, S. Nomura , A. Fujishima, Y. Einaga, *J. Electroanal. Chem.,* 612, 29 (2008).
[2] 宮村和宏, 亀子雄大, ダイヤモンド電極を用いた残留塩素濃度モニター,「センサ・マイクロマシンと応用システム」電気学会センサ・マイクロマシン部門39 3p-, 2022-11. (In Japanese)

KAWANO Tadashi
General Manager
Research & Development Division
HORIBA Advanced Techno, Co., Ltd.

MIYAMURA Kazuhiro
Advanced Technology R&D Department
Research & Development Division
HORIBA Advanced Techno, Co., Ltd.

Current Conditions of Small Water Supply System in Japan and Technical Needs

ITOH Sadahiko

Professor,
Department of Environmental Engineering, Graduate School of Engineering,
Kyoto University
Doctor of Engineering

Since the population has been decreasing in Japan, it is important to focus on the area with small population or low population density. In this article, small water supply systems managed mainly by residents in small residence area were described. Various water supply methodologies and the needs of water treatment facility installed were shown. Based on the reality of waterworks, technical needs for supporting small water supply systems were discussed.

Keywords : Water supply system, drinking water, water treatment, depopulation

Introduction

Although Japan's potable water supply is a mature social infrastructure, it currently faces a number of important and urgent issues. The main issues are listed below[1].

(1) Depopulation and decline in water demand

Water demand continues to decline due to a decrease in domestic water consumption per capita and depopulation.

(2) Rapid increase in demand for facility renewal and decline in investment

The time has come to renew the water supply assets that have been developed to date. However, investment has been declining in recent years, and water supply facilities are aging.

(3) Aging of pipelines

Pipelines, which account for 70% of water supply assets, are aging, but the pipeline renewal rate is only 0.64% per year (as of the end of fiscal 2021), which means that it will take 156 years to renew all pipelines.

(4) Delays in earthquake-resistant measures

The earthquake-resistant measures rate is still not sufficient, at 42.3% for main pipelines, 43.4% for water treatment facilities, and 63.5% for service reservoirs (all as of the end of fiscal 2022).

(5) Problems with business management and water tariff setting

Although waterworks are supposed to be self-supporting, many of those are operating at a loss. Tariffs should be set based on asset management, considering future renewal demand, but in many cases this is not being done.

(6) Reduction in staff and difficulties in technology transfer

The number of employees at waterworks is decreasing and the age of those is increasing. As a result, technology transfer is becoming difficult, and business management itself is becoming difficult.

Against this backdrop, the Waterworks Law was revised in 2019[2]. The most important point of this revision is that the purpose of the law has been changed from "systematic development of water supply" to "strengthening the infrastructure of water supply." In other words, with the serious issues mentioned above, it is not only difficult for small and medium-sized waterworks to overcome these issues, but there are also cases where it is becoming difficult to continue operations in the future. This amendment is considered as a major revision because it changed the purpose of the law itself.

This article focuses on small water supply systems as a symbol of the problems with which water supply in Japan is faced, introducing the trends of the systems regarding

both water supply methodologies and the needs for water treatment facilities. Based on the trend introduction, the needs are discussed to support the small water supply systems.

Existence of small water supply systems

Water supply systems serving 5,001 or more people are called potable water supply systems, and those serving 101 to 5,000 people are called small water systems. These are the main types of water supply treated as "water supply" under the law. (There are several other types, such as dedicated water supply systems.) The penetration rate of these types of water supply reached 98.1% in 2020. However, it would be premature to conclude that universal access to water supply is being achieved. There are still local governments where the water supply coverage rate is in the 50% to 60% range, and there is no prospect of a rapid increase in the coverage rate in these areas. Furthermore, even though the coverage rate is in the 98% range, this means that the remaining 2% or so of the population, or more than 2 million people, do not have access to water supply.

In Japan, there are many small water supply systems that are not subject to the Waterworks Law because the water supply population is 100 or less. These include drinking wells, drinking water supply facilities, and small community water supply systems. Not being subject to the Waterworks Law means that these systems are not required to comply with water quality standards or conduct water quality examinations. Since they are not considered as "water supply", this paper refers to them as "small water supply systems."

Most of these are very small facilities managed by local residents, but they face issues such as ensuring the safety of drinking water, increasing maintenance costs due to aging, and resilience to disasters such as earthquakes.

With the ongoing depopulation in various parts of Japan, there is a growing need to focus on small-scale water supply systems, including the small water supply systems mentioned here. From this perspective, authors including myself published "Small Water Supply Systems: Toward a Sustainable Supply of Safe Drinking Water"[3] in 2024. That is the first book to discuss the small water supply systems in Japan comprehensively. While looking at the current situation directly, the book outlines the direction that the water supply in Japan should take as a whole and suggests recommendations from various perspectives.

The current situation and trends in small water supply systems

Among the small water supply systems, there are cases where management by residents is difficult or has reached its limits, and conversely, there are good examples of the systems that have been established in a sustainable manner. There are also cases where new technologies that meet social needs have been successfully created. This section discusses current trends and future directions, focusing on two aspects: water supply methodology and water treatment facilities.

Selection of water supply methodology

There are areas where it is difficult to maintain a centralized water supply system with water treatment facilities and distribution networks, which are referred to as "areas where pipeline maintenance is difficult." In addition, in many cases, it is inefficient or impractical to connect unserved areas to existing centralized potable water supply systems that is the conventional method. In the future, it will be necessary to select water supply systems that are appropriate for local conditions, such as decentralized systems and water transmission by transportation.

The decentralized system is one in which raw water intake, water treatment, and water distribution are all carried out within the local area. A unitized portable equipment is one of the options for the water treatment facilities to be introduced in such areas. Photo 1 shows an example of a facility in Hamamatsu City (supplying drinking water to about 50 people). The water treatment facility on the left side of the photo provides the workflow, which are coagulant injection, sedimentation, rapid filtration, and disinfection. The service reservoir is on the right side of the photo.

Photo 1 Water supply facility installed in Hamamatsu City, Shizuoka Prefecture

The decentralized systems are clearly less expensive in terms of initial costs than the system connecting to the potable water supply, but in this case, it is necessary to address concerns such as facility management responsibilities, maintenance entities, required water quality examinations, and secured fire protection water supply.

Furthermore, instead of the centralized water treatment, the decentralized water treatment close to the point of use is becoming one of realistic options. Examples of the options include Point-of-Entry (POE) systems, which use small-scale water treatment facilities installed at the entrance of buildings to treat water and to supply the water to households, and Point-of-Use (POU) systems, which is even smaller scale and treat water at each faucet.

In Higashi-Chichibu Village, Saitama Prefecture, in addition to the option of introducing the small-scale water treatment facilities similar to those in Hamamatsu City as mentioned above, a plan has been proposed to discontinue the existing water treatment plant and to install small-scale water treatment facilities in each household. A conceptual diagram is shown in Figure 1. It would be difficult to respond to subsequent depopulation if the water treatment plant would be renovated completely, but this system has the advantage to respond to depopulation because water is treated in each household.

Higashichichibu Village plans to introduce this system on a trial basis and to verify its effectiveness through water quality examinations and other measures.

In addition, on Kuroshima, a remote island off the coast of Sasebo City in Nagasaki Prefecture, the introduction of the Point-of-Entry (POE) system has been proposed and is being implemented.

This kind of water supply system can be introduced in a short period of time because the system requires neither a network of long pipelines nor large-scale installation work while the system is relatively cheap. However, in this case as well, it is necessary to organize measures to address the concerns mentioned above.

By the way, the law defines “water supply” as a facility that supplies water through pipes but does not assume that water is transported and distributed. However, the needs for transporting water exist in various places because the difficult cases are increasing for the areas (where pipeline maintenance is difficult) to maintain the centralized water supply systems that have been built up to today. For example, in Shitara Town, Aichi Prefecture, the plan to transport water was proposed in the past but was rejected after Aichi Prefecture pointed out that it would not be water supply anymore.

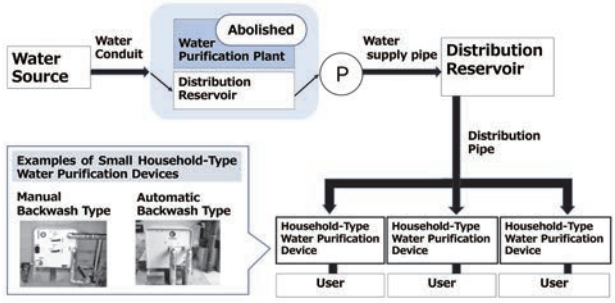

Figure 1 A scheme of installing point of entry type water treatment facility.

Photo 2 An example of water transmission by transportation in Miyazaki City.

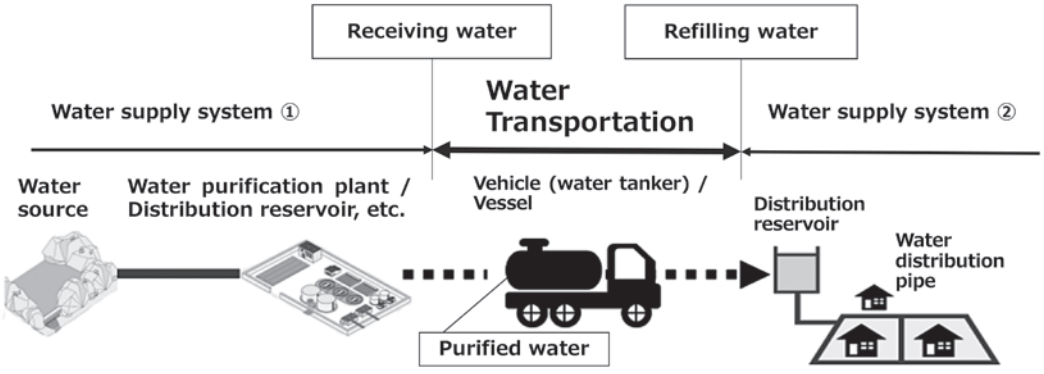

Figure 2 Illustration of water transmission by transportation.

Under these circumstances, the Ministry of Health, Labour and Welfare issued "Points to note regarding water transmission by transportation"[4] in 2023, stating that water transmission by transportation is feasible as a part of waterworks. A conceptual diagram is shown in Figure 2. Since this is the transmission part of the water supply systems, the term "water transmission by transportation" is used instead of "water supply by transportation." Since the water is transmitted in the part of the water transmission, the part is still not considered as the water supply. However, since the service reservoir and beyond can be considered as the part of the waterworks, it is feasible as a part of waterworks. This can be considered as an example of a flexible response without major institutional changes such as legal revisions. As a result, many waterworks can now consider to introduce the water transmission by transportation although they gave up to introduce it. An example of water transmission by transportation in Miyazaki City is shown in Photo 2 showing that the water is supplied from the supply tank vehicle to the service reservoir.

The evaluation example of the advantages of the water supply methodology mentioned above[5] is shown in Figure 3. The area in Nara Prefecture equipped with the small water system has been evaluated. The two-dimensional plane with the horizontal axis representing the water supply population and the vertical axis representing the total length of the pipelines for supply and transmission shows the areas, where the normal water supply can cover, where introducing the water transmission by transportation is better, and where it is better to supply only non-potable water but to supply potable water with another methodology. The important point is to have clarified that the introduction of the water transmission by transportation is effective if the transportation to each household is available based on the condition of the area. It is recommended to discuss such studies actively and to select the realistic or smart option to meet the condition of the local area.

Needs for water treatment facilities

Fukuchiyama City, Kyoto Prefecture, has an ironic example in which no concerns have been raised about the future in areas without the water treatment facilities while concerns have been raised about the continuous maintenance of the water treatment facilities in areas with the water treatment facilities.

In Shizuoka City, measures to achieve sustainable water supply system for the future have been introduced based on the main concerns raised by residents including ensuring stable water supply, installing maintenance-free water intake and treatment facilities, and implementing reliable disinfection.

In addition, although a lot of the small-scale water treatment facilities have been introduced, their water treatment capability is approximately 50 m^3/day but even smaller-scale water treatment facilities have been required. Therefore, the needs for the water treatment facilities suitable for each small community should be extremely small-scale, easy to maintain, and low-cost facilities.It is expected that facilities and new technologies to meet the needs are developed.

On the other hand, the approaches have been proposed

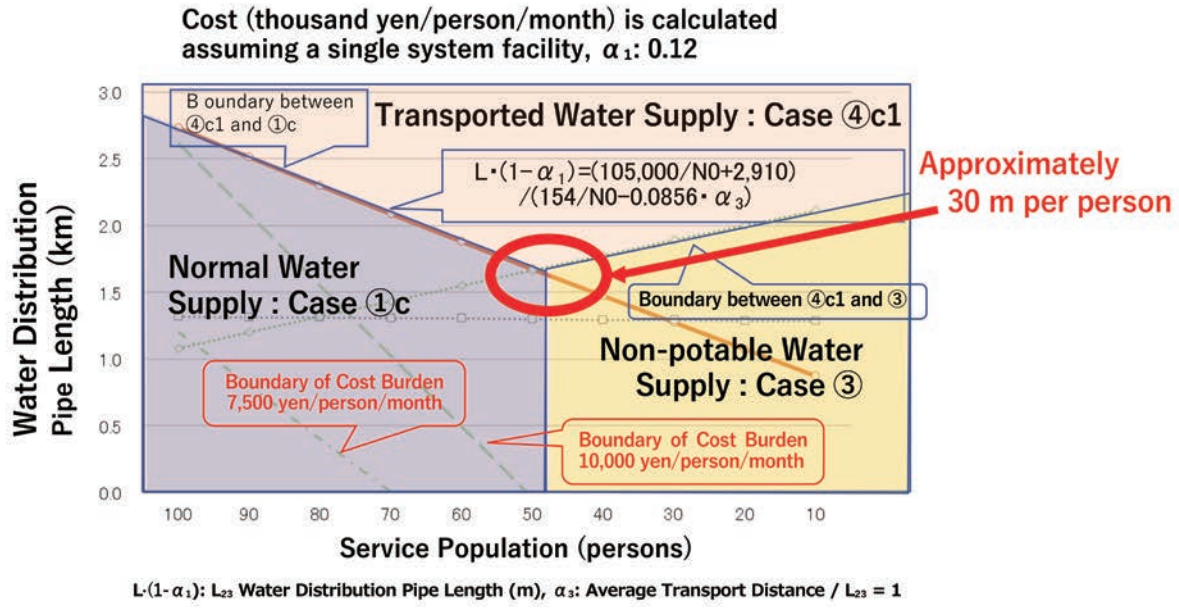

Figure 3 An example of evaluating water supply methodologies.

regarding the social infrastructure development in the depopulating society, which is not limited to potable water supply facilities[6], [7]. In the past, various types of infrastructure have been developed focusing traditionally on durability and permanence (long-term usability). It can be said that efforts have been made to build water supply facilities and equipment that are robust and long-lasting. In contrast, in a shrinking society, it will be necessary to adopt the concept to shorten their lifespan (or to combine extending lifespan and shortening lifespan) by modularizing the infrastructure. The term "shortening lifespan" can also be replaced with "planned service life." With this approach, we can respond to the future demand change of the area or, in some cases, can decide to withdraw the development. In the future, we believe that it will be necessary to adopt the concept of designing and introducing facilities and equipment that will last for about 10 years. Leasing contracts, which some companies have already started to offer, will also be an option.

In fact, there is an example in Kochi Prefecture where new technologies that meet the above social needs have been successfully developed.

In the mountainous areas of Kochi Prefecture, there are many water supply facilities where residents themselves secure and manage their own domestic water. Kochi Prefecture launched the "Kochi Prefecture Domestic Water Model Development Project" for those facilities and conducted the commissioned work in fiscal 2014.

Through this project, a simple slow sand filter facility (two-tank slow sand filter facility) has newly been developed for small-scale area. The structure of the facility and its surface are shown in Figure 4. The facility consists of two tanks with the gravel layer and the sand layer separated, which is the key feature of the facility. The water in the gravel layer flows upwards and is coarsely filtered. The filtered water flows into the sand layer downwards and is filtered. Simplifying each filtration layer in this way makes cleaning easier, which is the main maintenance work. In addition, no power supply is required.

Another feature of this device is its extremely small size, with a water treatment capacity of 3 to 6 m^3/day (corresponding to a filtration speed of 4 to 8 m/day). This is suitable for a water supply population of several to dozens of people. Furthermore, the facility itself is inexpensive, at 1.3 million yen per unit.

A notable feature of this case is that Kochi Prefecture identified the needs of mountainous areas, demonstrated the required facilities and equipment, and specified the technologies that needed to be developed. This enabled companies to clearly define their development targets and gain a clear outlook for business expansion throughout the prefecture. In fact, the contractor (company) stated that they would not have developed the facility and equipment from scratch without the prefecture's initiative.

In this way, the project promoted by Kochi Prefecture can be recognized as success in creating new technologies that match social needs. The role played by the prefecture was extremely important. The developed two-tank slow sand filtration facility has become the new technology that matches the needs for each small community[7] such as extremely small-scale, easy to maintain, and low-cost. We hope that it will be widely adopted throughout Japan.

Technological needs supporting small water supply systems

The above section introduced two aspects and their trends regarding water supply methodologies and water treatment facilities. At the same time, there are significant social needs to develop technologies supporting these water supply systems. This section provides an overview of various technologies currently under development and discusses technologies that are effective in alleviating the issues faced by the small water supply systems.

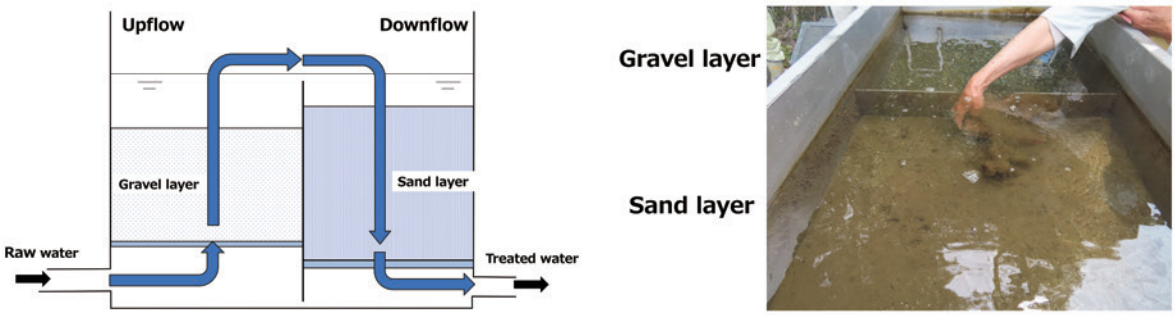

Figure 4 Slow sand filtration facility newly developed for small residence area.

Significance and trends in the introduction of data management and monitoring technologies

Small water supply systems rely on the self-help efforts of residents for transferring the know-how for operation and maintenance as well as managing data, which, in many cases, are done in analog form, i.e., through word of mouth and handwritten notes. This system has been increasingly difficult through the ongoing depopulation and the aging population.

This problem may be dramatically alleviated by information and communication technologies, which require little investment and are easy to operate. With the information and communication technology, data measured without human intervention can be recorded (logged), transmitted, and monitored remotely. If the communication environment is ready, it is possible to transmit not only numerical data but also real-time image data of the area, allowing visual confirmation of the area. However, such remote monitoring technology is generally expensive, and was mostly introduced to the public water treatment plants of the waterworks in the past while few technologies were introduced to the small water supply systems.

To date, the Ministry of Land, Infrastructure, Transport and Tourism has been implementing the "Model Project for Promoting the Use of IoT in Water Supply Services" (subsidy for earthquake-resistant infrastructure)[8] to improve business efficiency and provide high value-added water supply services through the use of advanced technologies such as CPS (Cyber-Physical System) and IoT (Internet of Things). In addition, the Ministry of Land, Infrastructure, Transport and Tourism; the Ministry of Economy, Trade and Industry; and NEDO (New Energy and Industrial Technology Development Organization) have collaborated to build a standard platform for utilization systems of the water supply information, with which a few services have been launched[9].

From the perspective of technologies suitable for the small water supply systems, low-cost and easy operation are essential. Therefore, it is necessary to reduce costs through standard design and mass production, and it is important to develop technologies as "mass-producible services" with a view to expanding their use beyond water supply.

Current situation of development and introduction with future expectations

This section provides an overview of the technologies developed to date and their potential for introduction into the small water supply systems. Some of the new technologies introduced here are summarized on an information website on the small water supply[10].

• Development of water quality management and monitoring technologies

Although the water quality examination has not been conducted on many of the small water supply systems, the cost of the water quality examination is a significant burden if the water quality examination is conducted on the systems. There are 51 items specified in the drinking water quality standards in Japan. It costs an average of about 210,000 yen when the examination is conducted by an inspection agency registered by the Ministry of the Environment. The Waterworks Law requires the regular examinations consisting of three quarterly examinations and eight monthly examinations in addition to the annual examination including all the items. If all the examinations are conducted, approximately 570,000 yen per year is required as the cost of these examinations. The water quality examination cost is a significant burden for small areas with a small water supply population. In fact, some of the small water systems have been downgraded to drinking water supply facilities due to the cost reduction of the expensive water quality examinations as a main reason. As a result, the drinking water supply facilities can be exempt from conducting the water quality examinations since the Waterworks Law does not apply to the facilities. In fact, as an example, in Nishigo Village, Fukushima Prefecture, the annual cost of 740,000 yen was significantly reduced to 59,000 yen through the downgrading. Considering these current situations, the author proposes to introduce a concept of "customized water quality standards", which involves selecting the examination items definitely necessary for the area and setting the frequency of the examinations[3].

If a system is available to monitor the operation including the water quality of the water supply facilities "at low cost", the system would provide a great advantage for maintenance and management.
Since communication technologies and terminals have become increasingly sophisticated and widespread in recent years, their utilization should be considered. Various services utilizing the communication infrastructure have already been introduced by private companies related to the water supply.

For example, in Yurihonjo City, Akita Prefecture, data on water quality, water levels, and water distribution volumes are managed collectively using telemeters as well as cloud-based remote monitoring and controlling systems for 16 facilities including water treatment facilities, service reservoirs, and water transmission facilities.

• Development of treatment and operation methods at low maintenance cost

The small water supply systems usually encounter no problems but often encounter big problems to remove turbidity and debris after rain. The easy-maintenance and low-cost water treatment systems are good to be introduced to these facilities. In addition, 56 types of portable water treatment facilities including water treatment devices have been classified according to their treatment capacity, device configuration, target substances to be removed, vehicles capable of loading devices, and operating methods[11].

Photo 1 shows that the small water treatment facilities dedicated for stream water was introduced in Hamamatsu City. As an example of such facility using IoT, a business entity has introduced the cloud-based remote monitoring systems[8], [12]. Although the technology is still under development, the low-cost LPWA (Low Power Wide Area) communication was introduced to the water supply system in a mountain community to reduce the cost for the residents to monitor the water level of the service reservoir[13].

• Examples of development of portable disinfection methods without replenishment

One of the maintenance burdens of small water supply systems is the replenishment of chlorine disinfectants. A portable disinfection method without replenishment of chemicals and frequent maintenance is required, and such technologies have already been developed and proposed in various products.

• Pipeline technology including water leak detection and easy temporary repairs

Since the small water supply systems have vulnerable pipelines, it is required to introduce the pipeline systems which can be repaired with low cost in the event of a disaster or pipeline damage. New technologies using IoT have been developed, and we can see its example in Wajima City in Ishikawa Prefecture[8].

• Inspection and chemical replenishment using robot

The introduction of technologies such as autonomous driving and drones is expected to reduce the burden of maintenance and to solve problems caused by decreasing number of technical staff. Currently, the robot technology in the water supply field has been introduced only to the limited application to observe pipes and tanks where humans cannot access. In the future, robots are expected to be used in a wider range of applications such as the maintenance of water supply facilities in general and the automatic operation of chemical replenishment.

Conclusion

In Japan, disparities in water supply are likely to widen in the future. This applies not only to large, medium, and small water supply systems, but also to small water systems such as small water systems and drinking water supply facilities. Water tariffs, which have traditionally varied by a factor of about 8, are expected to widen to a factor of 20 in the future[14]. Given this situation, we strongly consider that it will be necessary to develop diverse water supply systems and diverse water supply societies in the future.

In response to the many difficult challenges facing Japan's water supply system described at the beginning of this article, numerous creative ingenuities, ideas, and proposals are currently being put forward to strengthen the foundation of water supply businesses and, even more importantly, to enhance their sustainability. These valuable ideas and proposals need to be implemented in society, but first, the technologies to support them should be developed.

We hope that this article will serve as a reference to create diverse technologies in various fields. At the same time, it is essential for the water supply industry to establish systems and mechanisms that do not hinder the formation of diverse water supply systems and societies, and to ensure that these systems and mechanisms are operated flexibly.

References

[1] 水道事業基盤強化方策検討会：水道事業の基盤強化方策に盛り込むべき事項（2016）. (In Japanese)

[2] 水道法制研究会監修：水道法ガイドブック-令和元年度-, 水道産業新聞社, 197p.（2020）. (In Japanese)

[3] 伊藤禎彦, 浅見真理, 牛島健, 小熊久美子, 木村昌弘, 増田貴則, 山口岳夫：小規模な水供給システム～安全な飲料水の持続可能な供給へ向けて～, 水道産業新聞社, 236p.（2024）. (In Japanese)

[4] 厚生労働省医薬・生活衛生局水道課：運搬送水に係る留意事項, 令和5年7月（2023）. (In Japanese)

[5] 木村昌弘, 浅見真理, 伊藤禎彦：小規模水道における給水形態に関する系統的評価と簡便汎用モデルの適用, 水道協会雑誌, 93(9), 22-32（2024）. (In Japanese)

[6] 宇都正哲,植村哲士,北詰恵一,浅見泰司：人口減少下のインフラ整備, 東京大学出版社（2013）. (In Japanese)

[7] 伊藤禎彦：人口減少下における浄水処理装置・施設に関する課題とニーズ. 環境衛生工学研究, 33(2), 3-10（2019）. (In Japanese)

[8] 国土交通省：水道事業におけるIoT・新技術活用推進モデル事業 (In Japanese)

[9] 国土交通省：令和３年度全国水道関係担当者会議資料（2022）. (In Japanese)

[10] 水道技術経営パートナーズ株式会社：小規模水供給に関する情報サイト https://www.waterpartners.jp/smallscalewatersupply/0_format/newpage3-4.html（最終閲覧2024年12月）(In Japanese)

[11] 水道技術研究センター：緊急用浄水器・可搬型浄水装置. https://www.jwrc-net.or.jp/info/emergency/equipment.html（最終閲覧2024年12月）(In Japanese)

[12] 西原健志, 福田健吾, 一番ヶ瀬宏之, 須崎岐嗣, 矢野正人, 平尾嘉一, 沼島夏彦, 花本一将：小規模事業体におけるクラウド型遠隔監視システムの導入事例, 平成30年度全国会議（全国水道研究発表会）講演集, 704-705（2018）. (In Japanese)

[13] 渡邊真也, 小熊久美子：省電力長距離通信を利用した簡易無線モジュールによる小規模水供給施設の遠隔監視. 水環境学会誌, 46(1), 11-19（2023）. (In Japanese)

[14] EY Japan水の安全保障戦略機構事務局：人口減少時代の水道料金はどうなるのか？（2024年版）（2024）. (In Japanese)

Standardizing Early Oil Spill Detection for Drinking Water with Absorbance-Transmittance Excitation Emission Matrix (A-TEEM) Spectroscopy

Adam M. GILMORE

Oil spills into fresh water sources used for drinking water treatment present serious potential damage to the treatment plant infrastructure, the environment and consumer health. While the major fraction of most fuel and oil spill components are insoluble in water, smaller component molecules including Benzene, Toluene, Ethylbenzene and Xylene (BTEX) and other Polycyclic Aromatic Hydrocarbons (PAHs) are both soluble and fluorescent. These dissolved components, which can diffuse rapidly in the water body and are detectable in the µg/L range, can serve as early warning sentinels to prevent spill uptake using HORIBA's patented A-TEEM technology. Importantly, the A-TEEM facilitates spectral identification and linear quantification of these compounds in the presence of mg/L levels of natural and manmade Dissolved Organic Matter (DOM) by virtue of Inner-Filter Effect (IFE) correction of the fluorescence data. The A-TEEM detection limits are significant as exemplified by the carcinogen Benzene which is regulated in finished drinking water at 10 and 5 µg/L, respectively, by the World Health Organization (WHO) and United States Environmental Protection Agency (USEPA). Here we summarize the background and methodology associated with the recently published standard test method, D8431-22[1], with the American Society of Testing Materials (ASTM).

Keywords
BTEX, Extreme Gradient Boosting, Inner-Filter Effect, Naphthalene, Parallel Factor Analysis, Polycyclic Aromatic Hydrocarbons

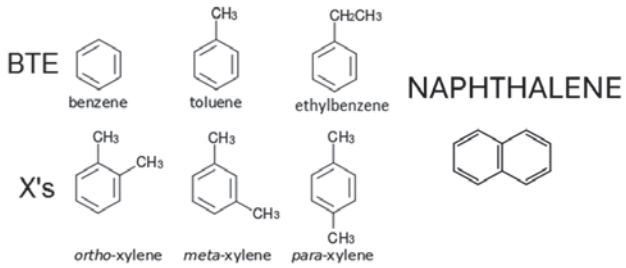

Figure 1 Chemical structures for Benzene, Toluene, Ethylbenzene (BTE), ortho-, meta- and para-Xylene (X's) and Naphthalene.

Introduction

The global demand of fuel oils conflicts directly with safe drinking water treatment with respect to the fact that both shipping and storage of oil can expose drinking water sources to spilled and leaked materials. Oil spills are dangerous to consumer health primarily as sources of carcinogens, including Benzene, that are regulated by the WHO and USEPA in the low µg/L concentration ranges. Oil spills can also significantly damage the environment, including natural flora and fauna, as well as damage the infrastructure of many types of drinking water treatment facilities. Thus, it is of direct benefit to be able to detect oil spills prior to uptake into a treatment facility as a primary means to protect the plant infrastructure and, most importantly, consumer health.

In most cases the majority of the mass of fuel oil spill components are insoluble in water and depending on their density may float or sink in fresh water. However, most fuel oils also contain a significant fraction of water soluble components in the form of BTEX and certain PAHs with relatively low molecular weight[2],[3]. Figure 1 shows the molecular structures for the BTEX and naphthalene compounds. These water-soluble components can diffuse and travel faster than the bulk of the insoluble oil in some streams and water sources. They are also highly fluorescent making them detectable as early warning spill indicators with HORIBA's patented A-TEEM technology[4],[5].

In this article we first describe the basic operation of the A-TEEM method with a special focus on how it facilitates rapid optical identification and quantification of BTEX and other components in the presence of an essentially ubiquitous background of naturally occurring DOM; DOM is usually present in the mg/L range in most fresh drinking water sources and finished water. Key aspects of the standard method development included evaluation of the method Ruggedness and Design of Experiment (DOE) which are discussed with a focus on the major potentially interfering signals from DOM and turbidity

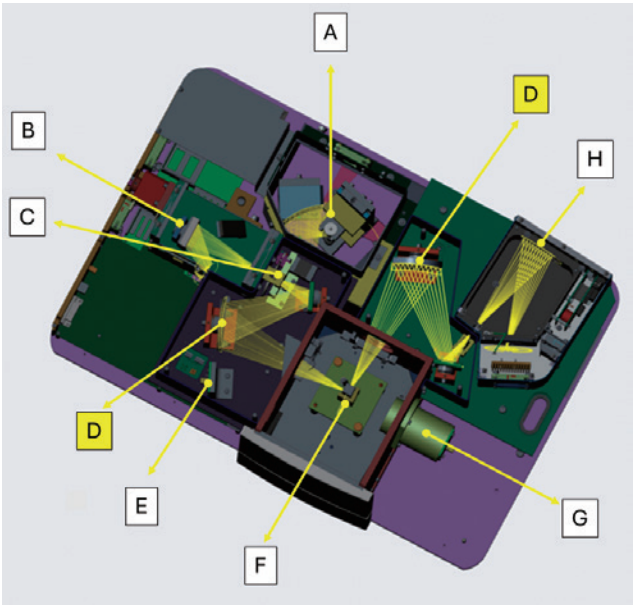

Figure 2 Patented Optical Bench Diagram for the HORIBA Aqualog® A-TEEM Spectrometer. (A). 150 W vertically mounted ozone-bearing exciting light source (200-1000 nm), (B). Double-subtractive monochromator (fixed 5 nm bandpass) with high-stray light rejecting holographic deep UV (250 nm) blazed gratings, (C). Order-sorted excitation optical path for absorbance and fluorescence excitation, (D). Geometrically matched all reflective excitation and emission sampling optics to eliminate color-dependent (chromatic) effects and ensure optical focus on the sample at all wavelengths, (E). A spectrally corrected reference diode detector (200-1000 nm) to account for changes in the light source intensity as a function of time and wavelength for signal stability, (F). A sample compartment with temperature, dry-gas, stirring and flow-cell compatibility, (G). A diode-based transmission detector capable of measuring from 200-1000 nm, and (H). A thermoelectrically cooled, aberration-corrected CCD-spectrograph (250-800 nm) with adjustable binning and gain to maximize the signal to noise with integration times ranging from 5 ms to 65 s.

(suspended particulates). The analytical methods including machine learning algorithms, and how these calibrations and validations are documented, are also discussed. The article concludes with a discussion of how this method can be applied with improved sensitivity to contemporary and future applications as well as a brief comparison to conventional, time consuming and expensive chromatographic methods.

Basic Theory and Operation of A-TEEM Spectroscopy

The patented A-TEEM technology[6], is exemplified in Figure 2 by the HORIBA Aqualog® (see caption for details). The optical bench consists of a powerful broadband (UV to NIR) white light source that is monochromated by a subtractive double monochromator followed by an automated order sorting filter wheel. The first order light is monitored immediately before the sample with a reference detector and then used for both the absorbance and fluorescence excitation source. The sample compartment uses all-reflective optics to geometrically and kinetically match the absorbance and the fluorescence excitation and emission paths. Fluorescence emission is measured

with a thermoelectrically cooled CCD-spectrograph. Operation involves scanning the absorbance and excitation wavelengths from red to ultraviolet (to minimize exposure to ionizing UV); at each abs/ex wavelength a complete emission spectrum is collected until a complete Excitation-Emission Matrix and matching absorbance spectrum is obtained. The signal processing is explained in detail elsewhere[6] noting the most significant feature of the A-TEEM analytical capacity is the coordinated correction of the primary and secondary inner-filter effects which would otherwise distort the EEM data with respect to Beer-Lambert linearity[6]-[9]. IFE correction is critical for the oil-spill detection method because the overlapping absorbance of the background DOM components, with concentrations that are both variable and usually much higher than BTEX, would lead to distorted, nonlinear estimates.

A-TEEM Signals for Naturally Occurring DOM and BTEX Components

As mentioned above naturally occurring DOM is normally present in all fresh drinking water sources and even in most finished drinking water since complete removal is not normally achieved with conventional treatments. The natural molecular composition of fluorescent DOM includes three major classes of compounds including humic acid-like, fulvic acid-like and aromatic amino acid like compounds. Combined these normally add up to at least 1 mg/L of total dissolved organic carbon but can vary widely to >10 mg/L or more in certain sources depending on weather and other conditions[6],[7]. Importantly, all three DOM component classes absorb light (excite) in the UV range from 240 nm. Their PARAFAC loadings also each exhibit distinct emission peak wavelengths with the humic acid like being the most redshifted (peak >450 nm) followed by the fulvic acid-like (peak around 415 nm) then aromatic amino acid-like (peak around 330-350 nm), itself being deepest DOM component in the UV range. Conventional wisdom explains that the relative red-shift for the higher molecular weight fluorophores is structurally associated with the higher extent of aromaticity (ring conjugation) with the single ring aromatic amino acid fluorophores showing the deepest UV emission for natural DOM.

The spectral signatures of the natural DOM A-TEEM signals described above contrast significantly with those from the BTEX and Naphthalene components as shown in Figure 3. Figure 3 compares raw surface water A-TEEM contour plots before (A: Control) and after (B: Spiked) spiking with 100 µg/L each of naphthalene and total BTEX. Naphthalene, which exhibits a very high fluorescence yield is most prominent with the excitation peaking around 275 nm and emitting around 325 nm. While this overlaps with the aromatic amino acid contours the absorbance (not shown) and emission contours are significantly different. BTEX in Panel 3B excites at a lower wavelength peak <270 nm and emits deeper in the UV peaking around 285 nm. Overall, it is clear both of these additions yield well distinguished spectral contours at the 100 µg/L concentration range. This is further exemplified in Figure 4 (adapted from reference[4]) which shows the PARAFAC loadings for raw fresh water samples from the same spiking experiments as Figure 3. The model yields four distinct components for the selected excitation-emission wavelength range; noting the humic acid like region is excluded (masked) for clarity. The 4 components in Figure 4 represent the A (Naphthalene), B (BTEX), C (Fulvic acid-like) and D (Aromatic amino acid-like) components. The component numbers (top of each panel) were assigned based on the score contribution(s) of each component to the overall model; the split-half validation matching for the model was 94.8%. Clearly, the most important distinguishing factor centers on the peak emission wavelengths for the BTEX compounds being considerably below 300 nm (peak for BTEX mixture spike is around 285 nm). This serves well to facilitate BTEX resolution since their emission is below that of any of the naturally occurring DOM components including the amino acid-like components. It is however important to consider that for most drinking water sources and finished water samples the amino acid-like signal intensity is the lowest

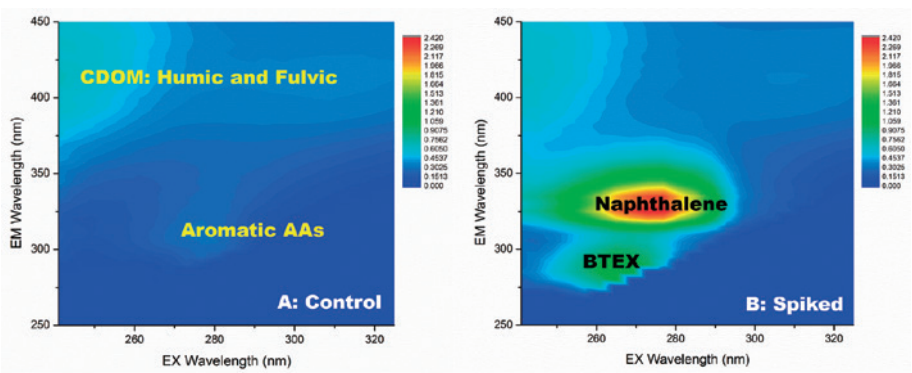

Figure 3 A-TEEM contour plots for a raw surface water control sample (A) with 1.86 mg/L dissolved organic carbon and a matching sample (B) spiked with 100 µg/L of Naphthalene and 100 µg/L of BTEX (25 µg/L of each compound). Signal contour areas associated with humic acid-like, fulvic acid-like and aromatic amino acid-like DOM components are labeled in Panel A. The signal contour areas associated with Naphthalene and BTEX are labeled in Panel B.

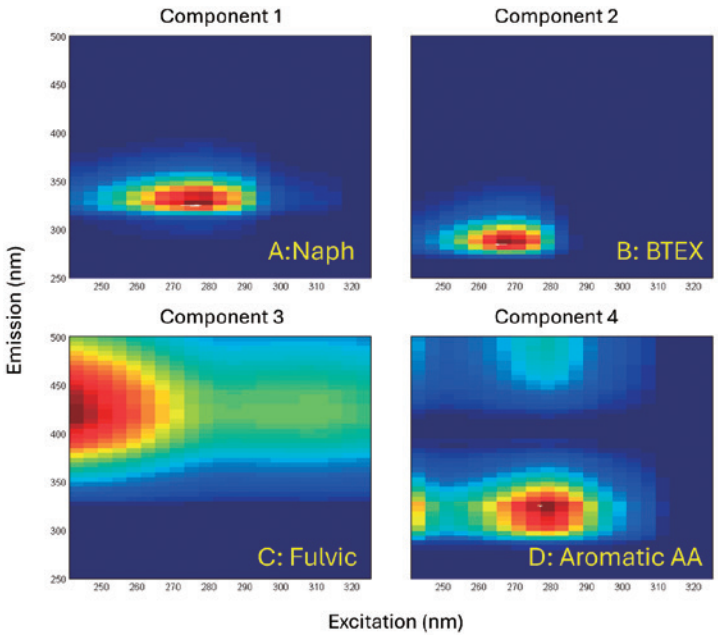

Figure 4 PARAFAC component loading plots for a 4 component model of the Raw water sample shown in Figure 3 spiked with varying levels from 0-100 µg/L of Naphthalene and 0-100 µg/L of BTEX. The component numbers 1 and 2 correspond to the assignments made based on linear regression correlations of the component scores for Naphthalene and BTEX (see ref.[4]); components 3 and 4 for fulvic acid-like and aromatic amino acid-like compounds were assigned based on earlier models from measured samples of Raw and Finished water from the same treatment plant.

of the three major DOM components. It however is more important to consider the BTEX absorbance/excitation and emission spectra overlap strongly with the UV absorbance for all three DOM components dictating that IFE correction is imperative for accurate BTEX and naphthalene quantification.

Experimental Design, Calibration and Validation for ASTM D8431-22

Having established the basis for BTEX and naphthalene detection above here we explain how this information was used to develop and publish ASTM D8431-22 for the purpose of early warning detection of these oil spill components. The method development began with a Design of Experiment (DOE) protocol for a Ruggedness test (see ASTM Practice E1169[10]) where all essential variables were varied to gauge their influence on the method calibration. Key variables tested included filtration (0.45 µm), turbidity from 0 to 20 Nephelometric Turbidity units, DOM concentration (0-15 mg/L), temperature and stirring. The use of 0.45 µm filters both mitigated the effects of turbidity and was needed to obtain the 'dissolved organic fraction' of which the water soluble BTEX and naphthalene are key constituents. It was determined the method was stable up to 15 mg/L DOM whereas beyond this nonlinear IFE effects due to Beer-Lambert linear deviation were observed; dilution could be applied to compensate for DOM concentrations >15 mg/L. Temperature was determined to be best stabilized at 20°C and stirring was insignificant for the dissolved components. Importantly, there was no significant evidence of loss by volatilization for the BTEX or naphthalene components using the method noting best performance includes rapid sampling and analysis and use of Teflon stoppered 4 ml quartz fluorescence cuvettes.

The Ruggedness test set the stage for the final method conditions for the sample preparation and instrument settings, see D8431-22[1] for details, noting accessing this controlled document requires a fee to ASTM. The basic outline of the method includes first standardizing the instrument response as a function of the integration time and CCD camera settings including the gain and binning. This is accomplished using a sealed Type I water Raman Scattering Unit (RSU) sample. The acquired RSU value acts as an external reference standard to account for changes in sample concentration independent of the aforementioned instrument settings. Samples are simply filtered (0.45 µm) through a nylon or glass fiber filter to avoid extractable compounds that may absorb in the UV range as an interference. The scan range was adjusted to include the BTEXN components with the excitation range from 240-325 nm with a 4 nm increment and the emission range from 250-800 nm with a 5 nm binning/interpolation. The default integration time was 1 s and Medium Gain with the sample compartment at 20°C. A blank file was acquired using these conditions with a sample of Type I water and a clean cuvette. The method cites ASTM guidelines for cuvette and glassware cleaning instructions for water-borne oil samples. Subsequent samples were evaluated against the blank sample and the time-date-stamped data files exported for multivariate model calibration and validation/application.

Table 1 Limits of Detection and Quantification* (low and high range) for *BTEXN* based on the Single Lab Study.

Analyte	Low Range	Detection Limit (µg/L)	Quantification Limit (µg/L)	High Range	Detection Limit (µg/L)	Quantification Limit (µg/L)
Benzene		2.52	7.62		6.45	19.55
Toluene		0.45	1.35		5.69	17.23
Ethylbenzene		0.45	1.35		5.69	17.23
Xylenes		0.45	1.35		5.69	17.23
Naphthalene		0.7	2.12		3.98	12.05

*Based on ASTM Practice E2617[11], the Limits of Detection and Quantification were calculated using the respective formulae: *LOD* = 3.3 *s*/*S* and *LOQ* = 10 *s*/*S*, where s is the standard deviation of the Y-intercept and S is the slope of the linear relationship between the regression model predicted and the target concentration values.

Calibration of the Extreme Gradient Boost (XGB) machine learning algorithms for regression (quantification) and discrimination (qualification model for Pass/Fail contaminant threshold testing) were made using the Eigenvector Inc. Solo software. Implementation of the regression and discrimination models used the HORIBA Multi-Model Predictor (HMMP) tool which is a commercial add-in application for Eigenvector Inc.'s Solo and Partial Least Squares toolboxes; the HMMP tool facilitates concurrent batch analysis of samples with either multiple regression models (possibly including multiple algorithms) simultaneously or a single discrimination model including multiple class assignments.

The machine learning algorithms for the method were calibrated and validated according to the ASTM guidelines defined in (E2617[11] and E2691[12]) which respectively deal with multivariate model calibration for empirical models and specifics for pharmaceutical and manufacturing applications. A specific experimental calibration design was applied for the standard preparations of the BTEX and naphthalene compounds to avoid to minimize issues with collinearity effects of the standards. Calibration curves were measured to determine the repeatability, recovery and the limits of detection and quantification for each individual compound and the sum of BTEXN. It was found that use of both high- (>50 µg/L) and low-range (<50 µg/L) calibrations for BTEX and (>20 and <20 µg/L) for naphthalene was useful to insure accurate detection across the wide working range of the method; noting naphthalene exhibited a significantly higher fluorescence yield per weight than any of the BTEX or natural DOM components. The single-lab calibration published in D8431-22 was all measured by spiking the raw source water before filtration to yield detection and quantification limits for the BTEXN compounds.

For the single lab calibration, the coefficient of determination (R^2) for the predicted values was >0.998 for all compound models in both the low and high range calibrations with the exception of Benzene which was 0.988 for the low range calibration. The recovery (%) values for all compounds in both the high and low range calibrations ranged from 99.4 % to 102.7 % except for Benzene in the low range calibration which yielded 21 % at 5 µg/L, which was the lowest concentration tested. Table 1 summarizes the limits of detection for all compounds including the sum of BTEXN for both the low and high range calibrations. Benzene yielded an LOD of 2.52 µg/L in the low range and 6.45 µg/L in the high range calibration. Benzene also yielded the highest detection and quantification limits for both the high and low range calibrations. This indicates Benzene, compared to the other compounds, has the lowest fluorescence yield and or it is associated with higher relative levels of background interference. This subject will be addressed in the scheduled full interlaboratory study. Possible improvements could include increasing the integration time to maximize signals in the Benzene region when signals fall below a threshold level; this would require adjusting the RSU factor to account for the concentration.

With respect to current WHO guidelines and USEPA maximum contamination limits (MCL) Table 2 lists the values for each BTEX compound. The LOD levels for all compounds in the low range calibration (Table 1) fall below both the guidelines and MCL values listed noting for Benzene the LOQ was above the USEPA MCL. It is important to note the WHO and USEPA MCL values represent the finished (distributed to customer) water values. This is especially relevant to the scope of D8431-22 which pertains only to raw untreated source water. Conventional water treatment processes may include treatment with activated carbon, polymers, coagulants for hydrophobic materials and filtration all of which would be expected to reduce soluble BTEX compound levels significantly via adsorption; noting volatilization would be another expected source of loss for BTEX during treatment and distribution.

Table2 Comparison of the WHO Guidelines and USEPA Maximum Contamination Limit (MCL) for the BTEX compounds in finished distributed to consumer) drinking water.

Compound (µg/L)	WHO Guidelines	USEPA MCL
Benzene	10	5
Toluene	700	1000
Ethylbenzene	300	700
Xylenes	500	10000

Conclusion

This article introduces and describes a new A-TEEM standard method for rapidly detecting water soluble oil spill components, primarily BTEX, in raw source water for early warning purposes to prevent uptake of potentially harmful materials by a drinking water treatment plant. The D8431-22 method was recently published by the ASTM D19.06 organics subcommittee on water quality based on a single-lab calibration study and is pending a full interlaboratory study due in 2027. The method is advantageous being rapid (<5 min per sample) and requiring minimal sample preparation (only filtration). The A-TEEM method is comparable in sensitivity requirements to the conventional Solid Phase Microextraction Gas-Chromatography Flame Ionization detection which can require up to 25 min run time among other time-consuming preparative steps. The D8431-22 method thus shows promise for rapid, accurate detection of BTEX in a wide variety of freshwater sources further noting it can be conceptually adapted to other types of water production as shown by Madhav and Gilmore[13] for hydroelectric dams and fuel oil spills during oil-assisted generator startup procedures.

* Editorial note: This content is based on HORIBA's investigation at the year of issue unless otherwise stated.

References

[1] *ASTM D8431-22.* Standard Test Method for Detection of Water-soluble Petroleum
Oils by A-TEEM *Optical Spectroscopy and Multivariate Analysis.*

[2] Bobra, M., "Solubility behaviour of petroleum oils in water," *Environment Canada Report,* (1992).

[3] Guard, H.E., NG, J. and Laughlin, R.B., "Characterization of gasolines, diesel fuels and their water soluble fractions," *Naval Biosciences Laboratory Report,* (1993).

[4] Adam M. Gilmore, Linxi Chen, "Water Soluble Fraction (WSF) contaminant detection using machine-learning Absorbance-Transmission Excitation Emission Matrix (A-TEEM) spectroscopy," *Proc. SPIE 11233,* Optical Fibers and Sensors for Medical Diagnostics and Treatment Applications XX, 112330H (20 February 2020); doi: 10.1117/12.2556434.

[5] Adam M. Gilmore, Linxi Chen, "Optical early warning detection of aromatic hydrocarbons in drinking water sources with absorbance, transmission and fluorescence excitation-emission mapping (A-TEEM) instrument technology," *Proc. SPIE 10983,* Next-Generation Spectroscopic Technologies XII, 109830E (13 May 2019); doi: 10.1117/12.2522498.

[6] Gilmore, A., Tong, M. System and Method for Fluorescence and Absorbance Analysis, *U.S. Patent 10,168,310 B2, 2019,* Issued January 1, 2019.

[7] Gilmore, A. Determination of water treatment parameters based on absorbance and fluorescence. *US 11874226B2.* Issued January 16, 2024.

[8] Gilmore, A., Tomioka, Y. Determination of water treatment parameters based on absorbance and fluorescence. *US 10184892.* Issued January 22, 2019.

[9] Gilmore AM. How to collect National institute of standards and Technology (NIST) traceable fluorescence excitation and emission spectra. *Methods in Molecular Biology.* 2014;1076:3-27.

[10] *ASTM E1169-21.* Standard Practice for Conducting Ruggedness Tests.

[11] *ASTM E2617–17R24.* Standard Practice for Validation of Empirically Derived Multivariate Calibrations.

[12] *ASTM E2891–20.* Standard Guide for Multivariate Data Analysis in Pharmaceutical Development and Manufacturing Applications.

[13] Madhav, H., Gilmore, A.M. (2024) Identification of oil contamination in process water using fluorescence excitation emission matrix (FEEM) and parallel factor analysis (PARAFAC). *Water Sci Technol* (2024) 90 (3): 908–919.

Adam M. GILMORE

Fluorescence Product Manager
Fluorescence Division
HORIBA Instruments Incorporated,
Ph.D.

Modular Water Supply Quality Monitor that Reduces Time Spent on Site

IRIE Kazuhiro

KOBAYASHI Issei

Monitoring the water quality at the end of water supply pipes is essential to supplying safe and secure tap water. In recent years, the introduction of systems has accelerated in capital cities in Southeast Asia, and the TW series of automatic tap water quality analyzers have been introduced in Malaysia and Thailand. Maintenance is essential for stable operation of the equipment, but there is a strong need to shorten on-site work as much as possible in terms of improving efficiency and ensuring the safety of workers working under high-temperature environments. We have recently developed the GX-100 modular water supply quality monitor to meet the aforementioned market challenges, and we would like to describe its features.

Keywords
module sensor, modular water supply quality monitor, reduced work time, smartphone, Bluetooth® communication, USB communication.

Introduction

In Japan, water quality standards for tap water are established under the Water Supply Act and related ordinances. Water quality inspections are conducted at various points, including the outlet of water purification plants, distribution reservoirs, and the endpoints of water supply pipes. The methods for these inspections are stipulated by Ministry of Health, Labour and Welfare Notification No. 99 (issued on March 21, 2024). As water quality checks by manual analysis take time, many local governments have adopted water quality measurement monitors. In order to ensure accurate measurements, water quality measurement monitors must be maintained at regular intervals. However, due to labor shortages caused by the declining birthrate and the retirement of engineers with technical expertise, there is a need for simpler and less time-consuming maintenance methods. In other countries, tap water supply standards are also set in each country and the water quality monitoring systems at the end of water supply pipes is being introduced. In Southeast Asia, maintenance is major stress factor for maintenance companies. In addition to the harsh environments with high temperatures and squalls, the scattered locations of measurement devices require technicians to spend a lot of time not only travelling, but also maintaining the devices. Furthermore, missing data due to long maintenance times poses a risk to the quality of tap water.

Although our previous products are compactly packaged with multiple sensors to save space, their maintenance take time. This is because multiple parts must be removed in order to remove the sensor unit. Furthermore, calibration can be performed only on site and takes approximately one hour for all sensors. With GX-100, on-site work can be completed in approximately 15 minutes by simply replacing the sensor that is already calibrated at the office or laboratory because calibration data is stored in the sensor module.

GX-100

GX-100 (Figure 1) employs a modular design to reduce on-site work time. Each module is described below.

Interface Module (IM): GX-100 communicates with external devices using this module.
It communicates with smartphones via Bluetooth® communication and connects to PCs via USB.

Pre-Processing Module (PPM): A filter is equipped to generate zero water* for calibrating turbidity, color, and residual chlorine. The lines are automatically switched between in normal measurement and in zero calibration. It also measures pressure, temperature, and flow rate.

Sensor Module (SM): There are three types of modules for sample measurement: turbidity/color SM, free residual chlorine SM, and conductivity/pH SM. These SMs can be attached and detached without any tools.

Flow Cell (FC): This cell has a sample flow path and electrical contacts to the SM.

* Zero water is water with zero turbidity, color, and free residual chlorine concentration.

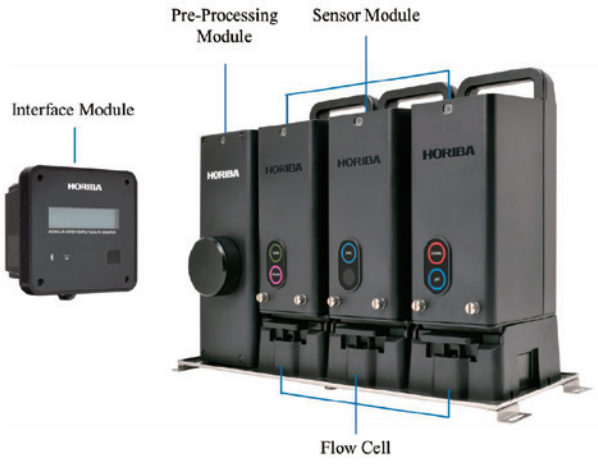

Figure 1 GX-100.

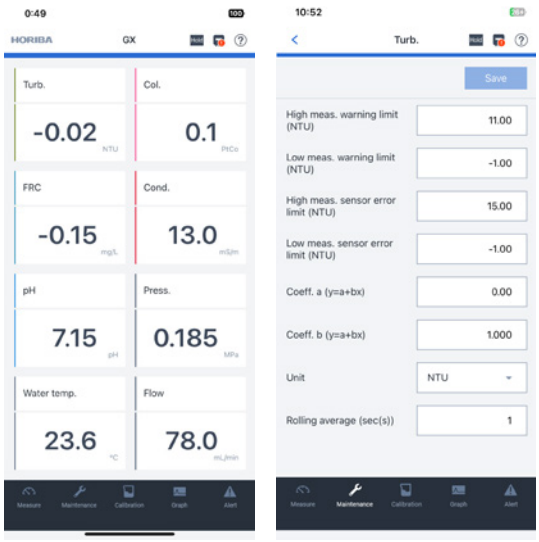

Figure 2 Measurement display of GX-100 application.

GX-100 consists of the above four modules. Measurement values can be checked and water quality meter settings can be changed using a mobile device or a PC with a dedicated application installed.

Compared to our previous products, GX-100 has a large screen with excellent visibility, allowing multiple measured components to be checked at once (Figure 2). GX-100 realizes reduced on-site time and easy maintenance through the modular design and the dedicated application. GX-100 also realizes maintenance cycle extension (reduce maintenance) with physical continuous cleaning function.

Easy maintenance

Frequently maintenance work is necessary to obtain stable and accurate measurements with a continuous water quality monitor. Work on site is required with our previous products, but it may be interrupted or postponed due to weather conditions. To alleviate this stress, maintenance work for SM of GX-100 can be performed not only on-site but also at the office or a laboratory. Unlike on-site, the office has all the necessary tools and reagents for maintenance. We believe that performing maintenance work in this environment reduces maintenance-related stress.

We also provide a dedicated kit for calibration, which reduces calibration time and the amount of calibration reagents required.

Our previous products are compactly designed with multiple cells connected directly to each other and cannot be easily disassembled. Therefore, more reagents are required because all measurement cells need to be filled

Figure 3 GX-100 calibration kit.

with calibration reagents when a sensor for a single measured component is calibrated. The calibration for X-100 can be performed by attaching each SM to the calibration kit (Figure 3) and by pouring the target calibration reagent. When using this calibration kit, the calibration can be performed simply by using USB communication to connect the SMs with the PC in which the GX-100 dedicated app is installed.

This dedicated application allows checking the current measurement values, past calibration history, and calibration values on a single screen, which prevents unintended calibration (Figure 4). The calibration kit is easy to carry because it does not require a power source, such as a pump, to pour the calibration reagent into the SMs. Calibration can be performed anywhere.

Reduce maintenance

If the maintenance is performed frequently, the stress to the operation of the water quality monitor remains unchanged despite of easy maintenance. The main factors requiring the maintenance are contamination, air bubbles, and flow rate. GX-100 has measures to reduce the frequency of maintenance. One of the measures is a continuous cleaning mechanism for the turbidity and color SM.
Although our previous turbidity meter series also has a cleaning function, the light path is blocked by the cleaning mechanism during the cleaning because the optical measurement is used as the measurement principle, resulting in missing measurement data.

For a sample containing a large amount of dirt, the cleaning frequency increases and the number of missing measurement data also increases, which may prevent the seamless acquisition of water quality trend data. For GX-100, the cleaning mechanism has been redesigned to eliminate the missing data, enabling continuous cleaning and continuous measurement.

The cleaning method generally used in our previous products is a mechanism employing a wiper that moves to clean the inside of a fixed glass cell. GX-100 employs a fixed cleaning wiper and rotates the glass cell to enable the continuous cleaning and the continuous measurement without blocking the light path. This continuous cleaning reduces the frequency of the maintenance by removing dirt and bubbles adhering to the surface of the glass cell.

The wiper unit (Figure 5) where the wiper is fixed has three functions.

The first is to fix the cleaning wiper. This wiper is designed to be easily replaced by the user without special tools or skills.

The second is to prevent stray light. GX-100 turbidity meter uses a 90-degree scattering method.
In this method, the light emitted from the light source is

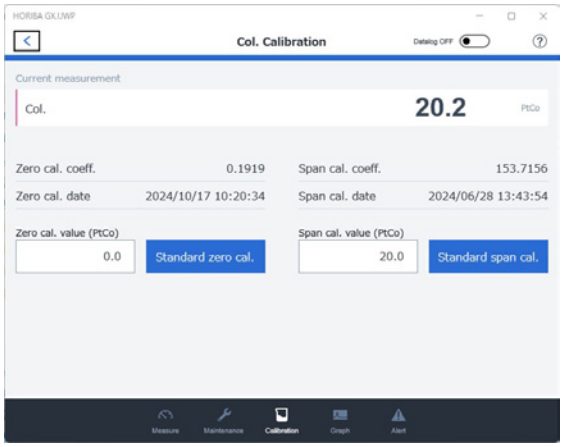

Figure 4 Calibration mode of app.

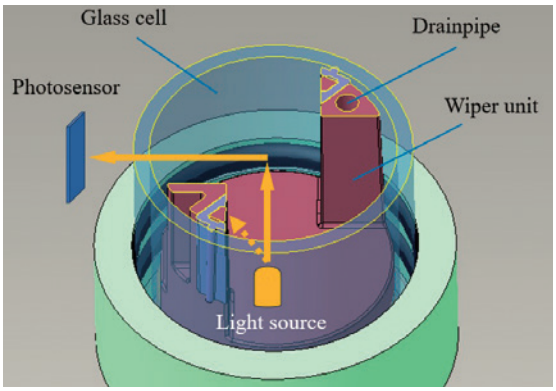

Figure 5 Wiper unit.

scattered by suspended substances and is received at a position 90 degrees to the light source. Ideally, only light scattered at a 90-degree angle should be detected. However, in reality, light other than pure scattered light, which is called stray light, also exists in the measurement cell. Light from the light source, as one of the stray lights, is directly detected by the photosensor. This stray light varies depending on the variation of the multiple components of the detection section and their operating temperature, causing measurement errors.
GX-100 prevents stray light by placing the wiper unit between the light source and the light receiving element located at a 90-degree angle, thereby reducing measurement errors.

The third is to remove bubbles remaining inside the measurement cell. Bubbles may form in the sample water when the sample water starts to flow or when the pressure or temperature of the sample water changes. These bubbles accumulate at the top of the cell and cause stray light, which leads to measurement errors. Therefore, a drainpipe is provided at the top of the wiper unit to prevent bubbles from remaining in the cell, thereby reducing measurement errors. The above three functions enable stable measurement of turbidity and color.

The second measure to reduce the maintenance is backwashing to ensure a stable flow rate necessary for measuring free residual chlorine.

As free residual chlorine meters produce unstable measurement values due to changes in the flow rate, it is necessary to supply new samples at a constant flow rate. The free chlorine electrode measures the current generated by the reduction reaction of free chlorine on the cathode surface. When the flow rate changes, the concentration of the free chlorine on the cathode surface becomes unstable. As a result, when the flow rate decreases, the supply rate of the free chlorine decreases and the measurement value of the residual chlorine also decreases.

The cause of this flow change is dirt adhering to the piping and filters, and maintenance such as disassembly and cleaning of the water quality meter was necessary to remove this dirt. GX-100 performs automatic cleaning by reversing the flow of the sample inside the water quality meter to remove minute dirt adhering to the piping and filters, thereby reducing the frequency of maintenance requiring disassembly.

The above measures enable stable measurement of turbidity, color, and residual chlorine, which are important water quality indicators for water supply, with low maintenance frequency.

Operation change of water quality meter by modularization

Maintenance of water quality meters is essential for stable water quality measurement, and therefore, water quality meters are maintained daily by engineers. We believe that the features of GX-100 described above will change the operation of the water quality meters.

First, since GX-100 employs the modular design, the only on-site work required is replacement of the SMs. Previous water quality meters required complex work at the installation site, which had to be performed by engineers on site. Furthermore, the distance between each site is far, and the number of sites that can be maintained in a day is limited. It took a long time to maintain the water quality meters at all sites. With GX-100, no tools are required to replace the SMs. The skill level of the workers is not an issue and on-site workers no longer need to be engineers.

Figure 6 Operational method of GX-100.

Table 1 Comparison of calibration time and reagent volume between GX-100 and TW series.

Maintenance Item	GX-100 (min)	Current Product (min)	Reduction Rate
Zero Calibration for Turbidity, Color, Free residual chlorine	10 min	10 min	
Turbidity span calibration	3 min	10 min	
Color span calibration	3 min	10 min	
pH calibration	8 min	20 min	
Total calibration time	22 min	50 min	56%
Maximum reagent amount required for calibration (per 1 parameter) *	300 mL	800 mL	63%

*Regarding the pH calibration, this is the amount of reagent required for one-point calibration.

Recently, the shortage of engineers has become a social issue, and we believe that GX-100 will play a major role in solving the issue.

Furthermore, SMs can be replaced in an environment with the necessary equipment, such as office or laboratory. Unlike before, it is no longer necessary to bring multiple tools and calibration reagents to the site. On-site work can be completed simply by bringing the replacement SM and a mobile device with the GX-100 app installed. (Figure 6)

The calibration time for SM is shorter than that of our previous products and the amount of calibration reagents to be used has been significantly reduced, resulting in lower running costs for maintenance. (Table 1)

Conclusion

Reducing on-site work is now essential for the operation of the water quality meters, and we have described the features and the operation methods of GX-100 that make this possible. Globally, it is expected that the population will continue to grow and the demand for high-quality water supply will increase. In order to ensure the quality of the water necessary for people's lives, it will become even more important to operate and maintain the water quality meters efficiently. We believe that GX-100 can solve this problem.

In addition, each country has its own specific measured components, and it is expected that the number of items that need to be measured to ensure the water quality will increase in the future. In order to meet these demands, we will continue to ensure the quality of the water supplies around the world with modularized SM, feature of GX-100, and with striving to stable the water quality measurement and to reduce the maintenance. We will continue to develop the water quality meters to meet the demands of each country.

* Editorial note: This content is based on HORIBA's investigation at the year of issue unless otherwise stated.

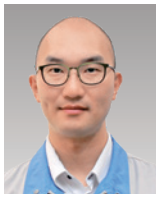

IRIE Kazuhiro

Water Solutions R&D Dept.,
Development Division,
HORIBA Advanced Techno, Co., Ltd.

KOBAYASHI Issei

Semiconductor Process Solutions R&D Dept.,
Development Division,
HORIBA Advanced Techno, Co., Ltd.

Development of the LAQUAtwin Series of Compact Water Quality Meters

TSUJI Kohei

KOMATSU Yuichiro

HORIBA has developed the LAQUAtwin series of compact water quality meters to meet the demand for checking water quality anywhere, anytime, by anyone. The lineup of measurement items so far includes pH, electrical conductivity, salinity, and sodium, potassium, nitrate, and calcium ions, for a total of seven types, but to meet diversifying measurement needs, a fluoride ion meter and an oxidation-reduction potential meter have been newly added to the compact product lineup. In this paper, we review HORIBA's characteristic water quality meters, LAQUAtwin series, and describe the two newly introduced models.

Introduction

Two-thirds of the Earth we live on is covered with water, and approximately 60% of the human body is made up of water. From rivers, lakes, and soil to foods and drinking water, water is essentially present in every aspect of our daily lives. It is useful to visualize the various properties of water that are essential for the survival of humans, animals, and plants. If water components can be measured easily and instantly without complicated operations, it will give us even greater peace of mind in our daily lives and may even lead to new discoveries, surprises, and excitement. However, in reality, it is necessary to prepare containers such as glass beakers for measuring samples and to prepare water quality measurement devices and sensors beforehand. In the measurement of ion components in aqueous solutions, which is one example of water quality measurement, atomic absorption spectroscopy (AA), inductively coupled plasma atomic emission spectroscopy (ICP), and ion chromatography (IC) methods used by professionals are common, which can initially cost 1 million yen or more. A less expensive method is the colorimetric method, which uses color-developing reagents, but this method involves visual inspection or the use of a colorimeter for quantitative analysis, and visual inspection does not allow for quantitative measurement. Typical ion components are widely distributed in concentrations ranging from approximately 100 ppm to 10,000 ppm, but the above-mentioned analysis methods are mainly used in the low concentration range, and dilution of the sample is essential for measurement. Additionally, these devices are expensive and perceived as professional-grade instruments, often associated with complex laboratory procedures. As a result, measurements are often not performed unless absolutely necessary. In order to solve these concerns of users, CARDY[1] was developed in the 1980s, followed by the compact water quality meter "LAQUAtwin" (Figure 1) developed to expanded measurement items with waterproof as the successor.

When the series was launched, seven types of water quality measurement devices were available for various applications, including pH, electrical conductivity, ions (Na^+, K^+, NO_3^-, Ca^{2+}), and salinity (NaCl concentration). The ion selective electrode method was used to measure ion components. The suggested retail price of the ion meter was only a few tens of thousands of yen, which was cost-effective in terms of running costs and measurement time.

Furthermore, since the measurement range was wide, from several ppm to 9,900 ppm, in most cases, measurements could be made without diluting the sample.

In 2024, we added the F^- ion meter and the Oxidation-Reduction Potential (referred to as ORP in the rest of this paper) meter to the LAQUAtwin series as new measurement items, and started their sales.
This paper introduces the features and measurement methods of the compact water quality meter "LAQUAtwin" and describes the two new sensors (F^- and ORP).

Device configuration

Figure 2 shows a typical measurement device configuration. In general ion measurement using electrochemical sensors, either an ion electrode or a pH electrode ②, together with a reference electrode ③, is connected to an ion meter ①. These electrodes are immersed in a sample solution ⑨, which is stirred using a magnetic stirrer ⑤ and stirrer bar ⑥ during the measurement.

In addition, in the ion measurements using electrochemical sensors, a thermistor ④ is used to control the sample temperature because it is necessary to measure the sample in the stable temperature using a constant temperature

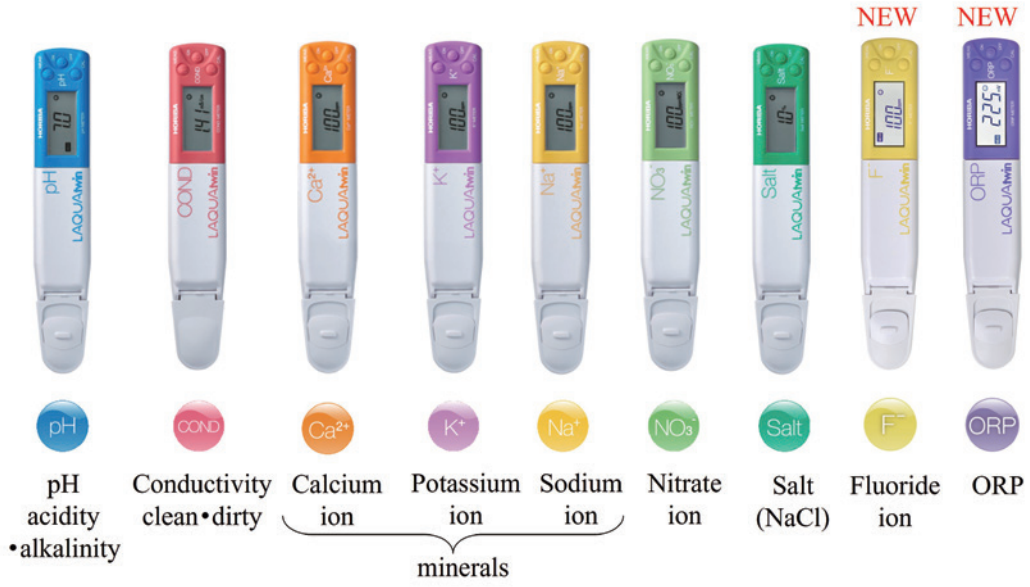

Figure 1 Overview of the LAQUAtwin series

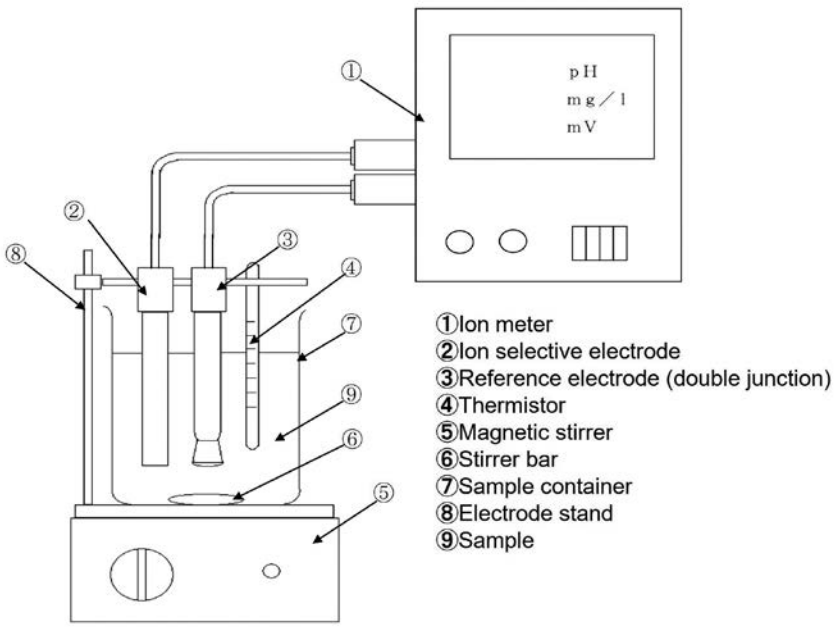

Figure 2 Ion measurement diagram with an ion selective electrode

chamber or similar device to avoid temperature effects. On the other hand, the compact water quality meter has been developed to adopt the flat sheet integrating the electrode ②, the reference electrode ③, and the thermistor ④ with a thickness of only approximately 0.8 mm, as shown in Figure 3. Since the flat sheet is arranged on the bottom of the small spoon-shaped container, the measurements can be made by simply dropping only 100 µL of the sample (300 µL of sample for ion measurement) onto the flat sheet and, additionally, the sample can be measured even if the sample is extracted directly from large quantities of sample such as rivers since the meter itself acts as a container. Furthermore, highly reliable data as the same as the data obtained in a laboratory can be easily obtained without any beaker in any places since the ion meter ① with the digital display is integrated into the compact water quality meter that is structured as IP67-compliant for waterproof and dustproof. The newly added F^- and ORP are also designed to be the same in this specification (Figure 4).

Moreover, since either the ion electrode or the pH electrode, together with the reference electrode, is arranged on the same plane of the flat sheet, and measurements can be made by simply bringing the sample into contact with both electrodes, the user can select the most appropriate measurement method depending on the measurement situation and sample type. This includes not only aqueous

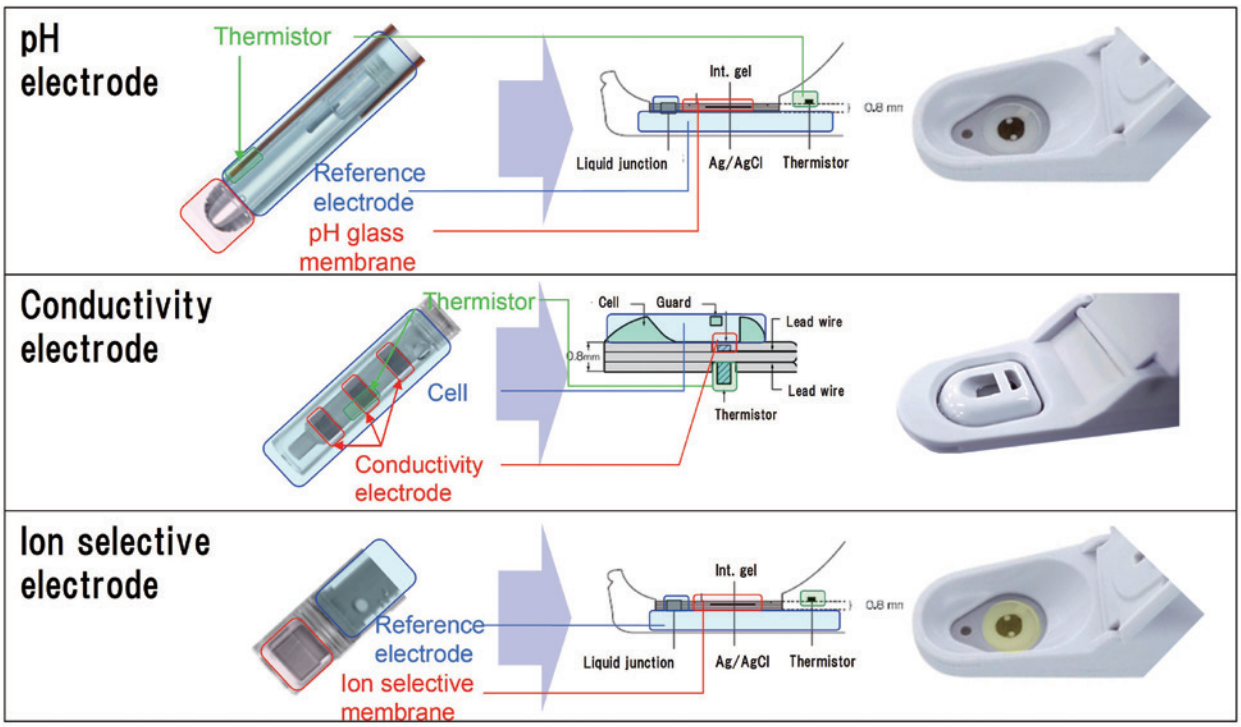

Figure 3 Diagram of Flat sensors

Figure 4 Flat sensor surface for Fluoride ion and ORP measurement

solutions, but also moisture-containing solid materials such as food, powders, paper, cloth, and other pre-wetted sheet-like materials (Figure 5).

For this reason, the unique flat sheet of LAQUAtwin enables highly reliable measurements that are unmatched by other similar models, as well as a variety of measurement methods depending on the measurement scene.

Fluoride ion meter features and its measurement scenes

Here, we introduce the newly developed fluoride ion meter. As same as the conventional LAQUAtwin ion sensors are designed, the gelatinized internal liquid with the flat sheet shape is left firstly, and then the lanthanum fluoride response membrane[2] is placed on the top of the internal liquid, and, finally, they are sealed by bonding together to form the flat sensor. This is the first sensor equipped with the solid membrane among LAQUAtwin ion meters, referring to the bonding technology based on our expertise in assembling the combination fluoride ion selective electrode sold by HORIBA.

Fluoride ions are present in environmental water at concentrations ranging from 0.1 to several tens of ppm, and excessive intake of the ions increases the risk of health hazards. In areas such as Asia and Africa where water supply and sewerage systems have not been well developed, well water and groundwater are still used for drinking but these water may contain the fluoride ions dissolved from rocks and soil in concentrations that exceed WHO water quality standards. The ability to easily check water quality in such situations contributes to ensuring safe and reliable drinking water.

In addition, wastewater containing the Fluoride ion is treated in the factories related to the semiconductor industry including those in Japan. The fluoride ion meter of the portable LAQUAtwin series have been introduced, enabling the measurement of the fluoride ion concentrations at multiple points in each wastewater line within factories, leading to the monitoring conducted together with the existing on-site water quality meter installed at the final line.

Even in laboratories where precise analysis is required, the operation time using the Ion chromatography method such as the time for dilution can be shortened if the fluoride ion concentration of the sample is known in advance. In this way, this product is also useful as a pretreatment tool for expensive and complex analysis methods.

ORP meter features and its measurement scenes

Here, we introduce the newly developed ORP meter. A platinum plate is used for the working electrode and the working electrode is fixed on the flat sheet using conductive adhesive to secure the electrical conductivity. This is the first sensor without the internal solution in the working solution among LAQUAtwin sensors that use the potentiometric method. In addition, although the conventional ORP electrode used the glass sealing to fix the plat-

Figure 5 Several measurement ways with a planer electrode.

inum working electrode, this sensor uses the bonding process for the integration, achieving the performance required for a compact water quality meter at a low price. The ferricyanide-based standard solution (Zobell's solution), used globally as an ASTM standard[3], is newly employed as the standard solution. The quinhydrone solution has been mainly used, especially in Japan, to check the ORP meter until now but the quinhydrone solution is prone to deterioration and cannot be stored, requiring preparation from powder to liquid each time for use, which is time-consuming. On the other hand, the ferricyanide-based standard solution is less prone to deterioration even when stored as solution and is less toxic, meeting the LAQUAtwin concept of easy measurement anywhere. The potential of the standard solution used in the ORP changes depending on the temperature change but the potential is automatically calibrated according to the temperature of the standard solution measured with the thermistor equipped on the sensor[4], [5], enabling improved measurement accuracy.

ORP measurement can be used to know if there are more the oxidizing substances or reducing substances in the water sample, which is one of the basic indicators of the water quality along with pH. In environmental water and wastewater treatment, measuring ORP together with dissolved oxygen allows detailed evaluation of microbial activity and treatment status based on the degree of anaerobicity. ORP is also used to confirm the quality of functional water such as reduced water. Although ORP is not an indicator of a specific component, ORP rather indicates the overall condition of the sample water by considering the various substances contained in the sample water, and ORP is frequently measured in combination with other measurement items around the world. The addition of ORP to the LAQUAtwin series is expected to create the synergistic effects with the existing products.

Reducing packaging materials to reduce the environmental impact

When the LAQUAtwin series was first launched, it was marketed as a portable laboratory, and the packaging materials were designed to match this concept with a high-quality decorative box. However, in light of the global trend recent years toward reducing environmental impact, it is important not to overlook the consumption of paper resources for packaging materials aimed at appealing design. As a result, the packaging design has been revised. Approximately 30,000 units of the LAQUAtwin series are sold annually. Therefore, even a small reduction in packaging materials can have a significant impact.
The new packaging design achieves a 60% reduction in paper weight compared to the previous model, resulting in an annual reduction of approximately 1.6 tons of paper consumption. Going forward, contributing to environmental sustainability will remain a key challenge in product development, and the LAQUAtwin series has become a pioneering initiative in this regard.

Conclusion

This paper reviewed the LAQUAtwin series, HORIBA's distinctive water quality meters, and discussed the overview of the two new models (F^- and ORP). The compact water quality meters introduced in this paper have not only simplified the water quality measurement in the environment and daily life, but have also opened up new application areas including derivative products in the water quality measurement. We will continue to contribute to activities such as solving environmental issues related to our daily lives and managing water quality through the expansion of the LAQUAtwin series as well as the development of the water quality measurement devices in the future.

* Editorial note: This content is based on HORIBA's investigation at the year of issue unless otherwise stated.

References

[1] K. Tomita, H. Okawa, J. Kojima, *Readout*, 1990, No.1, p.24-32
[2] M. S. Frant and J. W. Ross Jr., *Science*, 1966, Vol.154, p.1553-1555
[3] ASTM D1498-14(2022)e1, approved December 7, 2022.
[4] D. K. Nordstrom, *Geochimica and Cosmochimica Acta*, 1977, Vol. 41, No. 12, p.1835-1841
[5] Bates, R.G., *Determination of pH, theory and practice (2d ed.)* : New York, John Wiley & Sons, 1973, p.333-336

TSUJI Kohei
Advanced Technology Development Department, Development Division
HORIBA Advanced Techno, Co., Ltd.

KOMATSU Yuichiro
Quality Control Team, Quality Assurance Department
HORIBA Advanced Techno, Co., Ltd.

Innovations in Continuous pH Measurement Technology for Wastewater Treatment Processes

~Reduction of Maintenance Load: Industrial Self-Cleaning pH Electrode~

NISHIO Yuji

KOMI Takuhisa

In the pH measurement of industrial wastewater, contamination of the pH response glass by various organic compounds and microorganisms and clogging of the liquid junction of the reference electrode are problems because measurements are made continuously. Therefore, periodic cleaning and calibration are necessary to ensure stable and accurate measurements, which poses a significant burden on operators and a safety risk. To solve these problems, the authors commercialized pH electrode with a self-cleaning function. The electrode consists of a glass pH electrode coated with titanium dioxide (TiO_2), which is irradiated from a built-in UV-LED to the TiO_2 photocatalyst. The basic performance of the self-cleaning pH electrode is comparable to that of conventional pH electrodes, and in an implementation test in a microbial treatment tank, the self-cleaning pH electrode maintained sensitivity of more than 95% after more than 16 months of cleaning, while the current electrode required manual cleaning every month. In mounting tests at sites with large maintenance loads due to organic contamination, the self-cleaning pH electrode remained clean for a certain period of time, achieving no maintenance.

Keywords

pH, Glass electrode, Self –Cleaning, Maintenance free, TiO_2, Anti-fouling

Introduction

The world's population has exceeded 8 billion, and the impact of human activities on the global environment is increasing. While the population continues to grow, the amount of water available for drinking is 1% or less of the total water on the Earth. The conservation of the water environment becomes even more important in the future[1]. Therefore, it is important to measure and manage water quality for human beings to ensure the sustainable use of water resources. Sewage generated from daily life and various industrial activities is treated to protect the water environment of rivers and oceans before being returned to rivers. pH management is essential to optimize the process of purifying this sewage. For this purpose, in wastewater treatment facilities of general factories as well as sewage treatment plants, pH is measured and controlled at their many places. Among these places, organic matter with high concentration such as oil, sludge, and microorganisms are contained in raw water tanks, microbial treatment tanks, and final discharge tanks, which are for wastewater. Therefore, when pH electrodes are immersed in the above-mentioned samples for extended periods, contamination accumulates over time, making stable measurements difficult. The most common method for addressing contamination on electrodes is manual cleaning by operators, which places a heavy maintenance burden on operators and poses safety risks.

On the other hand, industrial pH electrodes are generally considered to be well established, and there has been little research and development on pH electrodes, leaving the above issue unresolved. Then, the authors developed a UV-LED-integrated pH electrode with a self-cleaning function that utilizes photocatalytic effects (photoinduced hydrophilicity and photodegradation) to address the fouling issue of pH electrodes. The reference electrode contains KCl granules in the internal solution and uses a water-insoluble gel with high UV transmittance. Additionally, a through-hole (open junction) was adopted in the liquid junction to eliminate clogging. The basic performance of the self-cleaning pH electrode is evaluated, and the results show that it has almost the same performance as the current product has although it is coated with titanium dioxide (TiO_2). Furthermore, field tests were conducted, and the results show that the electrode maintained surface cleanliness and performance in sites where organic fouling occur, such as the microbial treatment tanks, the raw water tanks, and the final discharge tanks, which are for domestic wastewater. This result indicates that the maintenance and calibration cycles can be extended significantly. This paper describes the development of the self-cleaning pH electrode that contributes to solving these maintenance burden issues.

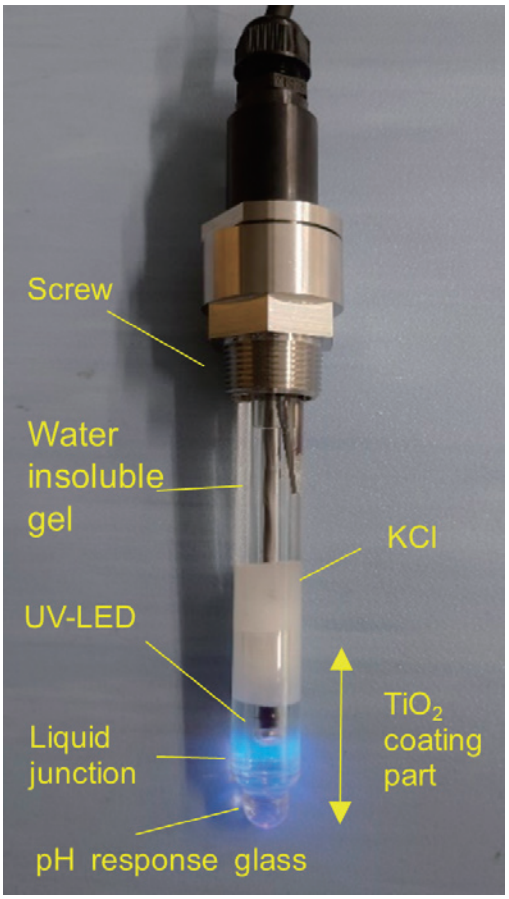

Figure 1 Picture of self-cleaning electrode 6122SA.

Electrode development and performance evaluation

Figure 1 shows the photograph of the newly developed UV-LED-integrated electrode with the self-cleaning function that utilizes photocatalytic effects (photoinduced hydrophilicity and photodegradation). Specifically, the electrode was structured so that the pH response glass membrane and the liquid junction were coated with TiO_2 and UV light was irradiated from the inside of the electrode. TiO_2 was coated approximately 30 mm from the tip of the electrode using the sol-gel method covering the pH response glass and liquid junction. Since titanium dioxide is an insulating material, the electrode does not respond when the pH response glass is covered completely. The reason why the sol-gel method was used is that the porosity film can be formed and its thickness can be controlled easily[2]-[4]. XRD (Smart Lab, manufactured by Rigaku) was used to check the presence of TiO_2 on the surface and a spectroscopic ellipsometer (UVISEL2, manufactured by HORIBA) was used to measure the film thickness. The transparent water-insoluble gel with low UV absorption was adopted as the internal solution of the reference electrode, eliminating the need for KCl solution replenishment[5]. In addition, the liquid junction was designed as an open junction that was not affected easily by

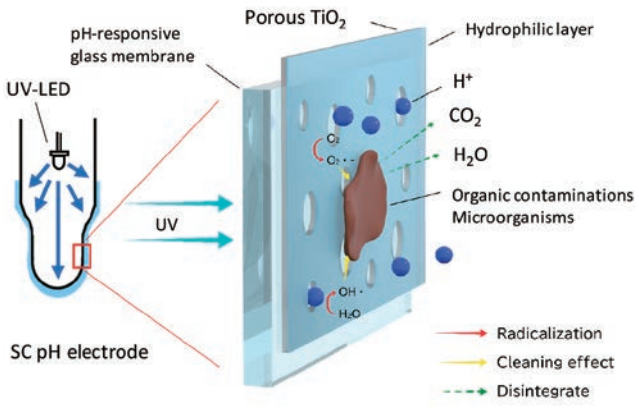

Figure 2 Schematic diagram of self-cleaning (SC) function.The rights to this illustration belong to HORIBA Advanced Techno,Co., Ltd.

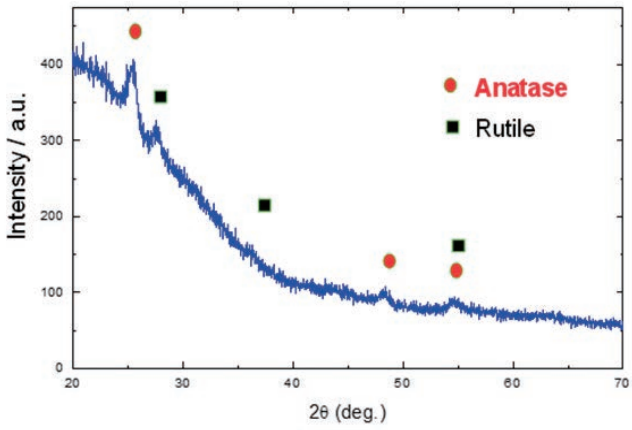

Figure 4 XRD Pattern of TiO_2 Coated Glass. Reprinted with permission from Ref. [1]. *Copyright 2018 EICA*

contamination[6]-[11]. The basic performance of the developed electrode was evaluated in terms of the asymmetric potential, the sensitivity, and the liquid junction potential by measuring the potential using the pH standard solutions.

Figure 2 shows a schematic diagram of the self-cleaning function of the electrode. The mechanism of the electrode is as follows. The surface of the pH response glass membrane was coated with porous TiO_2. UV light passed through the pH response glass membrane and irradiated TiO_2. Activated TiO_2 formed superoxide radical anions ($O_2^{\bullet -}$) and hydroxyl radicals ($OH^{\bullet}$) from oxygen (O_2) and water (H_2O) respectively. These active species decomposed organic matter. In addition, the photoinduced hydrophilic effect of photocatalyst washes away dirt, as this technology is used on the building exteriors. Hydrogen ions pass through the porous TiO_2 film and reach the pH response glass membrane.

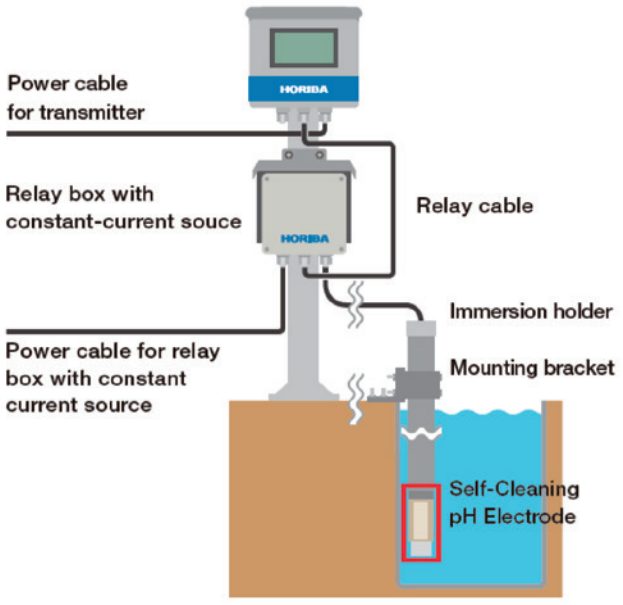

Figure 3 Schematic diagram of on-site installation (Immersion type). The rights to this illustration belong to HORIBA Advanced Techno, Co., Ltd.

Figure 3 shows a typical connection method from the pH meter to the electrode in this field test. Conventionally, the electrode cable was connected only to the transmitter. However, in the case of the self-cleaning pH electrode, a relay box with a constant current power supply was required to turn on the UV-LED. The anti-fouling effect was confirmed with the field test by immersing the electrodes continuously in a microbial treatment tank and in a raw water tank that are for domestic wastewater and are subject to the organic fouling.

Results and discussion

First, we checked that TiO_2, which was the photocatalyst, was formed as intended. TiO_2 was coated on commercially available glass plates using the sol-gel method. Figure 4 shows the result of XRD measurement on the coated surface. Diffraction patterns were observed including rutile-type and anatase-type. It was confirmed that the expected photocatalyst was formed as reported that the anatase-type TiO_2 was activated as a photocatalyst at wavelengths shorter than 388 nm. Next, the thickness of the TiO_2 film on the support tube was measured using the spectroscopic ellipsometer. The measurement point was set on the opposite side of the liquid junction through hole of the stem tube. Table 1 shows the results. The “roughness layer” in the table refers to the layer including surface irregularities. The average of the total value was 27.48 nm. Since the TiO_2 coating on the electrode contained a large amount of SiO_2, which was a component of the response glass membrane, the UV light emitted from

Table 1 Measurement of TiO_2 film thickness on stem tube using ellipsometer. Reprinted with permission from Ref.[9]. *Copyright 2024 Bunseki Kagaku.*

Sample number	1	2	3	average
Roughness layer (nm)	4.70	7.99	3.56	5.42
TiO2 layer (nm)	23.86	19.99	22.33	22.06
Total (nm)	28.56	27.98	25.89	27.48

inside the stem tube passed through the pH response glass membrane and was irradiated onto the outer TiO_2 coating film. The UV intensity was measured using the UV irradiance meter (YK-35UV, manufactured by Kenis) showing that the UV irradiance near the liquid junction was approximately 2.0 $mWcm^{-2}$.

Next, eight electrodes were assembled as composite electrodes as shown in Figure 1 and their basic performance was evaluated[12]. Table 2 shows the results. As shown in Table 2, the self-cleaning pH composite electrode developed by the authors responded as nearly identical to the theoretical sensitivity, approximately 96% or higher, in the range between pH 4.01 and pH 9.18. The calibration range of the asymmetric potential is ±90 mV, and the liquid junction potential of the self-cleaning pH electrode was within approximately 6 mV (equivalent to 0.1 pH) although the gel-type internal liquids generally tend to generate liquid junction potentials. These results were comparable to those of commercially available products and were within a range that would not cause practical problems.

Field tests were conducted at more than 20 locations using these electrodes. The measurement results, out of these tests, are reported, which were conducted at a microbial treatment tank (an aeration tank) for domestic wastewater, an inflow special manhole at a sewage treatment plant, and a final discharge tank at an inorganic material manufacturing plant. These sites are heavily contaminated with organic matter, such as microorganisms and sludge, and manual cleaning are required for these sites once a month. Figure 5 shows the condition of the electrode during the implementation test at the site for 16 months. The current to the UV-LED for the test was set at the normal setting of 100 mA. The test began in December, and slight contamination was observed during the summer months of July to September. During the other periods, the self-cleaning pH electrodes maintained cleanliness with no contamination observed on the glass membrane or around the liquid junction. The performance of the electrodes was checked every two to three months. Figure 6 shows the change in the sensitivity over time calculated using the equation shown in *2 (the Nernst equation) with a pH standard solution. At six to nine months elapsed, which was the summer months, the sensitivity decreased to approximately 80%, but remained above 95% during other periods. The possible cause is the slight contamination on the electrodes in summer, as shown in Figure 5. When microbial activity is high in summer, it seems that the decomposition rate is slow compared to the contamination rate. It is desirable to increase the current.

In addition, during this 16-month period, the liquid junction potential of the reference electrode in each standard solution was maintained within ±3 mV, and no clogging

Table 2 Standard property of the Self-Cleaning pH electrodes. (n=8) Reprinted with permission from Ref.[9]. *Copyright 2024 Bunseki Kagaku.*

Asymmetry Potential (mV)	pH6.86*1	-24.1±4.1
	pH4.01	144.3±4.3
	pH9.18	-155.9±4.6
Sensitivity (%)*2	pH6.86-4.01	99.9±0.5
	pH6.86-9.18	96.0±0.1
	pH4.01-9.18	98.1±0.7
Liquid junction potential (mV)*3	pH6.86	3.9±1.2
	pH4.01	2.0±0.7
	pH9.18	1.5±0.7

*1 Asymmetry Potential
*2 Sensitivity was calculated by the following formula.

$$\text{Sensitivity (a - b) (\%)} = \frac{-100F(E_b - E_a)}{2.3026RT(pH_b - pH_a)}$$

E_a and E_b represent the electromotive forces generated in the respective test solutions a and b, with reference to the comparison electrode. Here, R denotes the universal gas constant (8.3145 $J{\cdot}K^{-1}{\cdot}mol^{-1}$), T is the absolute temperature (K), and F is the Faraday constant (96485 $C{\cdot}mol^{-1}$).

*3 Liquid junction potential was calculated by the following formula. Liquid junction potential(mV)=(Potential in each standard solution / mV) - (Potential in 3.33 mol L-1 KCl solution / mV)

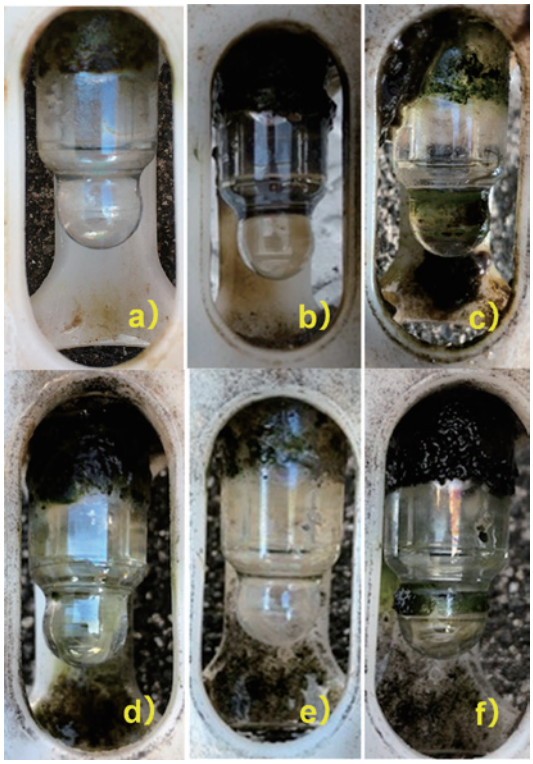

Figure 5 Photos of the change over time of the SC electrode in the microbial treatment tank : a) 5 months : b) 7 months : c) 9 months : d) 12 months : e) 14 months : f) 16 months. Reprinted with permission from Ref.[9]. *Copyright 2024 Bunseki Kagaku.*

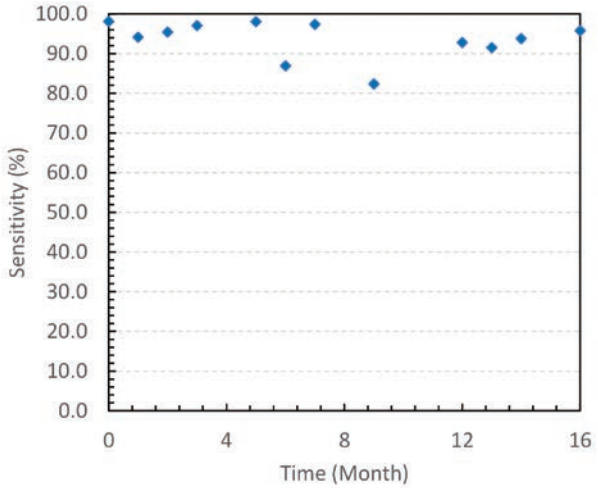

Figure 6 Change in sensitivity of Self-Cleaning pH electrode over time in microbial treatment tank. Reprinted with permission from Ref.[9]. *Copyright 2024 Bunseki Kagaku.*

occurred in the liquid junction. Although the KCl granules decreased gradually, some remained after 16 months. And the reference potential (potential difference in a 3.33 mol/L KCl solution between an Ag/AgCl electrode (#2565 of HORIBA Advanced Techno, Co., Ltd.) and the self-cleaning pH electrodes) maintained at 3 mV or less. These results suggest that the maintenance and calibration cycles can be extended.

In addition, it is confirmed that the life and performance of the reference electrode can be maintained for 16 months or more. Next, we report the results of continuous measurements at an inflow special manhole for domestic wastewater. This site is heavily contaminated with microorganisms and sludge as the same as the microbial treatment tank is, where the manual cleaning is required every two weeks. Figure 7 shows the condition of the self-cleaning pH electrodes by month. At this site, the self-cleaning pH electrodes under the continuous UV irradiation maintained cleanliness without any contamination on the pH response glass membrane or around the liquid junction that were coated with TiO_2 while the upper part of the stem tube was contaminated. Figure 8 shows the continuous measurement data for three months. The

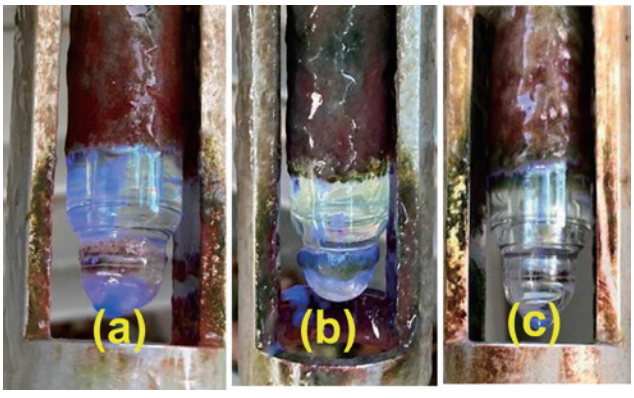

Figure 7 Results of continuous immersion tests in raw domestic wastewater tanks (a: 1 month, b: 2 months, c: 3 months)

pH was stably measured at around 7 without any abnormal value. This electrode maintained the sensitivity of pH between 4.01 and 9.18 at approximately 98% even after three months. In addition, the measured value (asymmetry potential) of the pH 6.86 standard solution was pH 6.74. At this site, maintenance-free operation was achieved for more than six times longer than the conventional operations.

Finally, the results of implementation tests are reported, which were conducted in a discharge tank at a chemical plant. The electrical conductivity of the tank was approximately 600 µS/cm, and the site was home to carp, resulting in a heavy microbial contamination on the electrodes. This site required manual cleaning every month. The continuous measurements were conducted immersing the self-cleaning pH electrodes set with the immersion holder as same as before. The test was conducted with the normal setting of the current to the UV-LED at 100 mA.

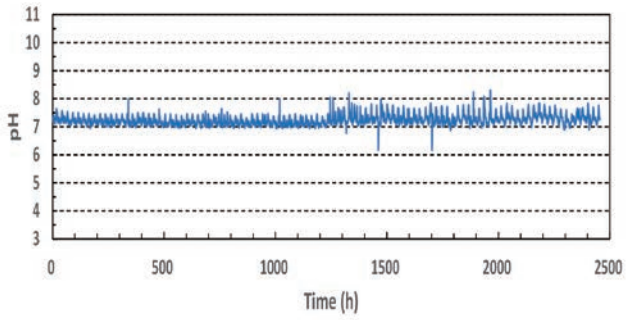

Figure 8 Continuous measurement data for raw domestic wastewater (inflow special manhole) Reprinted with permission from Ref.[8]. *Copyright 2023 Japan Sewage Association.*

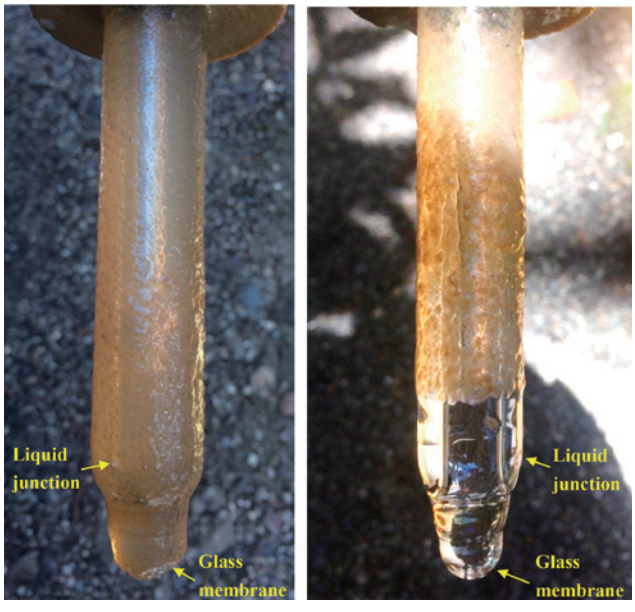

Figure 9 Change in sensitivity of Self-Cleanig pH electrode over time in microbial treatment tank. Reprinted with permission from Ref.[2]. *Copyright 2018 EICA.*

Figure 9 shows the photos comparing the conventional pH electrode with the self-cleaning pH electrode three months after the installation. The self-cleaning pH electrodes were coated three times with TiO_2 film before the test. At this site, the conventional pH electrode was covered with organic matter and biofilm. On the other hand, the self-cleaning pH electrode under the continuous UV irradiation maintained cleanliness without any contamination on the pH response glass or around the liquid junction[2].

Conclusion

In this paper, we have discussed the pH electrode designed to reduce the maintenance burden on users.
The self-cleaning pH electrode using TiO_2 photocatalyst demonstrated that TiO_2 photocatalyst could be applied to the pH glass electrode and that its basic performance was comparable to that of the conventional electrode. In addition, the maintenance-free operation is realized for a certain period of time with the anti-fouling effect in the implementation tests conducted in the sites where the continuous measurements are difficult due to the organic contamination such as microbial treatment tanks for domestic wastewater and return sludge tanks. Regarding the microbial treatment among these tests, it is possible to extend the calibration cycle up to approximately 16 times longer (maintenance frequency from once a month to once every 16 months). These results are expected to contribute significantly to the industry because the maintenance burden on users is greatly reduced. The electrode developed by the authors is applicable to sites with organic contamination but many issues remain unsolved such as anti-fouling to the inorganic contamination. In general, the pH electrode is considered as a matured device, but the authors will try to develop the pH electrode to satisfy the users because the authors believe that the pH electrode will have its potential.

Acknowledgment

We would like to express our sincere gratitude to Prof. Satoshi Kaneko (Mie University), Prof. Tadanori Hashimoto (Mie University), and other professors who provided guidance during this research, as well as to all the employees of our company who provided support.

* Editorial note: This content is based on HORIBA's investigation at the year of issue unless otherwise stated.

References

[1] L.A. Shiklomanov, John C. Rodda, World Water Resources at the Beginning of the Twenty-First Century, *Cambridge University Press*, 13 (2004)
[2] 西尾友志, 室賀樹興, 橋本忠範, 石原篤, EICA 環境システム計測制御学会, 23, 2/3, 69 (2018) (In Japanese)
[3] Y. Nishio, T. Muroga, T. Hashimoto, A. Ishihara: *ISA Analysis Division,* 2-(2), (2018)
[4] 西尾友志, 分析化学, 69, 7/8, 385 (2020) (In Japanese)
[5] 木下隆将, 伊東裕一, 西尾友志, 室賀樹興, EICA 環境システム計測制御学会, 25, 2/3, 59 (2020) (In Japanese)
[6] 西尾友志, 高味拓永, 橋本忠範, 石原篤, EICA 環境システム計測制御学会, 26, 2/3, 107 (2021) (In Japanese)
[7] 西尾友志, 橋本忠範, 月刊「計装」, 64, 9 (2021) (In Japanese)
[8] 西尾友志, 高味拓永, 橋本忠範, 石原篤, 日本下水道研究会, 8, 895 (2023) (In Japanese)
[9] 西尾友志, 高味拓永, 橋本忠範, 石原篤, 分析化学, 73, 4/5, 171 (2024) (In Japanese)
[10] 西尾友志, 高味拓永, e-Readout-014 Issued: June 4, 2024 (In Japanese)
[11] 高味拓永, 西尾友志, 室賀樹興, 橋本忠範, 石原 篤, EICA環境システム計測制御学会, 28, 2/3, 11 (2023) (In Japanese)
[12] JIS Z 8805 : 2011 pH 測定用ガラス電極 (In Japanese)

NISHIO Yuji
Advanced Technology Development Dept.,
Development Division,
HORIBA Advanced Techno, Co., Ltd.
Dr. Eng.

KOMI Takuhisa
Water Solutions R&D Dept.,
Development Division,
HORIBA Advanced Techno, Co., Ltd.

Joy and Fun for Future Scientists, Though Micro Plastic Detection Examination

MIKI Jumpei

Plastic is used in vast quantities around the world as an inexpensive and convenient material that is indispensable to our daily lives. However, in recent years, large amounts of discarded used plastics have been released into the ocean, causing social problems; it has been reported that the oceans in 2050 will contain more plastic waste than fish [1]. Among discarded plastics, microplastics (MPs), which are smaller than 5 mm in size, have the potential to affect the ecosystem. We have developed a simple observation kit to help children, who will be responsible for the future, learn about the plastic waste problem that is happening around them in an easy-to-understand manner. This paper briefly introduces the kit for simple observation of microplastics and hands-on learning activities using the kit.

Introduction

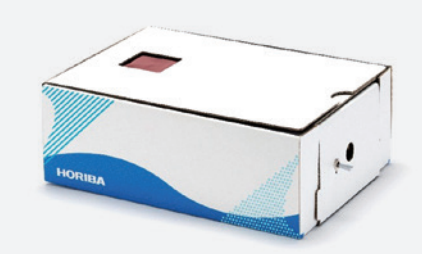

Figure 1 A simple observation kit “PLAWATCH”

HORIBA Techno Service, Co., Ltd. has developed “PLAWATCH” that is a simple observation kit to detect MPs, allowing ordinary citizens and children to detect the presence of MPs in their everyday environment using a smartphone (Figure 1).

For observation, samples such as sand collected on the seashores and in rivers are washed, and then stained using a mixture of the fluorescent dye “Nile Red” and an organic solvent (referred to as fluorescent staining solution in the rest of this document)[2]. The MPs mixed in the sand is stained through the pretreatment.

The stained sample is irradiated with green light from an LED using the fluorescent properties that Nile Red, contained in the staining solution, emits red fluorescence when excited by green light.
This causes only the MPs contained in the sand to emit red fluorescence (Figure 2). “PLAWATCH” is designed to capture only red fluorescence efficiently by blocking the green light with a red filter (made with cellophane or other material) (Figure 3) since green light as excitation light is not required.

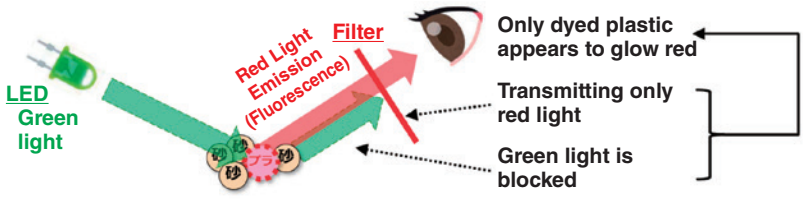

Figure 2 How MPs Emit Red light

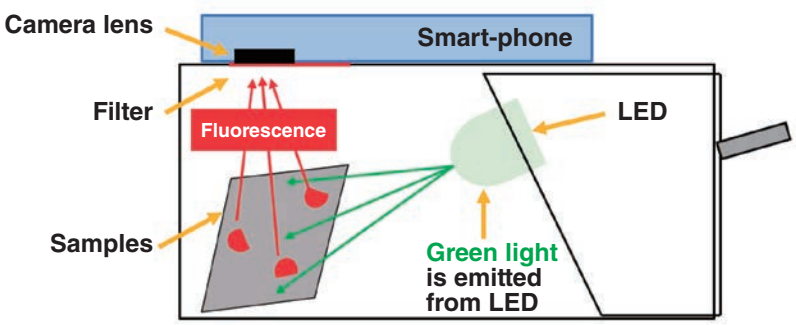

Figure 3 Schemic Diagram of Microplastic Simplified Observation kit (Cross-section)

A smartphone or a camera on tablet devices is placed on the top of the enclosure of "PLAWATCH" to be use as a detector for the observation. Using a camera of smartphone or tablet device allows anyone to observe and record images easily (Figure 4).

Based on the concept of minimizing the use of plastic, the "PLAWATCH" enclosure is made of paper (cardboard) to be environmentally friendly. In addition, the kit is designed for users to assemble by themselves, allowing them to experience the joy of manufacturing.

The sand was collected on the rivers and the seashores in Kyoto Prefecture (Kameoka City), Hyogo Prefecture (Nishinomiya City), Kanagawa Prefecture (Kamakura City), and Okinawa (Iriomote Island), and was investigated using the prototypes of "PLAWATCH".

We found that the plastic waste was accumulated and washed ashore on the rivers and the seashores in the many places where we visited (Figure 5), and then we confirmed that the MPs were mixed with the sand particles using the kit after the surface sand from the surrounding areas were collected, washed, and stained.

Furthermore, building on previous activities, we conducted an MPs observation session using "PLAWATCH" at a workplace tour for children (elementary school students) of HORIBA group employees in August 2024. We collected

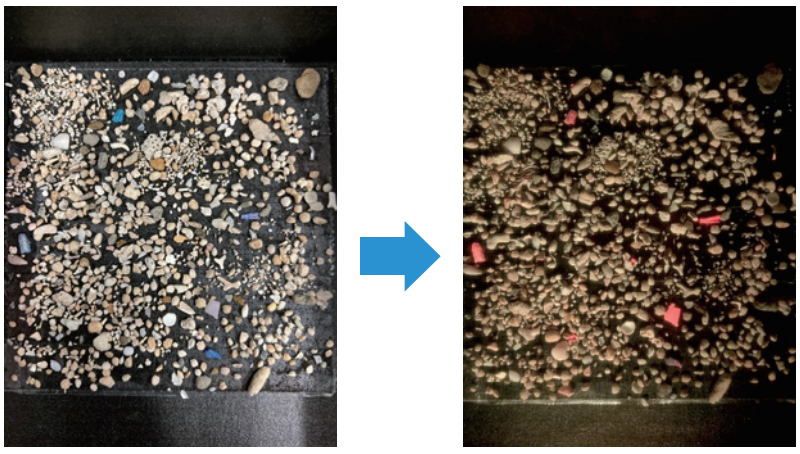

Natural light image　　Fluorescent Image

Figure 4 Comparison of Observation Fluorescence Imaging using PLAWATCH

Figure 5 Large amount of plastic waste washed ashore (on a remote island coast in Okinawa)

HTS engineers collecting sand for use at an event (at coast in Osaka)

Sand collected from various overseas locations (11 prefecutres,12 type)

Figure 6 Preparations for the event

sand from seashores across the country (Figure 6) with the cooperation of the service engineers in the offices of HORIBA Techno Service, Co., Ltd.

After giving an easy-to-understand explanation of the environmental impact of the MPs to the participated elementary school students, we conducted an experiment to observe how much the MPs were mixed in the sand from the seashores.

Each of the participated children selected the sand in which they were interested and observed the sand with “PLAWATCH” and their smartphone after the staining treatment with the fluorescent staining solution by themselves under the guidance of the staff. When they found MPs glowing red in the sand, they were surprised and reported to their parents, “I’ve found it!” (Figure 7).

Sand images taken by the children were overlaid on a map of Japan to create “MPs Map - What’s hidden in the sea sand?” (Figure 8). The observation results showed that MPs were observed in all of the sand collected. This result indicates that MPs are spreading in sand of seashores and rivers throughout the country. We hope that this kind of experiential learning will spark children’s interest in science experiments and environmental issues in the future.

Figure 7 Event highlights A child who participated in the event

Conclusion

Since the press release in October 2024 was very well received regarding the sale of this simple observation kit, we are now promoting further initiatives so that the kit can be used in the environmental education and the extracurricular activities for students.

The environmental education using “PLAWATCH” is also being conducted by educational personnel and research organizations. For example, we are conducting a survey of the MPs on rivers in Kameoka City in collaboration with TAKASAWA Nobue Laboratory at Kyoto University of Advanced Science (Kameoka City, Kyoto Prefecture). In addition, Prof. Makiko Okamoto, the University of the Ryukyus, conducted “Environmental Education through Fluorescent Visualization of Microplastics” using “PLAWATCH” for elementary school students on Iriomote Island in Okinawa in 2024, and we also participated in the local classes.

Additionally, teachers including Mr. Suzuki, Tokyo Metropolitan High School of Science and Technology, are conducting observations using “ PLAWATCH” as one of the ways to confirm that the MPs are contained in bird droppings[3]. In this way, we expect that the product application will expand further in the future.

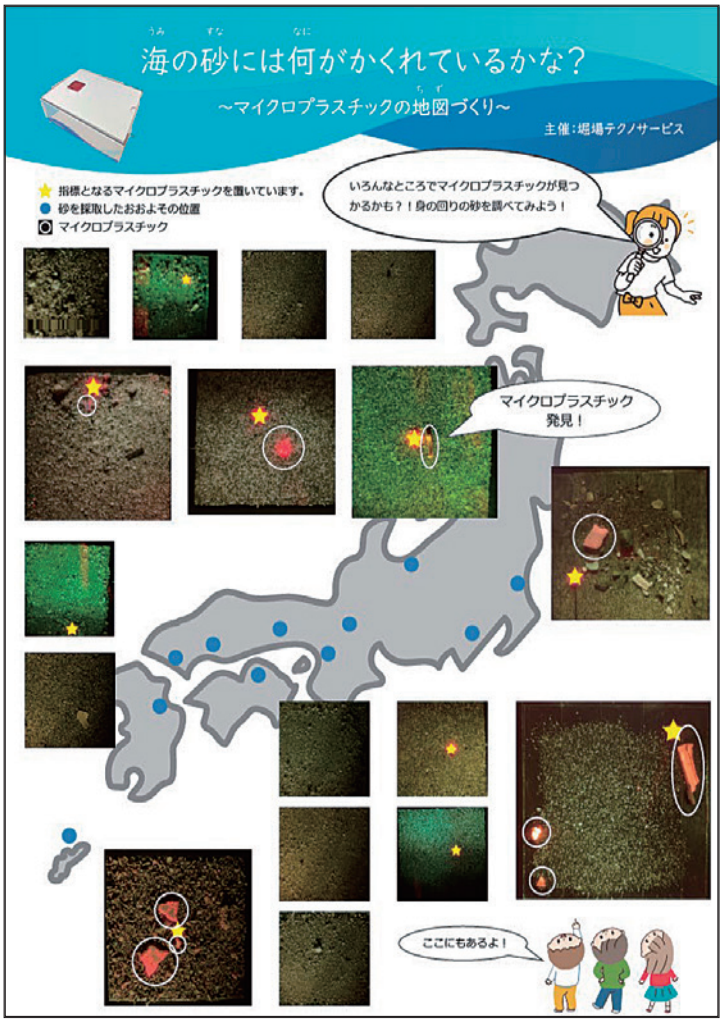

Figure 8 Japanese Map of MPs Observation Images Using the PLAWATCH

We are also working on developing an application that will enable the creation of a global distribution map of microplastics using images captured by "PLAWATCH".

* Editorial note: This content is based on HORIBA's investigation at the year of issue unless otherwise stated.

References

[1] 公益財団法人 日本財団. "2050年の海は魚よりもごみが多くなる？今すぐできる２つのアクション". 2022.08.25, https://www.nippon-foundation.or.jp/journal/2019/20107/ocean_pollution, (参照 2024-12-23). (In Japanese)

[2] Maes Thomas et.al., "A rapid-screening approach to detect and quantify microplastics based on fluorescent tagging with Nile Red", *SCIENTIFIC REPORTS*, 7(1), 1-10 (2017).

[3] 東京都立科学技術高等学校 科学研究部生活科学班. "鳥フンの調査結果から見えるもの". 日本動物学会 第94回大会, 2023.09.09. (In Japanese)

MIKI Jumpei

Engineering Dept.,
Analytical & Technology Division,
HORIBA Techno Service Co., Ltd.

HORIBA World-Wide Network

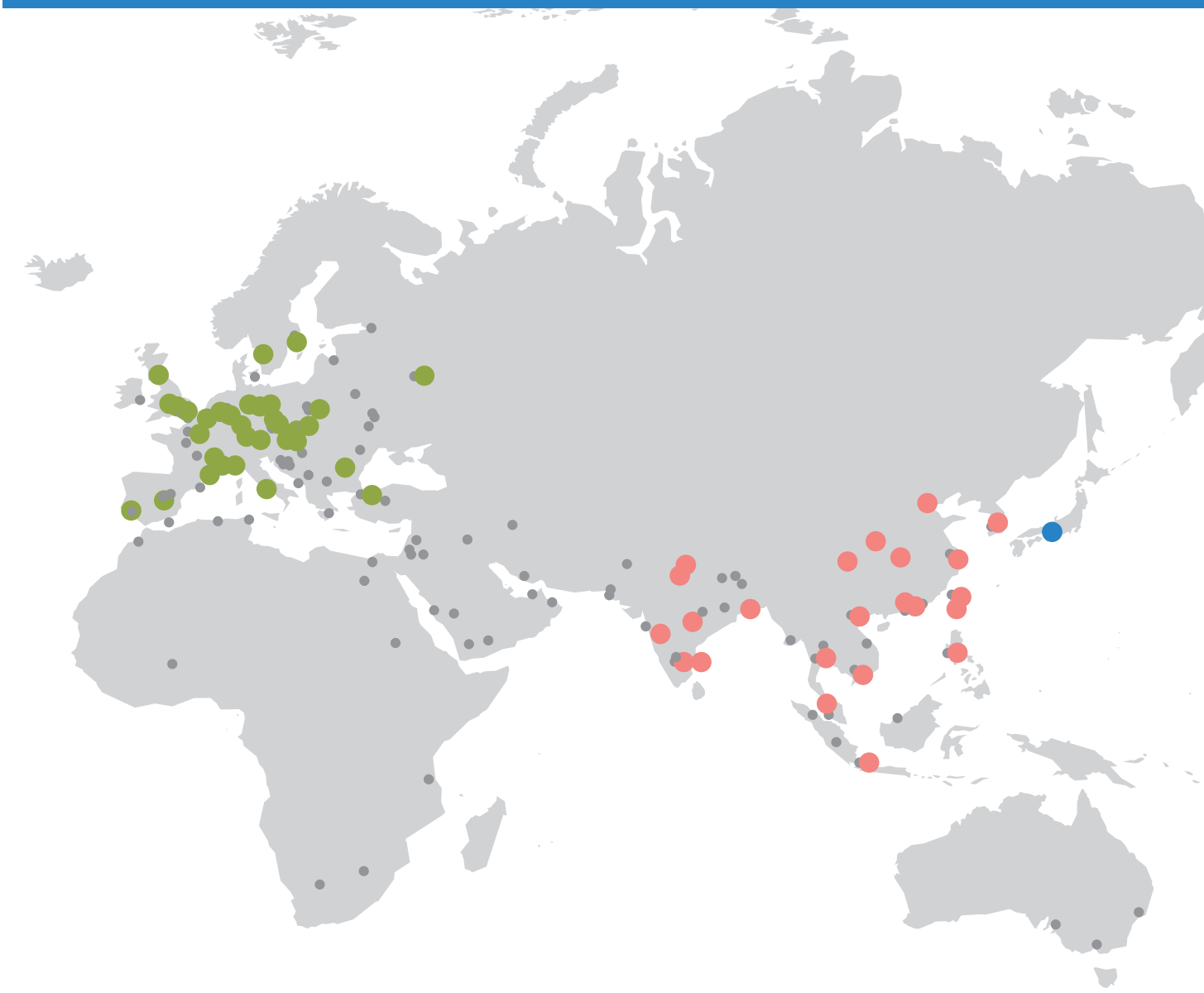

Austria
- HORIBA (Austria) GmbH - Tulln

Czech Republic
- HORIBA Czech
  Olomouc Factory / Prague Office

France
- HORIBA ABX SAS - Grabels
- HORIBA Advanced Techno France SAS
- HORIBA Europe Research Center - Palaiseau
- HORIBA FRANCE SAS - Lyon
- HORIBA FRANCE SAS, Lille Office / Montpellier Office / Vénissieux Office

Germany
- BeXema GmbH
- HORIBA Europe GmbH - Darmstadt Office / Dresden Office / Flörsheim Brake Test Center / Hannover Office / Korschenbroich Office / Leichlingen Office / Munich Office / Oberursel Office / Potsdam Office / Stuttgart (Neuhausen) Office / Wolfsburg Office
- HORIBA FuelCon GmbH - Barleben
- HORIBA Jobin Yvon GmbH - Oberursel
- HORIBA Tocadero GmbH

Italy
- HORIBA ABX SAS - Italy Branch
- HORIBA ITALIA Srl - Roma
- HORIBA ITALIA SRL - Torino Office

Netherlands
- HORIBA Europe GmbH - Netherland Office

Poland
- HORIBA ABX Sp. z o.o. – Warszawa
- MLU Sp. z o.o.

Portugal
- HORIBA ABX SAS - Portugal Branch

Romania
- HORIBA (Austria) GmbH - Romania Branch

Russia
- HORIBA OOO - Moscow / Zelenograd Office

Spain
- HORIBA ABX SAS - Spain Branch

Sweden
- HORIBA Europe GmbH, Sweden Branch - (Gothenburg) / (Sodertalje)

Turkey
- HORIBA Europe GmbH - Istanbul Office

United Kingdom
- HORIBA Jobin Yvon IBH Ltd. - Glasgow
- HORIBA MIRA Limited - Nuneaton / Quatro Park
- HORIBA Test Automation Limited. - Worcester
- HORIBA UK Limited - Northampton

You can find detailed information
on HORIBA Group locations here.

https://www.horiba.com/int/contact/worldwide-locations/

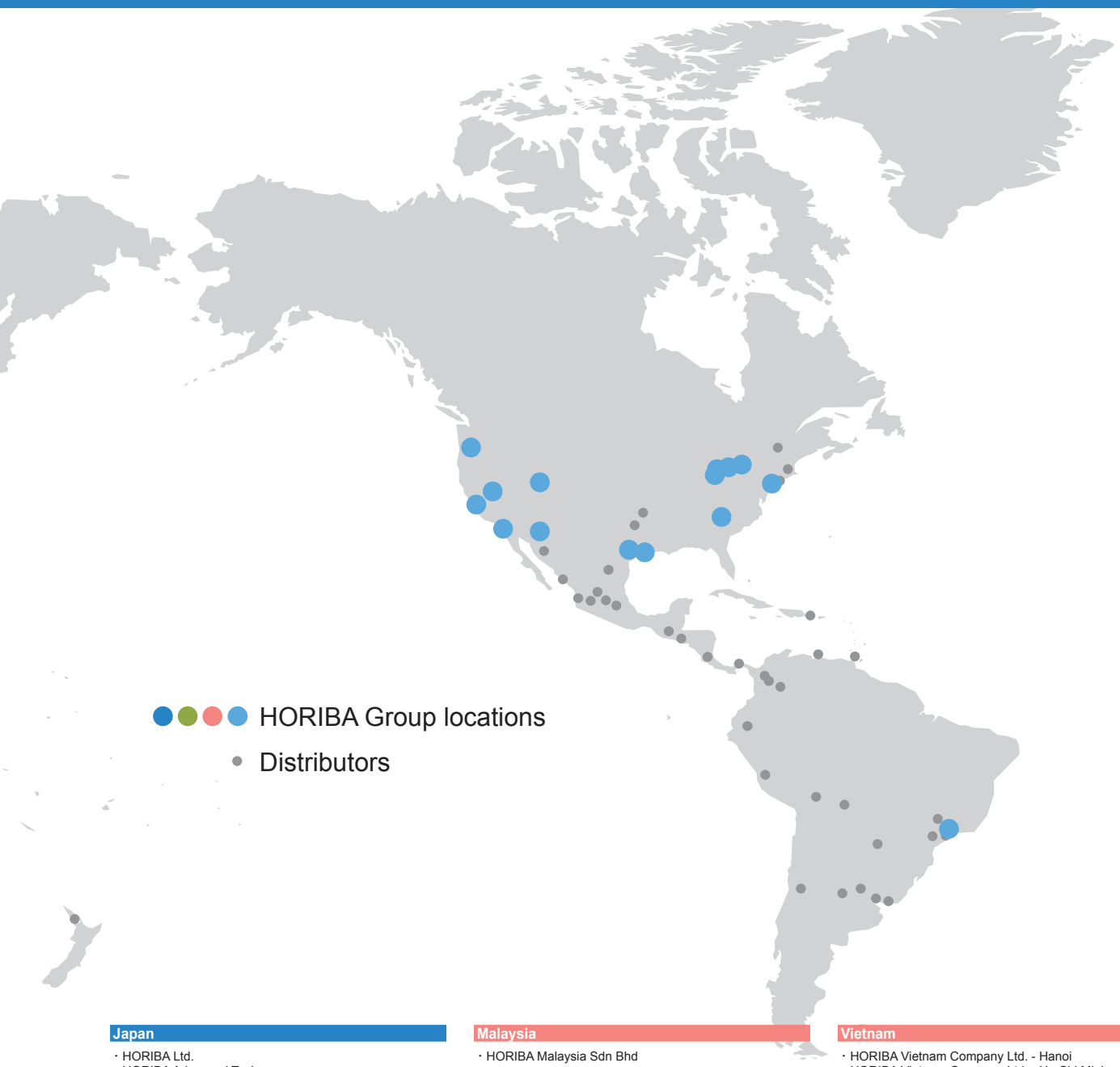

Japan

- HORIBA Ltd.
- HORIBA Advanced Techno
- HORIBA STEC
- HORIBA Techno Service

China

- HORIBA (China) Trading Co. Ltd. - Xi'an / Beijing / Beijing YiZhuang / Chengdu / Guangzhou Office / Shanghai / Shenzhen / Xiamen
- HORIBA INSTRUMENTS (SHANGHAI) CO., LTD - Shanghai
- HORIBA Precision Instruments (Beijing) Co., Ltd.
- HORIBA Technology (Suzhou) Co.,LTD.
- MIRA China Ltd. - Shanghai
- MIRA China Ltd. Xiangyang Workshop

India

- HORIBA India Private Limited - Bangalore Office / Chennai Office / Haridwar Factory / New Delhi / Technical Center / Kolkata Office / Nagpur Factory

Indonesia

- PT HORIBA Indonesia
- PT. HORIBA Indonesia - Tangerang

Malaysia

- HORIBA Malaysia Sdn Bhd

Philippines

- HORIBA Instruments (Singapore) Pte Ltd. - Manila Office

Singapore

- HORIBA Instruments (Singapore) Pte Ltd. –Singapore / West Office

South Korea

- HORIBA KOREA Ltd. - Anyang-Si / Dongtan Office / Ulsan Office
- HORIBA STEC KOREA, Ltd. - Gyeonggi-do

Taiwan

- HORIBA Taiwan, Inc. - Hsinchu
- HORIBA Taiwan, Inc. - Tainan Office

Thailand

- HORIBA (Thailand) Limited - Bangkok

Vietnam

- HORIBA Vietnam Company Ltd. - Hanoi
- HORIBA Vietnam Company Ltd. - Ho Chi Minh

Brazil

- HORIBA Instruments Brasil, Ltda. -São Paulo
- TCA/HORIBA Sistemas de Testes Automotivos Ltda. -São Paulo

Canada

- HORIBA Canada Inc. -Burlington / London Office

USA

- HORIBA Instruments Incorporated -Ann Arbor Office / Austin Office / Canton Office Fletcher Office / Houston Office / Irvine / Portland Office / Sunnyvale Office / Tempe Office / Troy Office / West Valley City Office
- HORIBA New Jersey Optical Spectroscopy Center
- HORIBA Reno Technology Center

Readout **HORIBA Technical Reports English Edition No.59**

Publication Date : December 26th, 2025
Publisher : HORIBA, Ltd.
Editor : NAKAMURA Hiroshi
Associate Editor : HAYASHI Susumu
Publication Members : URAKAMI Chikako, MATSUDA Tetsuya, HAMAGAMI Ikuko
SATAKE Hiromi, MISUMI Akihiro, SHIROSAKI Akari
DTP, Printing : SHASHIN KAGAKU Co., Ltd.
Information : R&D Planning Center, R&D Division, HORIBA, Ltd.
2, Miyanohigashi-cho, Kisshoin, Minami-ku, Kyoto 601-8510, Japan
Phone : (81)75-313-8121
E-mail : readout@horiba.co.jp

HORIBA

Explore the future